Title

Inferior-Colliculus Responses to Amplitude-Modulated and Unmodulated Acoustic Tones and Cochlear-Implant Pulse Trains

Permalink

https://escholarship.org/uc/item/33m1n11v

Author

Schoenecker, Matthew Charles

Publication Date

2010

Peer reviewed|Thesis/dissertation

Inferior-Colliculus Responses to Amplitude-Modulated and Unmodulated
Acoustic Tones and Cochlear-Implant Pulse Trains

By

Matthew Charles Schoenecker

A dissertation submitted in partial satisfaction of the

requirements for the degree of

Joint Doctor of Philosophy
with University of California, San Francisco

in

Bioengineering

in the

Graduate Division

of the

University of California, Berkeley

Committee in charge:

Professor Patricia A. Leake, Chair
Professor Edwin R. Lewis
Professor José M. Carmena

Fall 2010

Inferior-Colliculus Responses to Amplitude-Modulated and Unmodulated

Acoustic Tones and Cochlear-Implant Pulse Trains

copyright 2010

by Matthew Charles Schoenecker

Abstract

Inferior-Colliculus Responses to Amplitude-Modulated and Unmodulated
Acoustic Tones and Cochlear-Implant Pulse Trains

By

Matthew Charles Schoenecker

Doctor of Philosophy in Bioengineering

University of California, Berkeley

Professor Patricia A. Leake, Chair

Cochlear implants (CIs) are neural prostheses that currently provide acoustic sensation to more than 120,000 profoundly hearing-impaired people throughout the world. The majority of these CI users are able to understand speech without lip reading and to converse over the telephone. The most fortunate among them can even perform and appreciate music. Unfortunately, however, many CI recipients receive much less benefit from their devices. In order to examine the neuronal bases for these disparate outcomes, a recording system was developed to overcome specific technical limitations in previous studies that recorded neuronal responses to cochlear implant stimulation in animal models. This recording system was then used in two studies comparing responses to normal acoustic stimulation and electrical cochlear implant stimulation in guinea pigs and cats.

The design of the recording system included a 32-channel recording amplifier and a software technique for removing stimulus artifacts from recordings of neural responses to high-rate electrical stimulation. Contemporary cochlear implants often deliver current pulse trains with carrier rates of 1000 pulses/s or higher. In neurophysiology studies, this electrical stimulation produces artifacts that are typically much larger than neuronal responses. Therefore, the recording system was specifically designed to record neuronal responses and cancel these electrical stimulus artifacts. When biphasic full-scale-input pulses (1.5-V) are applied directly to the amplifier inputs, each recording channel settles to 20 µV in less than 80 µs. This fast recovery makes it likely that the recording electrode-electrolyte interface, not the recording electronics, will limit artifact settling times. Artifacts are blanked in software, allowing flexibility in the choice of blanking period and the possibility of recovering neural data occurring simultaneously with non-saturating artifacts. The system has been used *in-vivo* to record central neuronal responses to intracochlear electrical stimulation at rates up to 2000 pulses/s.

Using this recording system, systematic and quantitative comparisons of inferior-colliculus responses to acoustic stimulation and electrical stimulation in two configurations (monopolar and bipolar) were carried in guinea pigs and cats. Previous cochlear implant studies using isolated electrical stimulus pulses in animal models have reported that monopolar stimulus configurations elicit broad extents of neuronal activation within the central auditory system—much broader than the activation patterns produced by bipolar electrode pairs or acoustic tones. However,

psychophysical and speech reception studies that use sustained pulse trains do not show clear performance differences between monopolar and bipolar configurations. To evaluate whether monopolar intracochlear stimulation can produce selective excitation of the inferior colliculus, activation widths were determined along the tonotopic axis of the inferior colliculus for acoustic tones and 1000-pulse/s electrical pulse trains in guinea pigs and cats. Electrical pulse trains were presented using an array of 6-12 stimulating electrodes distributed longitudinally along a space-filling silicone carrier positioned in the scala tympani of the cochlea. The data indicated that for monopolar, bipolar, and acoustic stimuli, activation widths were significantly narrower for sustained responses than for the transient response to the stimulus onset. Furthermore, monopolar and bipolar stimuli elicited similar activation widths when compared at stimulus levels that produced similar peak spike rates. Surprisingly, monopolar and bipolar stimuli produced narrower sustained activation than 60 dB SPL acoustic tones when compared at stimulus levels that produced similar peak spike rates. Therefore, the conclusion from these experiments was that intracochlear electrical stimulation using monopolar pulse trains can produce activation patterns that are at least as selective as bipolar or acoustic stimulation, if stimulus intensities are appropriately matched.

The second study compared responses to acoustic and monopolar electrical stimuli that were sinusoidally amplitude modulated (SAM), in order to better model the complex signals delivered by CI processors. For both normal hearing listeners and cochlear implant users, SAM signals produce psychophysical interactions that can extend across large differences in carrier frequency or large intracochlear electrode separations. However, the neural correlates of these phenomena are not well understood. This study was designed to determine whether SAM stimuli elicit activation across a broader extent of the frequency axis of the inferior colliculus than unmodulated steady-state stimuli, and whether this activation is strongly phase locked to the SAM stimulus envelope. To address these questions neuronal activity in the inferior colliculus of guinea pigs, normal cats and chronically deafened cats was recorded in response to acoustic and electrical stimulation. Quantitative analysis of recordings indicated that the extent of inferior colliculus activation was up to 70% broader for SAM stimuli than for unmodulated steady-state stimuli in normal cats and guinea pigs and 160% broader in chronically deafened cats. This activity was also phase-locked to the SAM envelope across a broad extent of the frequency axis of the inferior colliculus. These results suggest that a number of cross-carrier frequency interactions for SAM stimuli could occur at the level of the inferior colliculus. They also show that direct comparisons of responses to acoustic and electrical SAM stimuli can reveal attributes of neural processing that underlie specific psychophysical findings in CI recipients—and thereby can provide a powerful basis for guiding development of new processing strategies for future cochlear implants.

Dedication

To my beloved family and friends

8-15-2010

Acknowledgments

Many people, I am sure, think that a doctoral dissertation is primarily about research. That it is primarily about numbers, or charts, or graphs. However, what I have come to realize in these last seven years is that a doctoral dissertation is primarily about people. On the one hand, it is about the people one is trying to help by advancing knowledge in a particular field. But perhaps on an even deeper level it is about the people that one comes to know, to learn from, and to admire along the way. Among the people whose help I have received are professors, coworkers, friends, and family. I would like to take this opportunity to thank just a few of these people who were instrumental in the completion of this dissertation.

There are some people who, through their dedication to being nothing less than excellent in their profession and through their constant concern for those who work with them, make a working environment not only bearable, but delightful. My dissertation chair, Pat Leake is one of those people. Pat has a remarkable ability to be both your biggest cheerleader and your most constructive critic. She combines constant vigilance, thinking ahead about the next step or two to three steps down the road for you with a very practical wisdom about what to do in the moment and what to leave undone. Her personal warmth, sense of humor, and individual concern remarkably go along with her status as somewhat of a star in the cochlear implant research field. Yet, she always uses that status not for her own aggrandizement, but to introduce her students and post-docs to anyone and everyone in the field who could help them. I also think that she is the only person who spent more time reading and editing my dissertation than I did. In short, I really could not have asked for a better chair, advisor, and colleague than Pat.

Ben Bonham, the co-advisor on my dissertation, also deserves more thanks than I could reasonably give him in a short paragraph. At UCSF I suppose all faculty members are intelligent, but the speed with which Ben can grasp and move forward concepts that I find difficult is at times alarming. It is hard to overstate how helpful it is to have someone who can quickly understand all your technical and scientific plans and immediately provide you with suggestions on how to make them better. But even more important is his commitment to using this ability to be a real mentor. I think what stood out most in this regard was his concern for my freedom in choosing a project and carrying it out, but at the same time his lively concern and timely interventions to make sure that my project (and my professional trajectory) were going in the right direction. And, he combines all this with a wry sense of humor and easygoing attitude that makes you want to hang out on the deck outside and have a malted beverage with him.

My third and "unofficial" advisor is Russ Snyder. Russ and Ben together helped me formulate most of the ideas that went into the experiments described in this dissertation. In addition Russ spent hours talking with me about the history of the cochlear implant field, its current status, and where it could go in the future. I credit him with teaching me much of what I know about auditory neurophysiology, but most of all I credit him with providing me with a sense of inspiration, wonder, and hope for what can be accomplished in the future. I also have to thank him for the enthusiasm and sense of humor with which he approaches his work, adding an irreplaceable energy to the lab environment when he is around.

about the fundamentals of what we were actually doing. The veterinary care staff (Beth, John, Janet, and Chantale) also did a wonderful job caring for the animals in the laboratory.

Craig Atencio did not actually work with me on the dissertation itself, but nonetheless it never would have been completed without him. First of all, it was he who initially told me about Pat Leake's research lab and told me that it could be a good fit for me. Afterwards our weekly lunches, tennis games, and other outings and conversations kept me mentally and physically healthy and helped me to keep my professional and personal goals high. He has been a true friend, which is what every person, graduate student or not, needs to succeed and thrive in life.

Other graduate student friends who deserve special thanks include Alejandro, Drew, and Matthias for helping me through circuits class and John Secord for coaching my swing in softball. Cherian is a latecomer on the scene who deserves thanks for being so cheerful in and out of the lab. All my graduate school, undergraduate, and high-school friends also should be thanked, but special mention has to be given to Jesse. Among many other contributions, it was he who got me interested in bionic devices, which bloomed into a graduate career in circuit design for studies of neural prostheses.

I thank everyone I left out for forgiving me this bald-faced ingratitude. Also, I thank Sports Illustrated for not printing my name next to that compromising photograph years ago.

But most of all, I would like to thank my family. If I were to thank each of them for their contributions to this dissertation and to my life, I would have to double the length of these acknowledgements, which nobody wants. However, each one of them should know how they have touched my life and have given me the inner confidence, without which seven years studying for a Ph.D. would have been impossible.

"It was the best of times, it was the worst of times," begins a well-known novel. For me, it was only the best of times—thank you to all of you who made these some of the best times in my life.

Table of Contents

Introduction

Cochlear implants (CIs) currently provide acoustic sensation to more than 120,000 profoundly or severely hearing-impaired people throughout the world (Zeng et al., 2008). The majority of these CI users receiving the latest technology are able to understand speech without lip reading and to converse over the telephone. The most fortunate among them can even perform and appreciate music. Unfortunately, however, many CI recipients receive much less benefit from their devices. The reasons for these intersubject differences in performance, however, are not yet clear. In performing the studies described here, one of the overall goals was to better understand the mechanisms that underlie and limit CI performance so as to facilitate the development of new devices and strategies to improve performance for all cochlear implant users.

Cochlear implant technology

The earliest applied cochlear implants were single-channel devices that provided acoustic information by temporally varying the electrical stimulus delivered at one intracochlear location. It was hoped that the ability of normal hearing listeners to detect and make use of amplitude modulation in acoustic stimuli (Churcher et al., 1934; Kay, 1982) would be useful in these cochlear implant users. Early results showed that although these single-channel systems provided some benefits in lip reading, sound identification, and speech production, they generally did not provide speech recognition ability (Bilger et al., 1977a; Bilger et al., 1977b).

Later, multiple-channel systems were introduced in an attempt to take advantage of the highly precise spatial frequency organization (tonotopic organization) of the cochlea. Because high frequencies are represented at the base of the cochlea and low frequencies at the apex, it was thought that introducing multiple intracochlear electrode contacts along the cochlear spiral would enable specific activation of separate frequency regions. Initially, multi-channel electrodes did provide some speech reception ability, with average performance of roughly 30% correct on sentence recognition tests in quiet using the Nucleus WSP II device by Cochlear Corp. in about 1985 (Zeng et al., 2008)). However, with the introduction of substantial improvements in speech processing (e.g. improved spectral representations and temporal interleaving of pulsatile stimulation to reduce channel interaction (Wilson et al., 1991)) sentence recognition scores in quiet rise to mean levels of roughly 80% correct by around the year 1994 (Zeng et al., 2008).

Since that time, mean performance for sentence recognition in quiet seem to have reached a plateau (Zeng et al., 2008). In addition, there are a number of other challenges that have proved difficult to overcome, such as improving speech recognition in noise, providing music appreciation, and improving the ability to understand tonal languages. Clever use of the insights provided by psychophysical testing and animal studies has enabled remarkable progress in cochlear implant designs over the past 50 or so years. However, there is still a large gap in our understanding of the fundamental neuronal mechanisms underlying cochlear implant hearing. It may be that a deeper understanding of these neural mechanisms will be necessary to make further progress in providing more natural auditory sensations to cochlear implant users.

Neurophysiologic studies of cochlear implant stimulation

Neurophysiologic studies in animal subjects can provide a means of better understanding cochlear implant function and guiding development of novel cochlear implant strategies. In human psychophysical studies, tests are devised to infer perceptual parameters such as frequency resolution and the ability to detect and discriminate temporal fluctuations. If comparable signals and protocols are selected for conducting animal neurophysiologic studies, such studies can provide a powerful means of demonstrating and quantitatively analyzing neuronal firing patterns that are correlates of specific psychophysical phenomena. Variables that are difficult to control in human studies (such as etiology and duration of deafness, variability in surgical positioning of the implant, etc.) can be easily controlled in animal studies. Furthermore, certain variables can be easily manipulated in animal studies that cannot be easily manipulated in human studies (such as the geometry and placement of the implanted electrodes, the density and location of stimulating contacts, etc.). Lastly, there are measurements that can be made very precisely in animal neurophysiologic studies, but which can only be imprecisely inferred in human studies, such as the relative extent of neural excitation using different stimulus configurations and the precise timing of neural responses relative to the stimulus.

Although studies of neurophysiologic responses to cochlear implant stimulation have been carried out in a number of locations along the auditory pathway, the auditory midbrain (inferior colliculus) offers several advantages for comparing responses to acoustic and electrical stimuli. The inferior colliculus is an obligatory auditory processing center—virtually all auditory information passes through the inferior colliculus on its way to the auditory cortex. Further, the inferior colliculus has a very precisely defined frequency organization (tonotopy): low frequencies are represented in laminae that are positioned more superficially, and high frequencies are represented in progressively deeper laminae along the dorsolateral-medioventral axis in the central nucleus of the inferior colliculus. Hence, a multi-site recording probe can be placed along this axis, and recordings of responses to acoustic stimuli can be made that provide a means of characterizing the ensemble responses of neurons across a wide range of frequencies. These baseline measurements can then be compared directly to responses of the same neural populations to electrical stimulation, after the recording probe is fixed in place and the animal is deafened and implanted with a model CI electrode. Furthermore, the inferior-colliculus frequency organization is highly consistent across animals, such that these studies can be carried out in chronically deafened animals. Although precise acoustic frequency representations cannot be determined in these subjects, a tonotopic map of the basal-to-apical intracochlear electrode positions can be characterized; and comparisons of the specificity of neuronal activation patterns can be made for different electrical stimuli within the same animal. Similar procedures are possible, but more difficult in other locations such as the auditory nerve (because of difficulties with surgical access when a cochlear implant is present) and the cochlear nucleus and auditory cortex (because of their somewhat less regular tonotopy).

Electrical stimulus artifacts

Cochlear implants often deliver current pulse trains with carrier rates of 1000 pulses/s or higher to enable the representation of high-frequency temporal envelopes (a carrier rate of at least 800 pulses/s is necessary to accurately represent typical envelope cutoff frequencies of about 400 Hz (Wilson et al., 1991; Zeng et al., 2008)). Using a predetermined processing strategy, these pulse trains are amplitude modulated by speech or sound signals. One approach for evaluating the

relative performance of different implants and processing strategies is to record and compare inferior colliculus responses to intracochlear stimulation in animal models as described previously (Bonham et al., 2008; Snyder et al., 2004; Snyder et al., 2008; Snyder et al., 2000). However, electrical stimulation produces artifacts that are often much larger than neuronal responses (particularly when stimulation is delivered in a monopolar configuration—one intracochlear stimulating contact and an extracochlear return contact). Because of the technological problems of overlapping responses and stimulus artifacts at higher pulse rates, studies of midbrain neuronal responses to cochlear implant stimulation in animals have typically used single, isolated electrical pulses or relatively low-rate pulse trains. Here, a novel 32-channel recording system is described with the ability to record neuronal waveforms and eliminate high-rate stimulus artifacts. This system was developed and applied *in vivo* to investigate responses to cochlear implant stimulation in different stimulus configurations.

Monopolar versus bipolar stimulus configurations

In all three of the major commercial cochlear implant systems currently available for clinical application, electrical current pulses from cochlear implants are delivered in monopolar configuration (one intracochlear stimulating electrode and an extracochlear return electrode), although the devices are capable of operation in bipolar configuration (one intracochlear stimulating contact and one intracochlear return contact). Monopolar electrical stimulation has been reported in animal studies to elicit neuronal activation that is broadly distributed across the tonotopic frequency organization of the auditory system. In contrast, acoustic stimulation and bipolar electrical stimulation have been shown to produce relatively narrow, selective distributions of neuronal activity (Bierer et al., 2004; Kral et al., 1998; Merzenich et al., 1977; Middlebrooks et al., 2007; Snyder et al., 2008). However, studies of human cochlear implant users have shown that they perform as well with monopolar stimulation as with bipolar stimulation on speech reception tasks (Kileny et al., 1998; Pfingst et al., 2001; Zwolan et al., 1996). One possible cause of the discrepancies between the two types of studies is that most of the animal neurophysiology studies were carried out using isolated electrical pulses and the human speech reception studies were carried out using high-rate pulse trains. In this study conducted in guinea pigs and cats, the abovementioned recording system was used to examine inferior colliculus responses to acoustic tones and electrical pulse trains delivered at a typically used clinical rate (1000-pulse/s). The goal of this study was to determine whether (and if so, under what conditions) sustained monopolar intracochlear stimulation can produce activation of the inferior colliculus that is as selective as bipolar or acoustic stimulation.

Responses to sinusoidally amplitude modulated stimuli

Sinusoidally amplitude-modulated (SAM) acoustic tones and intracochlear electrical pulse trains elicit auditory neuronal responses that phase lock to the SAM envelope. For both acoustic and electrical hearing, it is likely that this phase locking plays an important role in speech processing, sound source localization, and source identification. A number of psychophysical phenomena including modulation detection interference (Grose et al., 2005; Yost et al., 1989) and comodulation masking release (Hall et al., 1984; Verhey et al., 2003) imply that excitatory and/or suppressive effects of SAM tones in the auditory system extend well beyond a critical band (a critical band is roughly 1/3 to 1/2 octave (Zwicker et al., 1957)). Cross-critical-band phenomena such as modulation detection interference have also been shown to occur in cochlear implant users (Chatterjee et al., 2004). Whereas these cross-critical-band psychophysical effects

have been well studied, relatively little is known about how neuronal populations respond to carrier frequencies and intracochlear stimulus locations that differ by more than a critical band. In particular, although it is has been reported that the inferior colliculus exhibits wideband effects such as inhibition (Li et al., 2006), little is known about how populations of neurons across the tonotopic axis of the inferior colliculus respond to acoustic SAM tones or electrical SAM pulse trains. Therefore, a study in guinea pigs and cats was performed to determine whether acoustic and electrical SAM stimuli elicit activation across a broad extent of the frequency axis of the inferior colliculus relative to unmodulated steady-state stimuli, and whether this activation is strongly phase locked to the SAM stimulus envelope.

Organization of this dissertation

In Chapter 1 the design and verification of the novel 32-channel recording system are described. Results demonstrate that the system is able to record neuronal waveforms and eliminate stimulus artifacts at carrier rates of at least 2000 pulses/s. Chapter 2 reports data in guinea pigs and cats comparing responses to acoustic tones and 1000-pulse/s electrical pulse trains. These data indicate that sustained monopolar intracochlear stimulation can indeed elicit selective activation of the inferior colliculus. In Chapter 3 inferior colliculus responses to unmodulated and SAM acoustic tones and electrical pulse trains are characterized. Results show that SAM stimuli elicit activation across a broad extent of the frequency axis of the inferior colliculus relative to unmodulated steady-state stimuli, and that this activation is strongly phase locked to the SAM stimulus envelope.

Chapter 1: Fast Stimulus Artifact Recovery in a Multichannel Neural Recording System

ABSTRACT

We describe a 32-channel recording system and software artifact blanking technique for recording neuronal responses to high-rate electrical stimulation. When biphasic full-scale-input pulses (1.5-V) are applied directly to the amplifier inputs, each recording channel settles to 20 µV in less than 80 µs. This fast recovery makes it likely that the recording electrode-electrolyte interface, not the recording electronics, will limit artifact settling times. Artifacts are blanked in software, allowing flexibility in the choice of blanking period and the possibility of recovering neural data occurring simultaneously with non-saturating artifacts. The system has been used *in-vivo* to record central neuronal responses to intracochlear electrical stimulation at 2000 pulses per second. Simplicity of the hardware design makes the technique well suited to an implantable multi-channel recording system.

INTRODUCTION

Many contemporary neural prostheses stimulate neural tissue using high-rate electrical pulse trains. For example, cochlear implants typically deliver biphasic current pulse trains with carrier rates at or above 1000 pulses per second (pps). These pulse trains are modulated by speech or sound signals according to a predetermined processing strategy. One method of evaluating the relative performance of various processing strategies is to record and compare midbrain neuronal responses to intracochlear stimulation in animal models (Bonham et al., 2008; Snyder et al., 2004; Snyder et al., 2008; Snyder et al., 2000). However, electrical stimulation often produces artifacts that are much larger than the neuronal responses being studied. A neural recording system used in these studies would therefore benefit from a method of eliminating these artifacts. Furthermore, if the recording system were chronically implantable, it would enable assessment of long-term prosthesis performance and neural plasticity resulting from chronic neural stimulation. A conceptual schematic of such an implantable recording system is shown in Fig. 1.
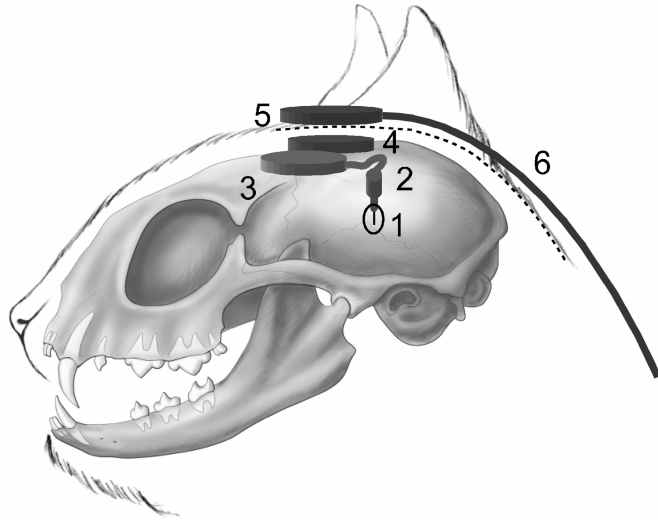
Fig. 1. Schematic of an implantable system for measuring midbrain responses to cochlear electrical stimulation. **1.** Neural probe in target tissue. **2.** Cable guide tube. **3.** Implanted circuitry for amplification, filtering and analog-to-digital conversion. **4.** Implanted circuitry for wireless data transmission and power reception. **5.** External magnetically-aligned data receiver and power transmitter. **6.** External cable connected to backpack-mounted circuitry. (Cat skull image © John Yesko, with permission.)

Stimulus artifact removal

A number of approaches to reducing electrical stimulus artifacts have been reported previously. In the sample-and-hold method, the ability of the amplifier to follow the input signal is disabled during a stimulus pulse, and the pre-stimulus voltage is usually stored on a capacitor (Freeman, 1971; Sher et al., 2007; Venkatraman et al., 2009). After the stimulus pulse is over, the amplifier is re-enabled. There are several drawbacks to the sample-and-hold method. First, neural activity occurring during the hold period is not recorded. This hold period cannot be changed after the recording occurs—if it is too long, excess neural information will be lost. If it is too short, the recorded waveform will be affected by stimulus artifact. Second, the hardware sample-and-hold function requires additional circuit complexity and, therefore, increased circuit size. Third, the amplifier circuit must be passed information about when the stimulus artifact will occur, which can be impractical for an implanted amplifier that is physically separated from the stimulating device. A recent variation on the hardware sample-and-hold technique entails increasing the high-pass cutoff frequency after the hold period (Brown et al., 2008; DeMichele et al., 2003). While the above drawbacks still apply to this technique, it does greatly decrease the post-artifact settling time of the system.

In an effort to overcome the disadvantages associated with the hardware sample-and-hold technique, investigators have developed algorithms for artifact reduction in software. Filtering algorithms can be used to remove the spectral components of artifacts while leaving the spectral components of neuronal action potentials intact (Gnadt et al., 2003; Litvak et al., 2003b; Middlebrooks, 2004). These algorithms work well when the stimulus repetition rate does not fall within the frequency spectrum of the neural waveforms of interest. However, for stimulation rates between 500 pps and 3000 pps, the spectra of the neural waveforms and artifacts overlap, making accurate separation difficult. Furthermore, these techniques are less effective for stimuli with time-varying pulse rates or pulse amplitudes (for example, the amplitude-modulated pulse trains typically used in cochlear implants). Software-based artifact template subtraction is one approach that can be used to recover neural waveforms in the presence of spectrally-overlapping artifacts (Azin et al., 2007; Hashimoto et al., 2002; Wichmann, 2000; Zhang et al., 2007). This method is also more difficult to implement for stimulus artifacts that change with time (Litvak et

al., 2001). Moreover, it is computationally expensive, making it less attractive for a multichannel recording system that removes artifacts during the course of an experiment. Subtracting artifacts using local curve fitting is more suitable for real-time artifact suppression, but the overall artifact recovery time with this method is still on the order of a millisecond (Wagenaar et al., 2002).

Heffer and Fallon described a sample-and-interpolate method that uses a wide-bandwidth amplifier for fast artifact recovery (less than 110 µs from the end of the stimulus) and software interpolation for artifact removal (Heffer et al., 2008). This method does not require additional hardware complexity, and there is no need for the recording amplifier to receive any signal indicating that a stimulus is occurring. The technique is flexible in that the artifact blanking period can be changed after recordings are made, and no neural information is lost during the stimulus artifact (provided that the amplifier does not saturate). Furthermore, this method can effectively remove artifacts that have frequency spectra overlapping the neural signals of interest or artifacts that change with time.

We have developed a 32-channel recording system for use with the sample-and-interpolate method or with a software artifact blanking method that we describe. Software artifact blanking has the same advantages as sample-and-interpolate but is more computationally efficient, making it attractive for artifact removal during an experiment. Because the recording system is designed using off-the-shelf components, it is low-cost and easy to implement. The system is appropriate for use in acute percutaneous recording preparations, but it is also designed for future miniaturization and use in fully-implanted applications. Using this system *in-vivo* we have demonstrated the ability to record multi-channel neuronal waveforms while eliminating spectrally-overlapping stimulus artifacts.

RECORDING SYSTEM DESIGN

Headstage

A block diagram of the recording system is shown in Fig. 2. The headstage receives inputs from a 32-site neural probe, amplifies the neural waveforms by 100 V/V, and digitizes them with 12-bit resolution at 23.4 kSamples/s. Amplification is carried out using 16 dual operational amplifiers (Texas Instruments OPA2345), and digitization is carried out using two 16-channel A-D converters (Analog Devices AD7490). The two A-D converters share a common serial bus with separate chip selects, allowing their outputs to be time-multiplexed on a single data output line. The amplifier gain of 100 V/V combined with the A-D converter input range of 2.5 V gives each channel a 25-mV input dynamic range (Table I). This relatively large dynamic range prevents saturation in the case of small electrical artifacts (in our auditory midbrain recordings, artifacts from intracochlear stimulation seldom exceed 10 mV). However, even in the case of larger artifacts that do saturate the amplifier, the recording amplifiers are designed to settle rapidly. A schematic of one "fast-recovery" amplifier channel is shown in Fig. 3.

7
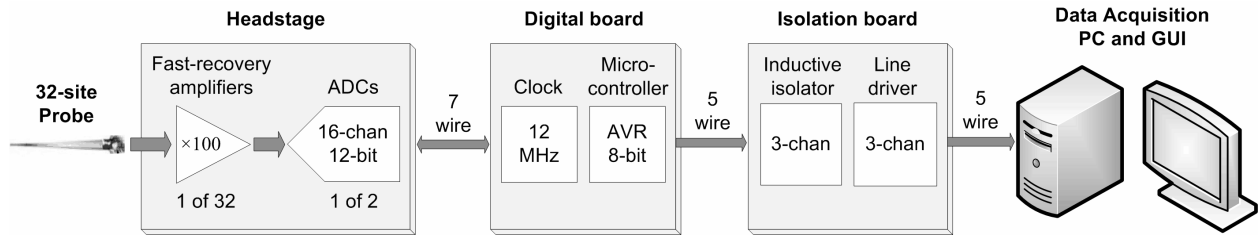
Fig. 2. Block diagram of tethered recording system for acute studies.

Table I. System design parameters

Parameter	Value
Number of recording channels	32
Sampling rate (per channel)	23.4 kSamples/s
A-D converter resolution	12 bits
Amplifier gain	100 V/V
Input dynamic range	25 mV$_{pp}$
Serial communication rate (to PC)	12 Mb/s
Headstage voltage supply	3.3 V
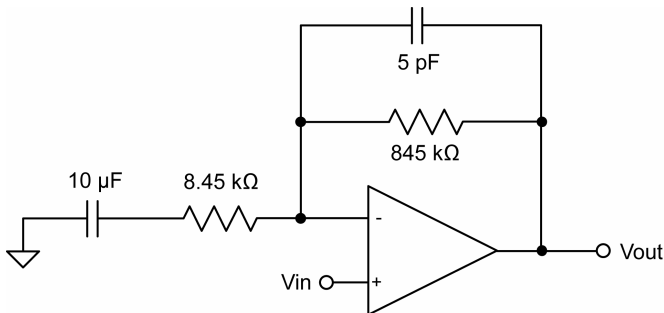
Fig. 3. Circuit schematic of one fast-recovery amplifier channel, designed for a passband of 1.9 Hz to 19.7 kHz.

Digital and isolation boards

The digital board contains clock-generation circuitry and a microcontroller (Atmel ATtiny2313), which sets up the A-D converters, then goes into idle mode. Data passes through the digital board to the isolation board via a 5-wire serial link. Using an inductive digital isolator (Analog Devices ADuM1401CRW) and a digital line driver (Texas Instruments 64BCT25244), the isolation board then transmits data to a digital I/O card (NI-PCI-DIO-32HS, National Instruments, Austin, TX) in a host PC for signal processing and display. The cost of the system (not including the PC) is approximately $1700 ($1400 for the digital I/O card, $150 for printed circuit board fabrication, and $150 for discrete circuit components). Detailed circuit schematics are included in Appendix I, and C code for the Atmel (AVR) microcontroller is included in Appendix II.

Signal conditioning for fast artifact recovery

The recording amplifiers are designed to have a relatively low high-pass cutoff (1.9 Hz) and a

8

relatively high low-pass cutoff (19.7 kHz) in order to settle quickly from electrical artifacts. In addition to enabling local field potential measurements, lowering the high-pass cutoff frequency reduces the magnitude of residual voltage artifacts from pulsatile electrical stimulation (McGill et al., 1982). Large residual voltages appear as artifacts in the post-stimulus waveform, making it difficult to detect action potentials using threshold crossing methods. In some cases the residual voltage can even saturate the recording amplifier. Fig. 4 shows a numerical simulation of 100-Hz and 2-Hz RC high-pass filter responses to a biphasic stimulus pulse. The 2-Hz filter has a post-stimulus residual voltage that is over 2000 times smaller than the residual voltage of the 100-Hz filter.
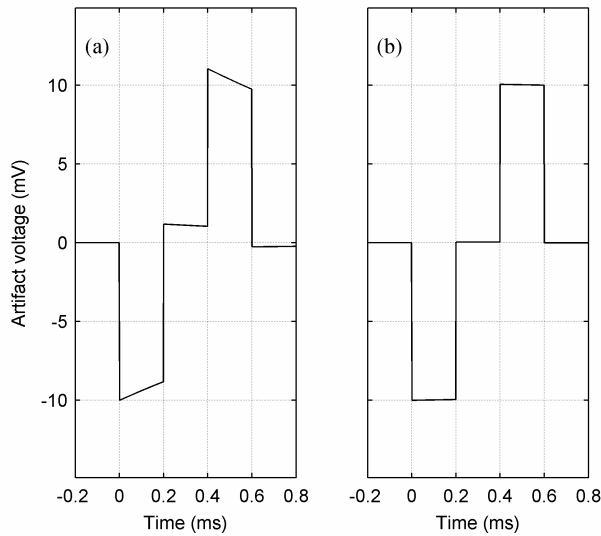
Fig. 4. The effect of high-pass cutoff frequency on amplifier response to a biphasic stimulus pulse. (Numerically-simulated input pulses have 10-mV amplitude, 200 µs/phase and a 200-µs interphase gap). **(a)** Decay toward baseline using a 100-Hz high-pass is considerable during the stimulus pulse phases and the interphase gap. The positive and negative decays do not sum to zero, resulting in a significant (-262 µV) residual voltage artifact following the second phase. This residual voltage artifact is large relative to most neuronal signals, and increases with stimulus pulse amplitude. **(b)** Decay toward baseline is considerably smaller using a 2-Hz high-pass filter, and produces a much smaller residual voltage artifact (-0.126 µV).

Settling time from the pulse peak to the residual voltage is determined by the amplifier slew rate, low-pass cutoff frequency, and filter topology. In comparison to low-pass cutoff frequencies typically used in neural recording amplifiers (6 kHz – 10 kHz), we chose a low-pass cutoff frequency that was relatively high (19.7 kHz) to decrease amplifier settling time (Table II). The low-pass cutoff is set by a combination of the feedback resistor, feedback capacitor (including parasitics), and op-amp gain-bandwidth product (GBW). Approximately 1 pF of parasitic board capacitance adds to the 5-pF feedback capacitor shown in Fig. 3. The circuit was designed to allow the loosely-specified op-amp GBW of 3 MHz to be low enough to affect the low-pass cutoff for two reasons. First, this system is intended as a prototype for an implantable system, for which minimum power consumption is a design factor. Second, the GBW provides a second low-pass pole for noise filtering without adding any hardware complexity. In a future design, the discrete amplifiers will be replaced by an integrated multichannel amplifier (with off-chip AC coupling capacitors) to decrease implant size and power consumption. Fig. 5 shows a photograph of the neural recording headstage.

Table II. Simulation of low-pass filter settling times

Filter topology	Cutoff frequency	Settling time to 0.2%
4th order Butterworth	8 kHz	340 µs
1st order RC	8 kHz	120 µs
1st order RC	19 kHz	50 µs

Biphasic pulse waveforms (with 10-mV amplitude, 40 µs/phase and 20-µs interphase gap) were low-pass filtered in software. Settling to 0.2% corresponds to residual artifacts of 20 µV or less.
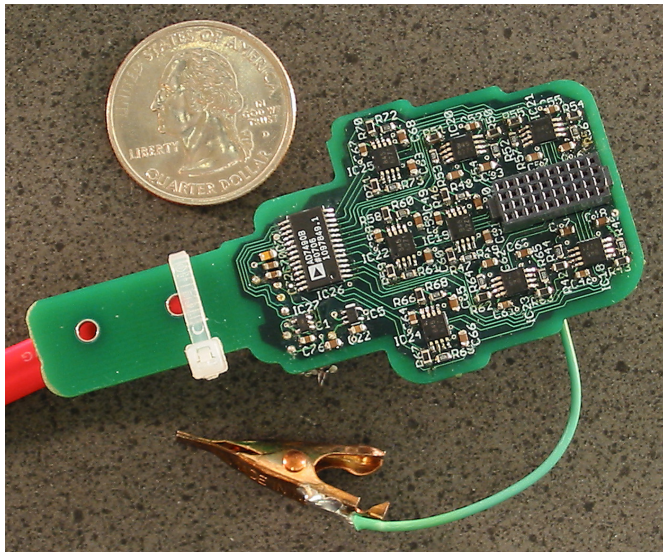
Fig. 5. Photograph of the neural recording headstage.

Software artifact blanking

The host PC receives a stimulus flag signal during each electrical stimulus pulse. The PC records the stimulus times and aligns them temporally with the incoming data from the recording headstage. A user-specified blanking time is added to each stimulus time to account for amplifier settling. For each recording channel, data occurring during a stimulus pulse artifact is replaced with the mean value of the data point before the stimulus and the data point after the stimulus (Fig. 6). The resulting waveforms are copies of the originals but with flat regions wherever a stimulus artifact had been. These waveforms are then band-pass filtered in software from 600 Hz to 3 kHz.

The 23.4-kSample/s sampling rate is adequate to represent the information content in this signal passband. However, the hardware low-pass cutoff frequency of 19.7 kHz is above the Nyquist frequency for this sampling rate so we expect some aliasing of higher frequency noise (thermal and external noise above 20.4 kHz can alias into the passband). In order to attenuate aliased external noise, we carry out recordings in an electrically shielded recording chamber. A higher per-channel sampling rate is possible with the A-D converters chosen. Together, the two A-D converters can sample the waveforms at up to 31 kSamples/s per channel in our design. This would be especially useful for reducing aliased thermal noise in applications that require a wider

passband (e.g. an 8-10 kHz software low-pass cutoff). However, use of a higher sampling rate would increase the aggregate data rate to the host PC. In our *in-vivo* recordings, the root-mean-squared noise when sampling at 23.4 kSamples/s is only 10% higher than when sampling at 186 kSamples/s. Because this noise increase is small, we have opted to sample below the Nyquist rate in order to limit the aggregate data rate to 12 Mb/s.
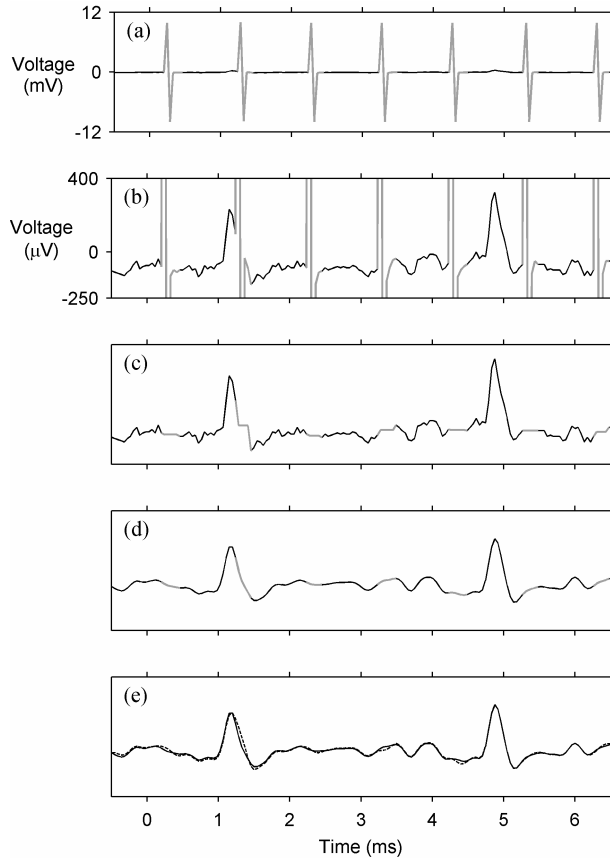
Fig. 6. Software artifact blanking algorithm. **(a)** An extracellular voltage recording with biphasic pulses added in software to simulate electrical artifacts. **(b)** Same as (a) but smaller voltage scale. **(c)** Artifacts are replaced with the mean of the pre- and post-artifact voltages (flat segments, 200 μs in duration). **(d)** The waveform is band-pass filtered from 600 Hz to 3 kHz. **(e)** Shows the original waveform filtered but without added artifacts or blanking (dotted line) superimposed on the waveform from (d) (solid line); the differences in the two waveforms show the distortion introduced by the artifacts and the blanking algorithm.

The dynamic quantization error introduced by the A-D converter is small relative to the size of neuronal action potentials, which range from 30 μV to 300 μV in our application. The 12-bit resolution and 2.5-V input range of the ADC result in a 6-μV least-significant bit. For dynamic signals, this causes a theoretical quantization noise of 1.7 μV_{rms}. This quantization noise is reduced by a factor of two by the software bandpass filter to a final value of 0.88 μV_{rms}.

Power consumption

Because the headstage and digital board are designed for future miniaturization and implantation (still using commercially available components), power consumption is a critical design parameter for these two boards. The operational amplifiers chosen have low supply current (maximum of 250 μA per channel) given their relatively high gain-bandwidth product of 3 MHz. The two A-D converters are specified for a maximum current draw of 1.8 mA each. The actual measured current for the headstage under normal operation is 6.5 mA from a 3.3-V supply (21.5 mW).

On the digital board, the majority of the current is consumed by the clock generator and discrete logic gates switching at or below the serial clock frequency of 12-MHz. The measured digital board current (6.5 mA from a 3.3-V supply) combined with the headstage current results in a total power consumption of 43 mW for these two boards. This power is now provided by a battery, but we have developed an inductive RF link that can transmit up to 200 mW wirelessly.

This RF power link and an optical data link will replace the wired link between the digital and isolation boards. Because the isolation board will remain on the external side of the link, power is not a critical design factor for this board. In the current design it receives its power from the host PC.

PERFORMANCE OF THE RECORDING SYSTEM

Amplifier characterization and artifact recovery

Table III gives a summary of the measured performance of the recording system. When a saturating, biphasic rectangular voltage pulse (1.5-V amplitude, 40 μs per phase, 20-us interphase gap) is applied directly to the amplifier inputs, the recording system settles within 20 μV (RTI) of the pre-stimulus baseline voltage in a maximum of 78 μs after the end of the pulse. For a non-saturating, 10-mV pulse, the settling time is a maximum of 63 μs. Under actual neural recording conditions, it is known that charging of the electrode-electrolyte interface capacitance at the recording site can create a residual artifact voltage and increase settling time (DeMichele et al., 2003). This effect is highly dependent on the characteristics of the recording site. For the recording probe and artifact levels tested in our *in-vivo* studies, this effect was small. However, this residual voltage could be problematic in some recording situations because it increases with larger artifact voltages and with smaller recording sites.

Table III. Measured circuit parameters

Parameter	Value
Settling time to 10-mV pulse[a]	63 μs (max.)
Settling time to 1.5-V pulse[a]	78 μs (max.)
Amplifier gain	101.2 (±0.3) V/V
Input referred noise (100 Hz – 3 kHz)	3.6 (±0.1) μV_{rms}
High-pass cutoff (-3 dB)	3.7 (±0.1) Hz
Low-pass cutoff (-3 dB)	19.0 (±1.0) kHz

Measurements reported here include data from all 32 channels. Unless otherwise noted, values are reported as mean (±SD). Stimuli were generated by a function generator and attenuated (101 V/V) by a 100-kΩ to 1-kΩ resistive divider. Amplifier inputs were connected together and to the output of the resistive divider. Noise measurements were made with amplifier inputs grounded.

[a]Stimulus is a rectangular biphasic pulse with 40 μs per phase (negative phase first) and a 20-μs interphase gap. Settling time is measured from the end of the pulse until the amplifier settles within 20 μV (RTI) of the pre-stimulus baseline voltage.

The input referred noise (100 Hz to 3 kHz) was an average of 3.6 μV_{rms}, well below the typical noise levels of our auditory midbrain recordings (7 μV_{rms} – 15 μV_{rms}). The high-pass cutoff of the system was measured at 3.7 Hz, which is about twice the designed value of 1.9 Hz; the root

of this discrepancy is a topic of ongoing investigation. However, even this measured high-pass cutoff is low enough to result in very small residual voltages (simulated residual of -0.5 µV for the pulse shown in Fig. 4). The average low-pass cutoff of 19 kHz is close to the designed value of 19.7 kHz. Its variation from a minimum of 17 kHz to a maximum of 21 kHz may reflect variations in op-amp GBW and parasitic board capacitance. This variation results in only a small variation in noise level (3.42 μV_{rms} to 3.68 μV_{rms} RTI).

In-vivo evaluation

We evaluated the recording system hardware and software artifact blanking technique under three *in-vivo* conditions. The first condition was to record central auditory neuronal responses to acoustic tones in normal hearing animals. These recordings were stimulus-artifact free, and so they allowed us to compare the number of events detected before and after applying the software artifact blanking technique. The second condition was to record responses to unmodulated intracochlear electrical pulse trains. We used this condition to differentiate stimulus artifacts from neural responses based on two properties: 1) artifacts would be constant throughout the pulse trains, but responses would change due to neural adaptation; 2) artifacts would occur almost immediately following stimulus onset and neural responses would have a delay due to synaptic latencies. The third condition was to record responses to amplitude-modulated pulse trains, which represents a difficult test for many artifact removal techniques (as described in the Introduction). We again used differences in neural and artifact latencies to discriminate between responses and stimulus artifacts.

All procedures were approved by the UCSF Institutional Animal Care and Use Committee. A 32-site silicon probe with linearly spaced iridium contacts (413-μm^2 contact areas, NeuroNexus Technologies, Ann Arbor, MI) was inserted into the central nucleus of the inferior colliculus (auditory midbrain) in anesthetized guinea pigs and cats. Neural responses to acoustic and intracochlear electrical stimulation were subsequently recorded.

Responses to acoustic tones. We recorded single and multi-unit midbrain activity in the guinea pigs and cats using the fast-recovery recording system while calibrated acoustic tones were presented through hollow earbars sealed within the ear canals (Fig. 7). Neuronal events were detected by setting a threshold at 3.5 times the root-mean-squared pre-stimulus voltage. Post-stimulus time histograms (PSTHs) of the threshold crossing events were constructed from 20 repetitions of each stimulus condition. Response PSTHs typically exhibited a peak with a delay (caused by basilar membrane mechanics and neural synapse latencies) of about 10 ms after tone onset (Fig. 7c). This peak was followed by a sustained response that remained relatively constant until approximately 8 ms after tone offset. By applying the software artifact blanking procedure to these artifact-free recorded waveforms, we quantified the changes that the blanking procedure caused in the recorded voltage waveforms and in the detected event rates.
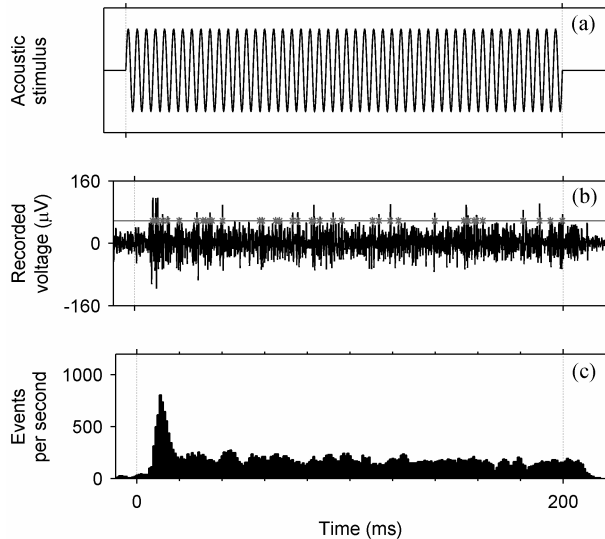
Fig. 7. Recording auditory midbrain responses to an acoustic tone in an anesthetized guinea pig. **(a)** Stimuli were 200-ms tones at 60 dB SPL with cosine on and off ramps. **(b)** Extracellular voltage recordings were made with 32-site silicon probes and the fast-recovery recording system. Multi-unit responses to one presentation of a 24-kHz tone are shown here. The horizontal line indicates threshold (3.5 times the rms value of the pre-stimulus recorded voltage); each threshold crossing is counted as an event (asterisks). **(c)** A post-stimulus time histogram of the threshold crossing events shows an onset response peak 10 ms after the stimulus begins and a smaller, sustained response continuing until 8 ms after the stimulus ends. This delay is due to basilar membrane mechanics and neural latency.

In one cat, we compared the software artifact blanking method to the previously reported sample-and-interpolate method. We implemented software artifact blanking as shown in Fig. 6c and 6d. For sample-and-interpolate, we replaced the blanking step (Fig. 6c) with linear interpolation. We then correlated the recorded voltage waveforms before artifact removal with those same waveforms after artifact removal. Using 200-μs blanking periods at 1000 blanks per second, the linear correlation coefficient was 0.8731 ± 0.0003 (mean $\pm$ SEM) for the software artifact blanking method and 0.8813 ± 0.0003 for the sample-and-interpolate method (nearly identical performance). Because the software artifact blanking technique was more computationally efficient (roughly 2.5 times faster) we opted to use software artifact blanking.

Next we investigated the effect of software artifact blanking on neural event detection. For one guinea pig, post-stimulus time histograms were constructed from acoustic-tone responses without blanking periods, with 1000 blanking periods per second (200-μs each), and with 2000 blanking periods per second. These post-stimulus time histograms were calculated using 20 trials and 6-ms bins, representing typical minimum values for data analysis (when better temporal resolution is required, shorter bins are often averaged over more presentations). Forty time bins, 11 stimulus frequencies (500 Hz to 28 kHz), and 31 recording sites were analyzed for a total sample size of 14 640. For the 1000-blanks-per-second condition versus the without-blanking condition the number of events detected was linearly correlated, with a slope near one (Fig 8a, slope=0.91, r^2=0.95,). This indicates that with 1000 blanks per second, roughly 91% of the events were detected. For the 2000-blanks-per-second condition, approximately 79% of the events were detected (Fig 8b, slope=0.79, r^2=0.92). Further analysis could reveal whether the undetected events following artifact blanking were randomly distributed or if they instead arose from a subset of functionally distinct events.
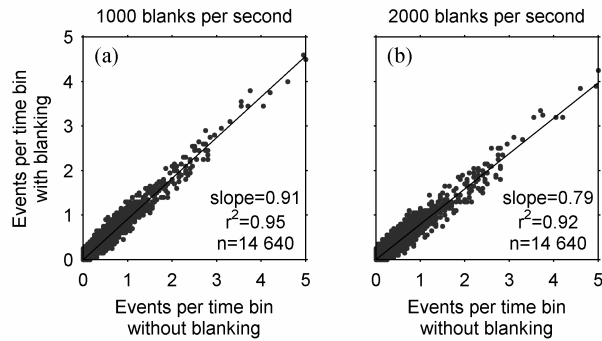
Fig. 8. Effects of the blanking algorithm on event detection. Using acoustic tone stimuli, post-stimulus time histograms were constructed from midbrain recordings with inserted blanking periods (as in Fig. 6) and without blanking periods. If the blanking algorithm had no effect on the bin counts, the points in the above plots would lie along a perfect diagonal with a slope of one. **(a)** For 1000 blanking periods per second the slope of the regression line was close to one (0.91) indicating approximately a 91% detection rate. **(b)** For 2000 blanking periods per second the slope decreased to 0.79. For both (a) and (b) the r^2 values were above 0.9.

Responses to unmodulated electrical pulse trains. To further evaluate amplifier performance and the artifact rejection procedure, we recorded midbrain responses to cochlear stimulation by electrical pulse trains in cats and guinea pigs that had been deafened and implanted with custom-designed auditory prostheses (Rebscher et al., 2007). Biphasic, rectangular pulses (cathodic phase first) were used with 40 μs per phase and 20-μs interphase gaps. The stimuli were delivered in monopolar mode (one intracochlear electrode with an extracochlear return electrode), which is known to produce particularly large stimulus artifacts in extracellular recordings. In our midbrain recordings, monopolar stimulation usually produced electrical stimulus artifacts on the order of a few millivolts, quite large relative to action potential amplitudes of 30 μV to 300 μV.

We recorded responses to 1000-pps pulse trains (Fig. 9a). Before artifact blanking (Fig 9b), recorded waveforms exhibited clear stimulus artifacts that were constant in amplitude throughout the stimulus (except for variations caused by differences in the stimulation and recording clocks). Neuronal activity was difficult to discern in these recorded waveforms, with the exception of some variation in the baseline reflecting evoked local field potentials. The artifacts began and ended coincidently with the stimulus, confirming that these were stimulus pulse artifacts rather than neuronal responses. In contrast, the underlying neuronal responses that were observed following application of the artifact blanking procedure lagged the onset of the stimulus by a short delay (4 ms – 7 ms, Fig. 9c and 9d). (Because electrical stimuli do not rely on basilar membrane mechanics, this delay is shorter than the 10-ms delay seen for responses to acoustic tones, Fig 7). The responses continued until approximately 4 ms after the end of the stimulus. PSTHs derived from these responses showed a pronounced onset peak and a smaller sustained response similar to PSTHs derived from responses to acoustic tones. The delay and variation in response rates to electrical pulses would not be observed if the threshold crossings were due to electrical artifacts.
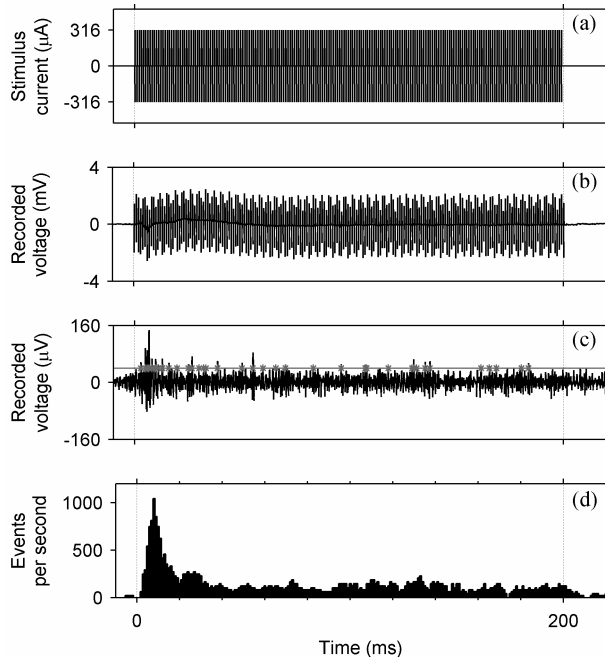
Fig. 9. Recording auditory midbrain responses to intracochlear electrical stimulation in an anesthetized guinea pig. **(a)** Stimulus was a 200-ms monopolar pulse train (316-μA biphasic pulses with 40 μs per phase and 20-μs interphase gaps, 1000 pulses per second). **(b)** Extracellular voltage recordings were made with 32-site silicon probes and the fast-recovery recording system. Shown here is the recorded waveform before artifact blanking. **(c)** Multi-unit responses to the stimulus pulse train after artifact blanking (note smaller voltage scale). **(d)** The post-stimulus time histogram (12 trials) shows an onset response peak and a smaller, sustained response similar to the acoustic post-stimulus time histogram (Fig. 7). However, the electrical response latencies are shorter (only 4 ms – 7 ms) due to the lack of a basilar membrane delay.

To evaluate the possibility of small residual artifact voltages contaminating the analog waveforms following artifact rejection, we compared post-stimulus time histograms of responses both with and without artifact blanking. We focused especially on the time bins when the stimulus turned on (-1 ms to 1 ms in Fig. 9d) and when the stimulus turned off (199 ms to 201 ms). If stimulus artifacts were present there should have been a large, sudden increase in the detected event rate when the stimulus turned on and a large, sudden decrease when the stimulus turned off. However, events rates due only to neuronal responses should not increase or decrease immediately because their synaptic latencies are greater than 2 ms. For one cat, we analyzed responses from 32 recording sites evoked by stimulation using each of five intracochlear stimulating electrodes at 4 dB – 6 dB above minimum response threshold (total of 480 post-stimulus time histograms, 20 trials each).

Without artifact blanking (Fig. 10a) the mean event rate rose significantly when the stimulus turned on (from 14 events per second to 1088 events per second, p<0.001, paired sign test) and fell significantly when the stimulus turned off (from 1166 events per second to 90 events per second, p<0.001). Note that the number of additional events during the stimulus was close to the pulse rate of 1000 pps. In contrast, with artifact blanking (Fig. 10b) the event rate did not change significantly when the stimulus turned on (p>0.05). (There were only a small number of spontaneous events, 12 per second, both before and after the stimulus began.) This shows that the residual artifact voltages after artifact blanking were below threshold (mean threshold across recording sites was 34 μV). The event rate *did* decrease significantly when the stimulus turned off (from 74 events per second to 60 events per second, p<0.001). One factor contributing to this small decrease could have been the summation of residual artifact voltages with otherwise sub-threshold sustained responses. To summarize the artifact-blanking results, when neural responses were not present, stimulus artifacts alone were not large enough to produce threshold crossings. When neural responses were present, the response was overestimated by about 14 events per second. In other recording situations, the occurrence and/or size of this overestimation is likely to

16

be dependent on factors such as artifact size, recording electrode characteristics, and stimulus pulse rate.
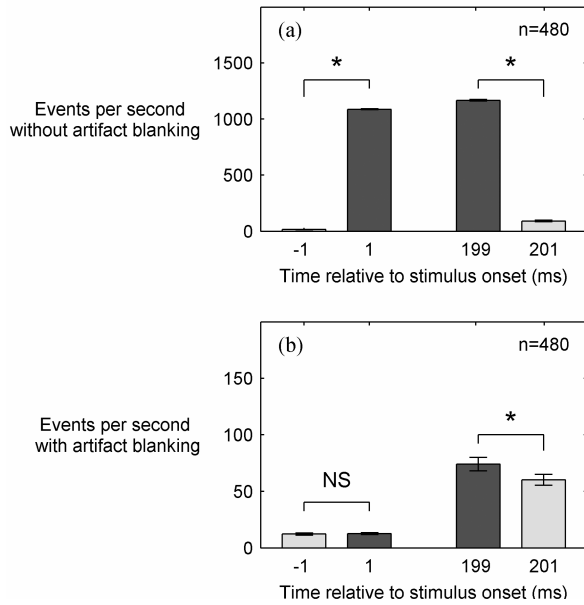
Fig. 10. Statistical test of artifact elimination in an anesthetized cat. Post-stimulus time histograms of responses to intracochlear electrical stimulation were constructed for two conditions: without artifact blanking and with artifact blanking. Stimulus duration (200-ms), rate (1000 pps) and timing were the same as shown in Fig. 9. **(a)** Without artifact blanking, there is a significant increase in the detected event rate when the stimulus turns on (-1 ms to 1 ms), and a significant decrease when the stimulus turns off (199 ms to 201 ms, [*]p<0.001, paired sign test, error bars are SEM). The differences are approximately 1000 events per second, which correspond to one additional event per stimulus artifact. **(b)** With artifact blanking there is no significant increase in the event rate from -1 ms to 1 ms (NS: p>0.05). There is a significant decrease in the event rate from 199 ms to 201 ms, but this decrease is small (14 events per second) relative to the decrease without artifact blanking. Note the 10 times smaller y-scale in (b) relative to (a).

We did not analyze the effect of the artifact blanking technique on sorting/classification of single-unit waveforms (spikes). Distortion introduced by artifact blanking would probably be largest when a blanking period fell directly on a sharp peak or valley in a spike. Results of distortion could include misclassification of a spike, changes in spike timing, or, in the worst case, missed detection of a spike. Use of shorter blanking durations when possible (e.g. when stimulus duration is short and / or artifact size is small) would decrease distortion and increase the detection rate. Fig. 11 shows three examples of spike waveforms before and after artifact blanking, including one case where the spike and stimulus artifact were coincident.

Before artifact blanking   After artifact blanking

(a)   (b)

(c)   (d)

(e)   (f)
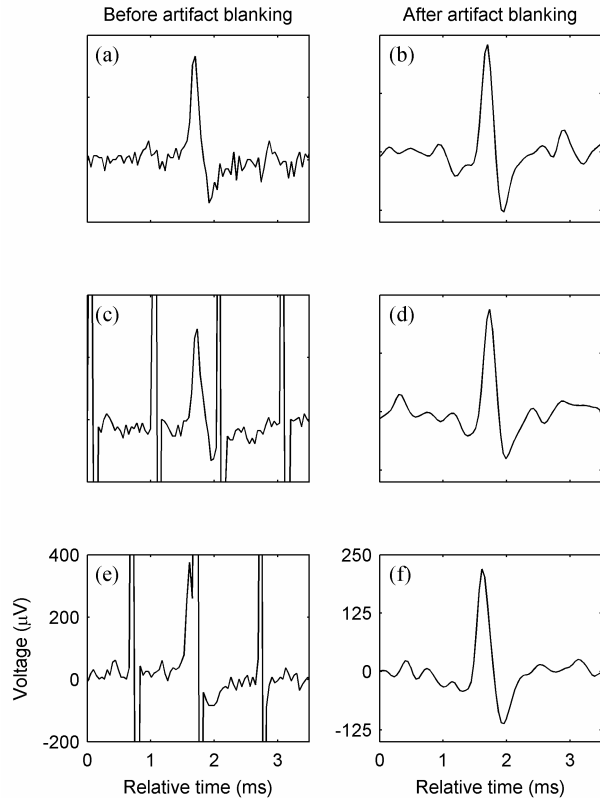
Fig. 11. Single-unit responses to electrical stimulation before and after artifact blanking. Stimulus was a monopolar intracochlear pulse train as shown in Fig. 9a (224-μA pulse amplitude). All recordings are from the same recording site, taken within a 20-second time span in the auditory midbrain of a guinea pig. The left column shows the recordings before artifact blanking and band-pass filtering. The right column shows the same recordings after artifact blanking and band-pass filtering. **(a-b)** A spontaneous action potential before the beginning of the stimulus pulse train. **(c-d)** An action potential falling between two stimulus artifacts. **(e-f)** An action potential coincident with a stimulus artifact.

Responses to sinusoidally amplitude-modulated electrical pulse trains. To further test the artifact-rejection capability of the fast-recovery recording system, we recorded midbrain responses to intracochlear, sinusoidally amplitude-modulated pulse trains (200 μA, 1000 pps, 50-Hz modulation frequency, 100% modulation depth) in an anesthetized guinea pig. The amplitude-modulated stimulus produced electrical artifacts at the input of each of the 32 amplifiers with peak amplitudes of about 2 mV (one recording channel shown in Fig 12a). The responses after artifact blanking (Fig 12b) and peaks in the post-stimulus time histogram (Fig. 12c) were delayed relative to artifact peaks by 4 ms – 6 ms. This delay represents neural synaptic latencies, and would not be present if the waveforms in Fig. 12b were electrical artifacts.
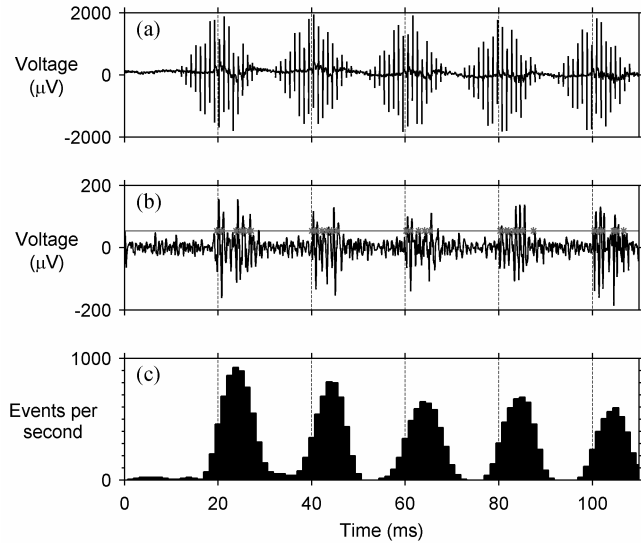
Fig. 12. Responses to a sinusoidally amplitude-modulated pulse train. **(a)** Recorded waveform includes stimulus artifacts and neuronal responses evoked by an intracochlear pulse train (1000-pps carrier, 50-Hz modulation). **(b)** Neuronal response waveform after artifact removal (note smaller voltage scale). **(c)** Post-stimulus time histogram peaks are delayed by 4 ms – 6 ms relative to the artifact peaks, reflecting synaptic delays from the cochlea to the inferior colliculus. This latency confirms that the waveform in (b) is biological in origin, and not electrical artifact.

We also recorded auditory midbrain responses to temporally interleaved, amplitude-modulated stimulus pulses presented using two intracochlear stimulus electrodes (1000 pps from each electrode for an aggregate rate of 2000 pps). Because the auditory midbrain is cochleatopically organized, we would expect that stimulation at different intracochlear locations would produce responses at different depths in the midbrain. Before artifact blanking, stimulus artifacts dominated the measured response and showed no cochleatopic organization. After artifact blanking, however, the inferior colliculus responses showed the expected cochleatopic organization. When stimulated alone, the electrode closer to the apex of the cochlea evoked midbrain responses at locations tuned to acoustic frequencies of approximately 10 kHz (Fig. 13a). These responses were phase locked to the stimulus modulation frequency of 125 Hz. When the electrode farther from the apex was stimulated alone, responses were centered at a deeper location in the midbrain tuned to approximately 17 kHz (Fig 13b). These responses were also phase locked to the modulation frequency of the stimulus (50 Hz in this case). Stimulating both intracochlear electrodes together in an interleaved fashion (Fig. 13c) produced responses at both locations activated by the individual stimulus electrodes. Analysis of these responses showed that there was relatively little interaction between these two stimulus electrodes (i.e. the responses in Fig. 13c are approximately equal to the sum of the responses in Fig. 13a and Fig. 13b). However, for different stimulus electrode pairs (not shown), as inter-electrode distance decreased, interaction increased.

19
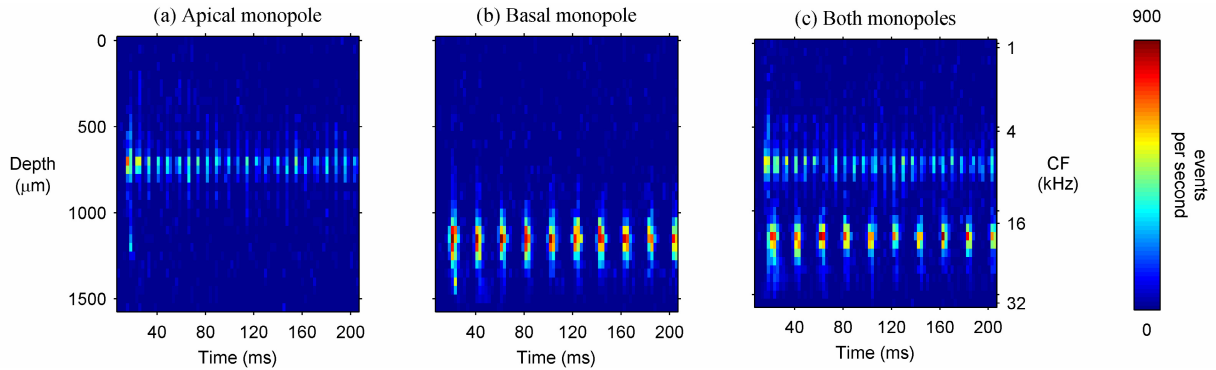
Fig. 13. Post-stimulus time histograms of midbrain responses to intracochlear electrical stimulation. Each row of pixels in the images above represents a post-stimulus time histogram (after artifact blanking) at one recording site with intensity of response indicated by color. The 32 recording sites are spaced linearly at 50-μm intervals—relative midbrain depth is indicated on the left y-axis. The characteristic frequency (CF, acoustic frequency that elicited a lowest threshold response at a given recording site) is shown on the right y-axis (log scale). Stimuli were monopolar pulse trains at 1000 pps with sinusoidal amplitude modulation (biphasic pulses, 40 μs per phase and 20-μs interphase gaps, 6-dB above response threshold). **(a)** Responses to an apical stimulus electrode are centered at a relative midbrain depth of 700 μm (10.4-kHz CF) and are phase locked to the 125-Hz modulation frequency of the stimulus. **(b)** A basal stimulus electrode (with 50-Hz amplitude modulation) elicits responses deeper in the auditory midbrain (1100 μm, 17.4-kHz CF). The responses are also phase locked to the stimulus modulation frequency. **(c)** Both electrodes are stimulated at 1000 pps in an interleaved fashion for an aggregate pulse rate of 2000 pps. Data from this panel can be used to evaluate stimulus electrode interaction.

CONCLUSION

A 32-channel recording system with fast-recovery from electrical stimulus artifacts was designed, implemented and tested *in-vivo*. Simplicity of the hardware design makes the system easy to implement, low-cost, and suitable for miniaturization and incorporation in a fully-implantable recording device. The system was able to record neuronal responses to intracochlear electrical stimulation at clinically relevant rates of at least 2000 pulses per second, making it a useful tool for the study of channel interaction in cochlear implants and other neural prostheses.

Chapter 2: Monopolar Intracochlear Pulse Trains
Selectively Activate the Inferior Colliculus

ABSTRACT

Previous cochlear implant studies using isolated electrical stimulus pulses in animal models have reported that intracochlear monopolar stimulus configurations elicit broad extents of neuronal activation within the central auditory system—much broader than the activation patterns produced by bipolar electrode pairs or acoustic tones. However, psychophysical and speech reception studies that use sustained pulse trains do not show clear performance differences for monopolar versus bipolar configurations. To test whether monopolar intracochlear stimulation can produce selective activation of the inferior colliculus, we determined activation widths along the tonotopic axis of the inferior colliculus for acoustic tones and 1000-pulse/s electrical pulse trains in guinea pigs and cats. Electrical pulse trains were presented using an array of 6 – 12 stimulating electrodes distributed longitudinally on a space-filling silicone carrier positioned in the scala tympani of the cochlea. We found that for monopolar, bipolar, and acoustic stimuli, activation widths were significantly narrower for sustained responses than for the transient response to the stimulus onset. Furthermore, monopolar and bipolar stimuli elicited similar activation widths when compared at stimulus levels that produced similar peak spike rates. Surprisingly, we found that monopolar and bipolar stimuli produced narrower sustained activation than 60 dB SPL acoustic tones when compared at stimulus levels that produced similar peak spike rates. Therefore, we conclude that intracochlear electrical stimulation using monopolar pulse trains can produce activation patterns that are at least as selective as bipolar or acoustic stimulation, if stimulus intensities are appropriately matched.

INTRODUCTION

Monopolar electrical stimulation (one intracochlear stimulating contact and an extracochlear return contact) delivered by a cochlear implant has been reported to elicit neuronal activation that is broadly distributed across the tonotopic frequency organization of the auditory system. In comparison, acoustic stimulation and bipolar electrical stimulation (one intracochlear stimulating contact and one intracochlear return contact) have been shown to produce relatively narrow, selective distributions of neuronal activity. This has been demonstrated in animal studies in which neuronal responses were recorded in the auditory nerve (Kral et al., 1998), inferior colliculus (IC) (Merzenich et al., 1977; Middlebrooks et al., 2007; Snyder et al., 2008), and auditory cortex (Bierer et al., 2004). However, studies of human cochlear implant users have shown that they perform at least as well with monopolar stimulation as with bipolar stimulation on speech reception tasks (Kileny et al., 1998; Pfingst et al., 2001; Zwolan et al., 1996). Furthermore, cochlear implant users can pitch-rank monopolar electrodes (Boex et al., 2006), and some identify monopolar percepts as having a tonal quality (Tong et al., 1980); both of these results seem inconsistent with broad, non-selective neuronal activation.

These discrepancies between studies of speech reception in humans and the extent of neuronal activation in animals could be caused by differences in the applied stimuli. Specifically, one potentially important difference is that studies of speech reception in humans have used electrical

pulse trains delivered at medium to high pulse rates (250 pulses/s, 1000 pulses/s or higher) (Friesen et al., 2005; Kileny et al., 1998; Pfingst et al., 2001; Zwolan et al., 1996), whereas studies of extent of neuronal activation in animals have typically used single, isolated electrical pulses (due to difficulties with overlapping responses and stimulus artifacts at higher pulse rates). It is known that the extent of IC responses to sustained acoustic tones narrows after the initial, broader "onset" response (Harris et al., 1997). We hypothesized that, in a similar fashion, electrical pulse trains delivered to the auditory nerve by a cochlear implant would elicit broad onset responses followed by narrower sustained responses.

Another difference in stimuli is that human cochlear implant studies have used comfortable or loudness-balanced levels (Morris et al., 2000; Shannon, 1983b), whereas animal studies of neuronal activation have typically compared responses at equal decibel levels above threshold (Snyder et al., 2008). It has been shown that monopolar stimulation elicits selective neural activation at lower current levels and over a narrower dynamic range than bipolar stimulation (Ryan et al., 1990; Snyder et al., 2008). Furthermore, loudness grows faster in response to monopolar stimulation (Chatterjee, 1999), suggesting that comparing responses to monopolar and bipolar stimuli at equal decibel levels above threshold may not be equivalent to comparing them at equal loudness. Instead, because it has been proposed that firing rate (spike rate) may be a neural correlate of loudness in central auditory neurons (Cai et al., 2009; Joris, 2009), we hypothesized that comparing responses to monopolar and bipolar stimuli that elicit similar spike rates would show that they elicit similarly selective activation widths—results that would better correspond to the human psychophysical findings.

By recording neuronal responses to acoustic tones and 1000-pulse/s electrical pulse trains in guinea pigs and cats, the present study sought to determine whether sustained monopolar intracochlear stimulation can produce selective activation of the inferior colliculus. First, we asked whether the extent of inferior colliculus activation produced by 1000-pulse/s monopolar electrical stimuli is narrower for the sustained response than for the onset response. Second, for levels that produce similar peak spike rates, do sustained periods of monopolar, bipolar, and acoustic stimulation produce similar extents of inferior colliculus activation?

METHODS

To determine whether sustained monopolar intracochlear stimulation can produce selective activation of the inferior colliculus, we conducted a series of acute neurophysiologic experiments in adult guinea pigs and cats. In these experiments, we recorded neuronal activity in the central nucleus of the inferior colliculus in response to acoustic and intracochlear electrical stimuli. All procedures were approved by the UCSF Institutional Animal Care and Use Committee.

Anesthesia and surgery: acute neurophysiology experiments

Guinea pigs. Procedures for positioning a multi-site recording probe in the inferior colliculus and recording responses to acoustic and electrical stimuli in guinea pigs were similar to those described in a previous study (Snyder et al., 2004). In brief, three guinea pigs were anesthetized with a mixture of ketamine and xylazine while the heart rate, respiratory rate, and core body temperature were monitored. An intra-tracheal breathing tube was placed via a tracheotomy to ensure a clear airway. The skin over the calvarium was incised and the head was held stationary

by a bar affixed to the calvarium with bone screws and dental acrylic. The right ear was deafened by puncturing the tympanic membrane and mechanical dislocation of the ossicular chain. After reflecting the right temporalis muscle, a portion of the skull about 1 cm in diameter was thinned with a dental burr and elevated. The overlying cortex was then aspirated to expose the right inferior colliculus.

Each guinea pig was transferred to a sound-proof recording booth, and a silicon recording probe (NeuroNexus Technologies, Ann Arbor, MI) with 32 linearly spaced recording sites was inserted along the tonotopic axis of the IC central nucleus at an angle of approximately 40° from vertical in the coronal plane using a micromanipulator. Acoustic stimuli were delivered to the left ear canal near the tympanic membrane via a sealed and calibrated interface. Responses to acoustic tones from 500 Hz to 32 kHz were recorded, and the depth of the recording probe was increased until all but the deepest recording sites showed responses to the acoustic stimuli. Multiple IC penetrations were sometimes necessary to find a location with robust sustained responses. Once such a location was found, the recording probe was fixed to the skull with dental acrylic and sticky wax, and responses to acoustic tones were recorded. After rotating the animal to allow access to the left ear, the left round window was exposed and the guinea pig was deafened by intracochlear infusion of 2-3 drops of 10% neomycin sulfate in saline. A space-filling intracochlear stimulating electrode with a linear array of 10 – 12 hemi-spherical platinum-iridium (90:10) contacts with diameters of about 150 μm^2 (Fig. 1) (Rebscher et al., 2007) was inserted into the scala tympani through the round window, and responses to electrical stimuli were recorded.
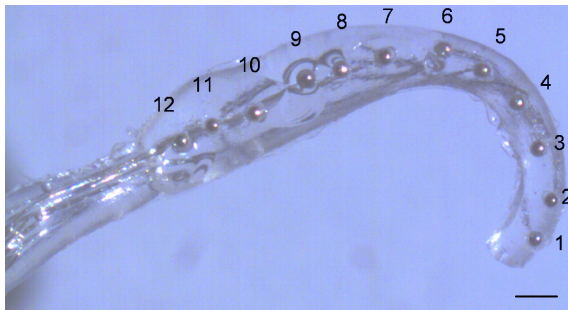
Fig. 1. Photograph of a guinea pig intracochlear stimulating electrode. Monopolar (MP) channel numbering convention is MP 1 to MP 12 from apical to basal. Bipolar (BP) numbering convention is BP 2,1 where 2 is the stimulating contact and 1 is the return contact. Contact spacing is 0.5 mm for guinea pigs and 1 mm for cats (cat array has six to eight contacts). Scale bar is 0.5 mm.

Cats. Surgical procedures for the IC exposure, deafening, implantation and adjustment of the depth of the recording probe in the IC were the same as described for guinea pigs with the following exceptions. Cats were pre-anesthetized with inhaled isoflurane, and a surgical plane of anesthesia was induced with intravenous sodium pentobarbital in LRA delivered by an infusion pump. Cat intracochlear stimulating electrodes had a linear array of six to eight hemi-spherical contacts (diameters 250 – 350 μm^2) and were specifically designed for the cat cochlea (Rebscher et al., 2007). That is, the silicone rubber carriers were molded to be relatively space-filling within the basal turn of the cat scala tympani, and stimulating contacts were positioned at 1-mm intervals (roughly one critical-band distance in the cat cochlea). Of the eight cats studied, two had normal hearing prior to the experiment (referred to hereafter as normal cats), and six had been chronically deafened and implanted with cochlear implant electrodes (with varying electrical stimulation regimens and drug treatments, see Appendix III). In the chronically deafened cats, the depth of the IC recording probe was determined by presenting electrical pulses

on the most basal channel of the stimulating electrode and increasing the depth of the recording probe until there were responses on all but the deepest and most superficial recording sites. This method of placing the recording probe made it likely that the recording sites were primarily or exclusively in the central nucleus of the IC.

Stimulus generation

Calibration methods and apparatus for generating acoustic and electrical stimuli were similar to those described previously (Snyder et al., 2004). In brief, stimuli were generated under the control of an Intel-based personal computer and synthesized digitally by a dedicated digital signal processor (Multi I/O Processor RX8, Tucker Davis Technologies, Alachua, FL) with 100 sample/s time resolution and 16-bit precision. Acoustic stimuli were programmably attenuated (PA5, Tucker Davis Technologies) amplified by an audio amplifier (Servo 170, Samsung Electronics, Ridgefield Park, NJ) and delivered to the animals via a speaker and earbar through a sealed interface. Calibration of the acoustic intensity at each frequency was performed using a probe microphone (type 4182, B&K, Buffalo, NY) with the probe positioned in the earbar. Electrical stimuli were delivered via an 8-channel optically isolated voltage to current converter under the control of the RX8 digital signal processor. The specific acoustic and electrical stimuli used in the present study are described below.

Acoustic stimuli. Tones from 500 Hz to 32 kHz with 50 ms duration and 2-3 ms cosine on and off ramps (levels 0 dB SPL to 70 dB SPL, frequencies and levels in randomized order) were presented in the guinea pigs and normal cats to determine the characteristic frequency (CF) of each IC recording site. (Characteristic frequency for a given recording site is that frequency which elicits a response at the lowest stimulus level). Next, tones from 5 kHz to at least 20 kHz (1/4 octave spacing) were presented with a duration of 200 ms. In guinea pigs, these tones were presented at 60 dB SPL; in cats, they were presented at 40 dB SPL, 60 dB SPL, and 80 dB SPL.

Electrical stimuli. Electrical pulse trains were presented in either a monopolar or bipolar stimulus configuration. Numbering convention for monopolar and bipolar channels are described in Figure 1. Pulse trains were delivered at 1000 pulses/s with 200 ms duration, and each pulse was charge-balanced biphasic with the cathodic phase first (40 μs per phase, and 20-μs interphase gaps). Stimulus levels were from -2 dB SL (sensation level, or level relative to threshold) to at least 6 dB SL with 2-dB steps in guinea pigs and 1-dB steps in cats (in one cat 2-dB steps were used). Channels that could not deliver stimuli at 6 dB SL without causing stimulation of the facial nerve were excluded.

Multi-site recording

Probes used for IC recording had 32 linearly spaced recording sites with inter-site spacings of 50 μm for guinea pigs and 100 μm for cats (NeuroNexus Technologies, Ann Arbor, MI). Recording site areas were 413 μm^2 or 177 μm^2. The inter-site spacings were chosen to place at least one recording site in each IC frequency band lamina (Schreiner et al., 1997) while spanning the relevant portion of the IC frequency axis. Neuronal signals were acquired with a custom designed data acquisition system and stimulus artifacts were removed offline in software (see Chapter 1; responses to acoustic and electrical stimuli were processed identically to facilitate comparison between them). On most recording sites, spikes from several undiscriminated neurons (multi-unit spikes) were detected by setting a voltage threshold at 3.5 times the root-

mean-squared pre-stimulus voltage on each recording site. When the recorded voltage crossed this threshold, a spike time was registered. On some recording sites spikes from one or a few neurons could be isolated based on their large spike amplitudes by empirically selecting a higher detection threshold.

Data Analysis

To visualize both the spatial distribution of neuronal activity across the tonotopic axis of the IC and changes in this activity over the duration of the stimulus, temporal response images were constructed for each stimulus condition (Fig. 2). First, post-stimulus time histograms were constructed for responses at each recording site. Next, for each recording site, the mean spontaneous spike rate was subtracted from the post stimulus time histogram bins (to emphasize driven activity). Then, for damaged recording sites (open or short circuits on the recording probe, two out of 32 sites on average) post stimulus time histograms were interpolated from the recording sites adjacent to the non-functioning sites. Finally, the post stimulus time histograms for the 32 recording sites were arranged in depth order to form a temporal response image. To remove non-spike, stimulus-evoked activity from the recorded waveforms, we used a template subtraction technique (Fig. 3) that has been used in previous studies of IC responses to cochlear implant stimulation in cats (J.C. Middlebrooks, personal communication, 2010). A template was formed by averaging the responses to all the trials for a given stimulus condition, and this template was subtracted from each single trial waveform.
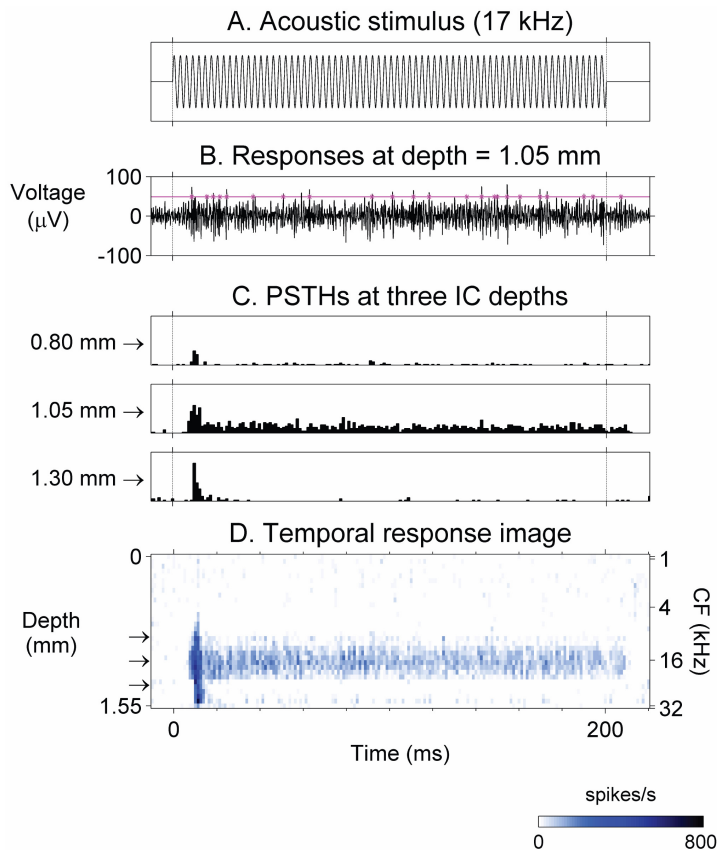
Fig. 2. Construction of temporal response images. **A.** Stimulus was a 60 dB SPL pure tone at 17 kHz; dotted vertical lines indicate stimulus on and off times. **B.** Multi-unit activity elicited by stimulus in (A) recorded on one of 32 linearly spaced recording sites positioned along the tonotopic axis (depth) of the IC. Horizontal line indicates spike detection threshold and asterisks indicate threshold crossings. **C.** PSTHs were computed from spike times at each recording site depth (three examples are shown here). Depths at the left of each panel are relative to the most superficial recording site. **D.** The 32 PSTHs were assembled in depth order to form a temporal response image. Each row in the image shows a PSTH at a given depth, with response strength indicated by color. Arrows indicate depths of the PSTHs shown in (C). CF (right axis) is the frequency that elicits a response at the lowest stimulus level for a given IC recording depth. (Abbreviations: IC, inferior colliculus; PSTH, post stimulus time histogram; CF, characteristic frequency).
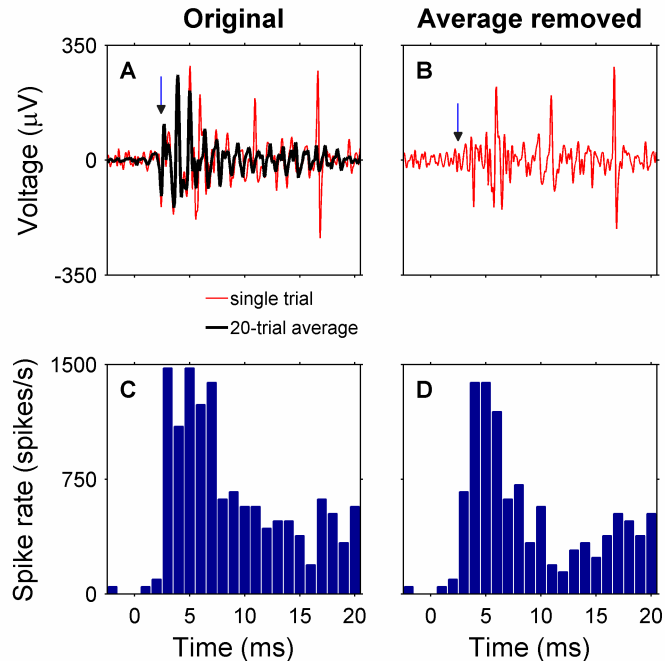
Fig. 3. Template subtraction procedure. For each stimulus condition, a template of the across-trial average was subtracted from each single-trial waveform. **A.** Initial response at one IC recording site to a 200-ms intracochlear pulse train in a cat (monopolar channel 4, 350 µA, 2 dB SL). At 3 ms, there is a small peak (indicated by the vertical arrow) that is very consistent from trial to trial. It has shorter than 4-ms latency, very little trial-to-trial jitter, and variable amplitude with stimulus level (not shown), all characteristics that make it unlikely to be an inferior colliculus spike. **B.** After subtracting the average template from the single-trial waveform, the peak at 3-ms (arrow) has been eliminated. **C.** A PSTH (20 trials) of the original responses shows a prominent peak at 3 ms. **D.** After subtracting the average template, the PSTH peak at 3-ms has been attenuated.

In order to quantitatively characterize IC responses, peak spike rates and activation widths were computed for an onset time window and a sustained time window for each stimulus condition. Onset time windows extended from 7 – 17 ms after stimulus onset for acoustic stimuli and 4 – 14 ms for electrical stimuli, whereas sustained time windows extended from 17 – 200 ms for acoustic stimuli and 14 – 200 ms for electrical stimuli. Peak spike rate for each time window was defined as the highest spike rate on any IC recording site (Figs. 4 and 5). To determine activation width, first we defined a spike rate criterion, chosen to be five times the mean spontaneous spike rate (after deafening), averaged across all recording sites. This criterion was chosen to be well above spontaneous activity but also well below peak spike rates for 60 dB SPL acoustic tones. The activation width for each time window then was calculated by counting the number of recording sites with responses exceeding the spike rate criterion and multiplying this count by the inter-site spacing (Fig. 4). Stimulus channels were excluded from the analysis if they elicited threshold-level activation near the boundary of the IC recording array. In these cases activation at higher stimulus levels was likely to extend beyond the recording array, making activation width measurements inaccurate.

26
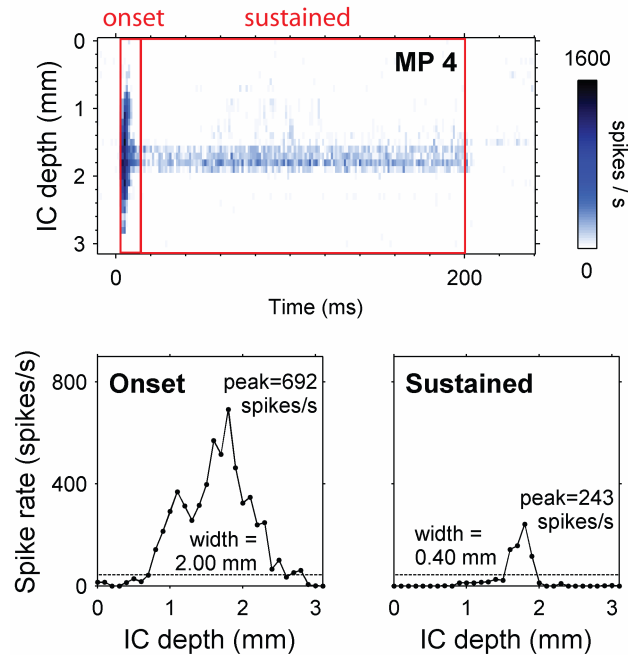
Fig. 4. Activation width and peak spike rate calculations. Top panel: temporal response image for a 200-ms pulse train on monopolar channel 4 in a cat (level = 500 µA, 6 dB SL, stimulus begins at 0 ms). Onset and sustained time windows are 4 – 14 ms and 14 – 200 ms, respectively. Bottom panels: spike rate versus IC depth averaged over the onset time window (left panel) and sustained time window (right panel). Each data point shows the spike rate from one IC recording site. Activation width is calculated by counting the number of recording sites with spike rates above the spike rate criterion (dotted line—five times the mean spontaneous rate averaged across all recording sites) and multiplying this count by the recording site spacing (50 µm in guinea pigs and 100 µm in cats).
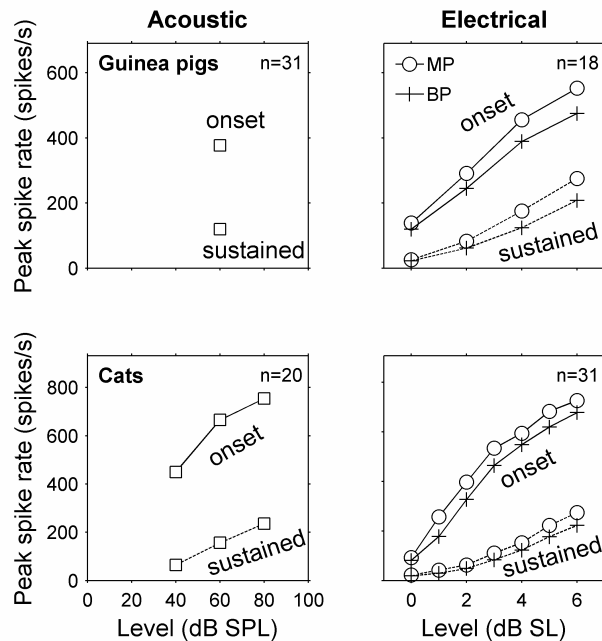
Fig. 5. Peak spike rate increased with stimulus level in guinea pigs and cats. Acoustic data are means from 31 stimulus frequencies in three guinea pigs and 20 stimulus frequencies in two cats. Monopolar and bipolar data are means from 18 stimulus channels in three guinea pigs and 31 stimulus channels in eight cats. Individual rate-level functions that contributed to the means were consistently monotonic as well (not shown).

Activation widths were also expressed in octaves. To calculate the number of octaves per millimeter of IC depth, a regression slope was computed for characteristic frequency versus depth in the IC central nucleus of the guinea pigs and normal hearing cats. The mean slopes of the regression lines were 2.8 octaves per millimeter in guinea pigs and 2 octaves per millimeter in cats. The mean slope for the normal hearing cats was also used as an estimate of the slope for

27

the chronically deafened cats. Activation widths in millimeters were then multiplied by these mean slopes to obtain values in octaves.

Activation widths for electrical and acoustic stimuli were compared at equal peak spike rates by interpolating responses to increasing electrical stimulus levels (Fig. 6). First, for each monopolar stimulus channel an acoustic frequency was chosen that elicited activation at a similar location in the inferior colliculus. Then, the activation width and peak spike rate for this acoustic tone frequency at 60 dB SPL were calculated. Next, the activation width and peak spike rate for the monopolar stimulus channel were calculated at various stimulus levels and plotted with the activation width on the ordinate and the peak spike rate on the abscissa. Finally, the monopolar activation width versus peak spike rate plot was interpolated to find the monopolar activation width that corresponded to the peak spike rate of the acoustic stimulus. This procedure was carried out for onset and sustained responses; it was also used to compare each bipolar stimulus channel with a matching 60-dB acoustic tone. Comparisons between electrical and acoustic stimuli were not made in one of the two normal cats because connecting the electrical current stimulator to this cat raised the background noise levels markedly. This increase in noise did not occur in any of the other cats or in the guinea pigs.
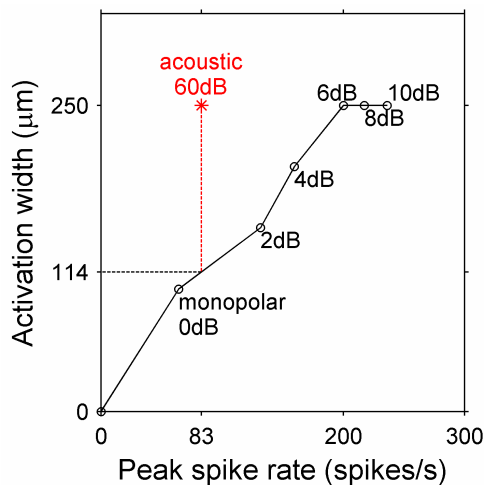
Fig. 6. Comparison of activation widths for equal peak spike rates in one guinea pig. Sustained activation widths versus peak spike rates are plotted for a monopolar stimulus channel (MP 5) at levels from 0 dB SL to 10 dB SL and for an 8.5-kHz acoustic tone at 60 dB SPL. (This acoustic frequency produced peak excitation at roughly the same inferior colliculus depth as MP 5). The acoustic tone had a sustained activation width of 250 μm and a peak spike rate of 83 spikes/s. The monopolar activation width (114 μm) at that same peak spike rate was found by interpolating between the points at 0 dB SL and 2 dB SL. This procedure was also used for comparing acoustic to bipolar stimuli, and for comparing monopolar to bipolar stimuli at equal peak spike rates.

In addition to the electrical-to-acoustic comparisons, monopolar and bipolar activation widths were compared to each another at equal stimulus levels (in dB SL) and also at equal peak spike rates. Monopolar and bipolar channels that had the same stimulating contacts were paired (e.g. MP 2 was paired with BP 2,1). Comparisons at equal spike rates were made as follows. For each bipolar stimulus level and corresponding peak spike rate the monopolar levels were interpolated to find the monopolar activation width at that same peak spike rate (as shown in Fig. 6 for acoustic-to-monopolar comparisons).

Within each stimulus type (acoustic, monopolar, or bipolar), onset responses were also compared to sustained responses by calculating normalized activation areas (Fig. 7). This was done to investigate the possibility that onset and sustained responses had different activation widths but the same overall shape (i.e., that spike rate adapted by a uniform factor across the recording array from onset to sustained response). First, onset and sustained peak spike rates and IC depths were normalized to a maximum value of one. Then, the normalized activation area was calculated for

28

each time window as the area under the normalized spike rate versus IC depth curve. A large area indicated a broad response shape and non-selective activation, whereas a small area indicated a narrow shape and selective activation. If the onset and sustained areas were equal, it would indicate that the sustained response could be a uniformly-scaled version of the onset response.
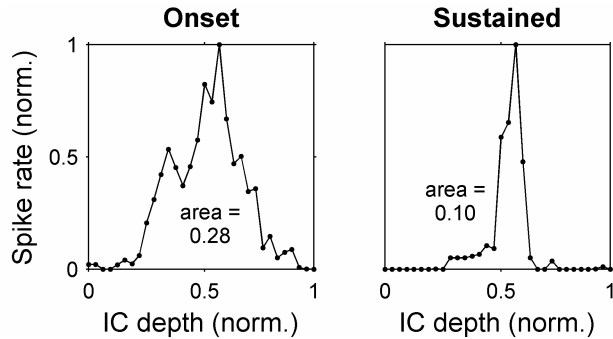
Fig. 7. Normalized activation area calculation. Spike rate versus IC depth are shown for the same responses as in Fig. 4, but with vertical and horizonal axes normalized to one. The area under each curve is taken as an indicator of how narrowly-tuned the responses are, independent of absolute spike rate (smaller area = narrower tuning). (Abbreviations: norm., normalized).

Statistical analyses. Data from guinea pigs and cats were analyzed separately. For acoustic stimuli, onset and sustained activation widths were compared using a two-way repeated measures ANOVA with the SPSS software package ("general linear model" command). Each stimulus frequency in a given animal was considered a subject, and the within-subject effects were time window (onset or sustained) and stimulus level (dB SPL). For electrical stimuli, activation widths were compared using a three-way, repeated measures ANOVA. Each stimulating contact in a given animal was considered a subject, and the within subject effects were time window (onset or sustained), stimulus level (dB SL), and stimulus configuration (monopolar and bipolar). The results of this ANOVA were used to compare onset to sustained activation widths and to compare monopolar to bipolar activation widths at equal dB SL.

These ANOVA tests were then repeated for the dependent variables of peak spike rate, activation width at equal peak spike rates (for monopolar and bipolar stimuli), and normalized activation area. For each ANOVA in cats, an additional between-subject effect of treatment group was tested (see Appendix III for treatment group details). The effect of treatment group was not significant for any of the tests ($p > 0.09$). Therefore, data from all the cats were pooled.

Because the assumption of normality was not always met in the parametric ANOVA tests, significant main effects of time window on activation width and normalized activation area were confirmed separately for each stimulus type (acoustic, monopolar, and bipolar) using a two-way non-parametric ANOVA (Friedman's test in the Matlab software package) with main effects of time window (onset or sustained) and stimulus level (dB SL). The higher p value resulting from the parametric or non-parametric test is given. For the monopolar – bipolar comparisons, means and 95% confidence intervals from the parametric ANOVA are given in the text, but medians and interquartile ranges are shown in the figures to provide a non-parametric description of the data.

Activation widths for peak spike rates matched to 60-dB acoustic tones were compared among acoustic, monopolar, and bipolar stimuli using a one-way non-parametric ANOVA (repeated

measures Friedman's test). Separate tests were performed for the onset and sustained time windows using a Bonferroni correction for two comparisons.

In order to compare activation widths for acoustic, monopolar, and bipolar stimuli at equal peak spike rates, it was necessary that peak spike rates increase monotonically with stimulus level. ANOVA results showed that peak spike rate increased significantly with acoustic and electrical stimulus level, (partial eta squared > 0.71 for a linear contrast, p<0.001, Fig. 5). For monopolar and bipolar stimuli in cats, the linear relationship between peak spike rate and stimulus level was particularly strong (partial eta squared = 0.93, p<0.001). In addition, individual peak spike rate versus stimulus level functions were consistently monotonic (not shown).

RESULTS

Exemplary raw data are illustrated in Figure 8 comparing responses in the IC elicited by stimulation with acoustic tones or 1000-pulse/s electrical pulse trains delivered in monopolar or bipolar configurations. For acoustic pure tones, a systematic shift in IC depth occurs with increasing frequency (from 6 kHz to 20 kHz), reflecting the frequency organization of the IC, with lower frequency CF neurons located more superficially and progressively higher frequency CFs on deeper recording sites of the probe (Fig. 8A). Similarly, the responses to 1000-pulse/s monopolar (Fig. 8B) and bipolar (Fig. 8C) pulse trains showed a systematic shift in IC depth with stimulation of different intracochlear electrodes, with the most apical electrodes eliciting responses superficially in the IC and progressively more basal electrodes producing responses at deeper probe sites. This systematic relationship between IC depth and cochlear place of stimulation was characteristic of recordings in all animals (guinea pigs and cats; normal and deafened subjects); we never saw a reversal in the systematic progression of IC depth with increasing CF or basal-to-apical intracochlear electrode sequence.

The data shown in Figure 8 also demonstrate the finding that the extent of IC activation was usually quite broad for onset responses and much narrower for the subsequent sustained responses. This was true for responses to acoustic stimuli, as well as responses to monopolar and bipolar electrical pulse trains. Quantitative analyses of IC activation widths demonstrated that onset responses were significantly broader than sustained responses for all three types of auditory nerve stimulation in both guinea pigs (Fig. 9) and cats (Fig. 10). In addition, activation widths increased significantly with level (p<0.001), and there was a significant interaction between the effects of time window (onset vs. sustained) and level (p<0.01). This interaction generally manifested itself as an increase in the effect of time window with increasing stimulus level (Figs. 9 and 10). For acoustic tones at 60 dB SL, sustained activation widths were on average 58% (95% confidence interval of 49–66%) narrower than onset activation widths in guinea pigs and 68% (43–95%) narrower in cats. Monopolar and bipolar pulse trains at 6 dB SL elicited sustained activation widths that were 56% (43–69%) and 69% (56–81%) narrower, respectively, than onset activation widths in guinea pigs and 74% (63–85%) and 78% (65–91%) narrower in cats.
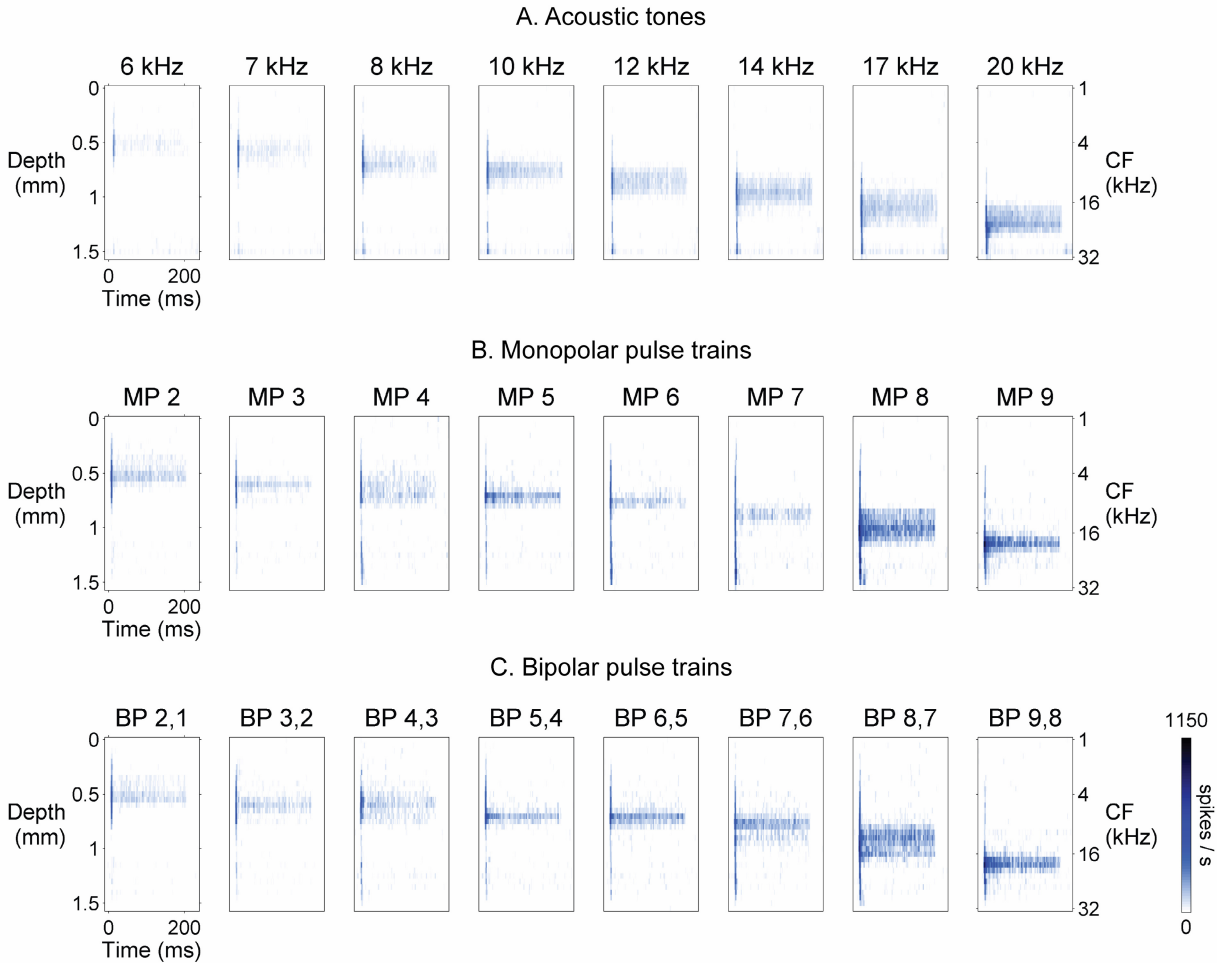
Fig. 8. Examples of temporal response images for acoustic, monopolar, and bipolar stimulation in one guinea pig. Response images to 200-ms long stimuli are constructed as in Fig. 2 (0 ms indicates beginning of stimulus). **A.** Acoustic pure tones at 60 dB SPL elicit responses at progressively deeper locations in the inferior colliculus as stimulus frequency increases, showing the stereotypical tonotopic (frequency) organization of the inferior colliculus. Initial "onset" responses to tones are broadly distributed across the inferior colliculus, whereas sustained responses are more narrowly distributed, indicating that sustained responses are more selectively tuned to stimulus frequency. **B.** Like acoustic responses, responses to monopolar pulse trains (4 dB SL) shift to deeper locations in the inferior colliculus with increasingly basal intracochlear stimulation (stimulus channel shown above each panel). Also, monopolar onset responses are more broadly distributed across the inferior colliculus than subsequent sustained responses, indicating more selective sustained tuning to electrical stimulus channel. Note that the distributions of responses to monopolar pulse trains and acoustic tones appear to be similar. **C.** Responses to bipolar pulse trains (4 dB SL) follow the same trends as seen for monopolar pulse trains.

When spike detection thresholds were raised to limit our analysis to one or several large-spiking units on several recording sites, we found that these units also had broad onset and narrow sustained tuning to monopolar electrical pulse trains at 1000 pulses/s (Fig. 11). In addition, direct comparisons of post stimulus time histograms for the unit responses (Fig. 12) and multi-unit responses (Fig. 13) on the same recording sites revealed similar patterns of neuronal excitation and suppression.

31
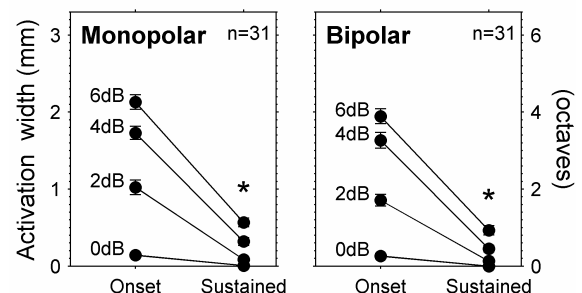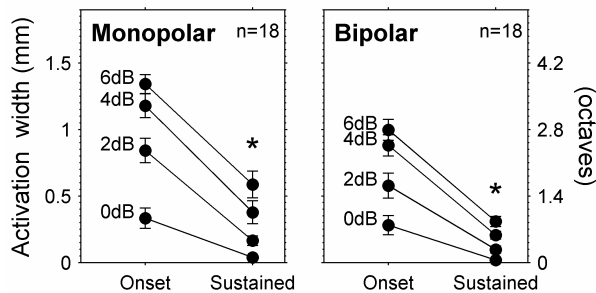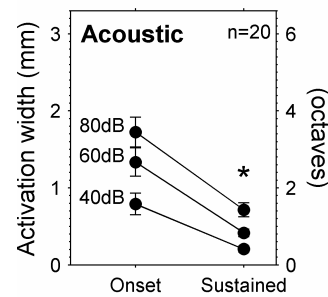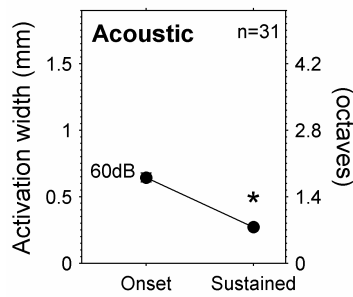
Fig. 9. Sustained activation widths were narrower than onset activation widths in guinea pigs. The left vertical axes show the extent of activation along the tonotopic axis of the inferior colliculus. The right vertical axes show this extent in units of octaves. Means and standard errors of the means are shown for a total of 31 acoustic tone frequencies and 18 monopolar and bipolar electrical stimulus channels in three guinea pigs. Acoustic level is dB SPL and electrical levels are dB SL. *$p<0.001$ for main effect of onset vs. sustained time window.

Fig. 10. Sustained activation widths were narrower than onset activation widths in cats (Figure layout as in Fig. 9). Values shown are for 20 acoustic tone frequencies in two normal cats and 31 monopolar and bipolar electrical stimulus channels in two normal and six chronically deafened cats.

We found that *for stimuli delivered at equal dB levels* monopolar stimuli produced broader (multi-unit) activation widths than bipolar stimuli in both cats and guinea pigs ($p<0.05$), whereas *for stimuli eliciting equivalent spike rates* monopolar and bipolar stimuli produced nearly identical onset and sustained activation widths in cats and similar sustained activation widths in guinea pigs. For equal peak spike rates in cats, monopolar and bipolar activation widths were not significantly different ($p>0.33$, Fig. 14). At 6 dB SL the differences between monopolar and bipolar activation widths were -2 % (-9–5%) for the onset time window and 4% (-13–21%) for the sustained time window. (At 6 dB SL the mean monopolar sustained activation width was 440 μm (0.89 octaves) so 4% corresponds to a difference of only 18 μm (0.035 octaves)). For equal peak spike rates in guinea pigs, the monopolar configuration produced significantly broader activation than the bipolar configuration ($p<0.001$, Fig. 15). At 6 dB SL, mean monopolar activation was 18% (6–29%) broader than bipolar activation for the onset time window and 30% (1.3–57%) broader for the sustained time window. However, median monopolar and bipolar sustained activation widths were very similar (Fig. 15 F and H).

32
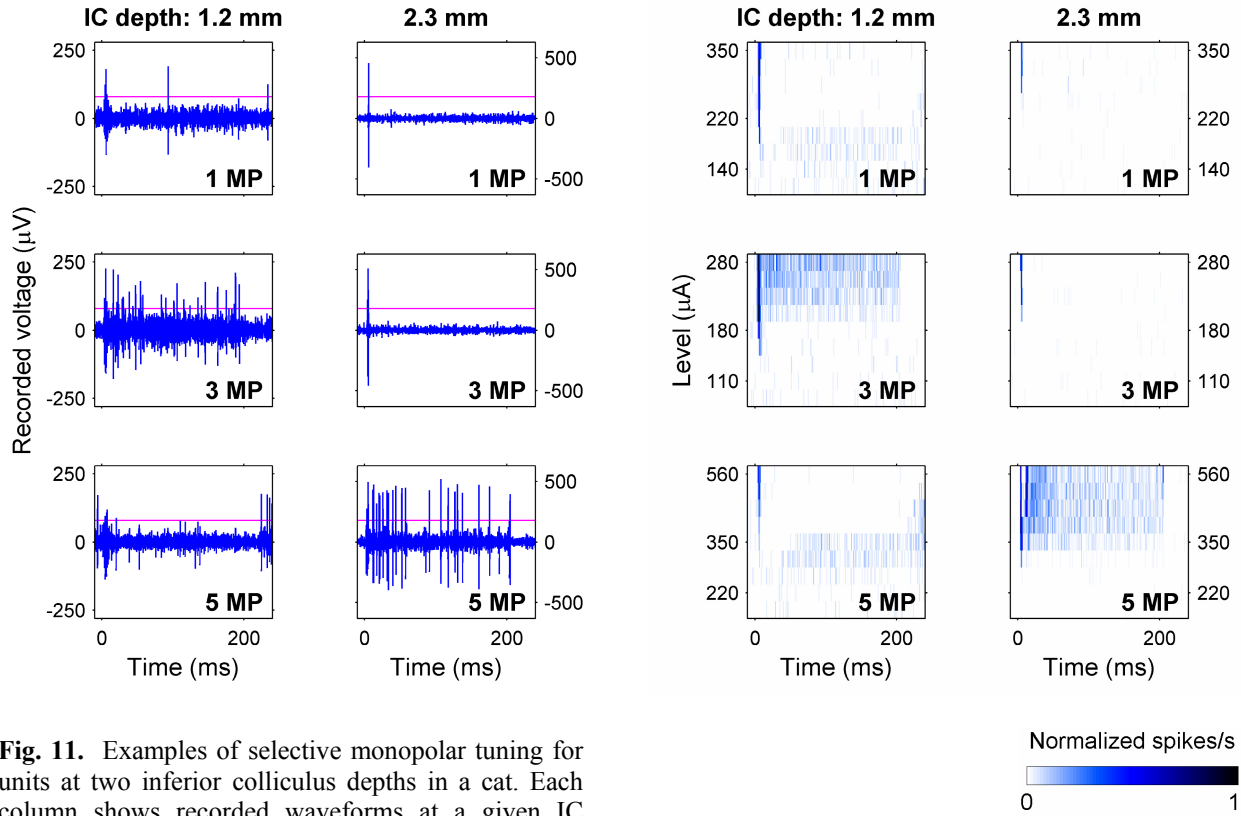
Fig. 11. Examples of selective monopolar tuning for units at two inferior colliculus depths in a cat. Each column shows recorded waveforms at a given IC depth in response to three stimulating channels (channel number inset bottom right). A threshold (horizontal line) was empirically chosen to detect only one to several large-spiking units. Recordings from the 1.2-mm deep recording site (left panels) show sustained responses to channel 3 MP but not to 1 MP or 5 MP. In contrast, the recording site at 2.3 mm (right panels), shows sustained responses to 5 MP but not to 1 MP or 3 MP. Both recording sites show onset responses to all three stimulating channels. Current levels were as follows: 1 MP – 280 μA, 3 MP – 250 μA, and 5 MP – 450 μA. Pulse trains began at 0 ms and ended at 200 ms.

Fig. 12. Post stimulus time histograms for the unit responses from Fig. 11 at various stimulus levels. In each image, the rows represent PSTHs at different stimulus levels with response strengths indicated by color. For the 1.2-mm deep recording site, at higher levels 3 MP produced sustained responses whereas 1 MP and 5 MP inhibited spontaneous activity (after a brief onset response). In contrast, for the 2.3-mm site 5 MP produced sustained responses, but 1 MP and 3 MP produced only onset responses.

33
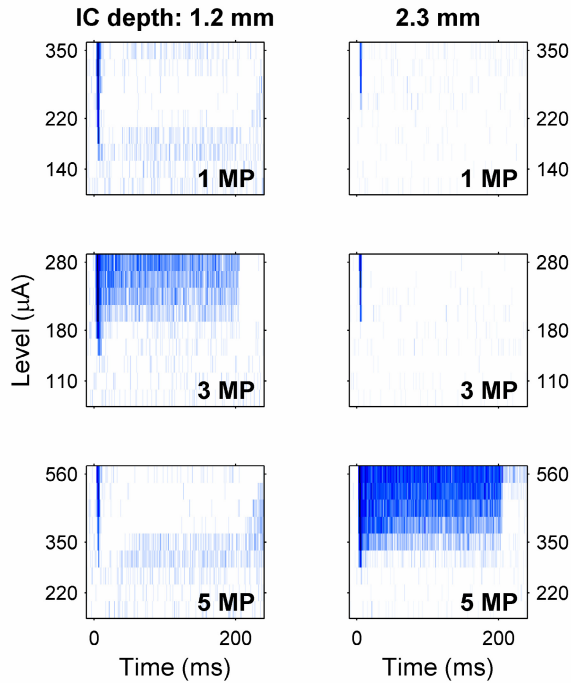
Fig. 13. Post stimulus time histograms for multi-unit responses at various levels. Spike detection thresholds were lowered to multi-unit detection levels (3.5 times the pre-stimulus rms voltage), and PSTHs were computed for the same responses as in Fig. 12. The excitatory and inhibitory tuning of the multi-unit responses shown here are similar to those of the unit responses shown in Fig. 12.
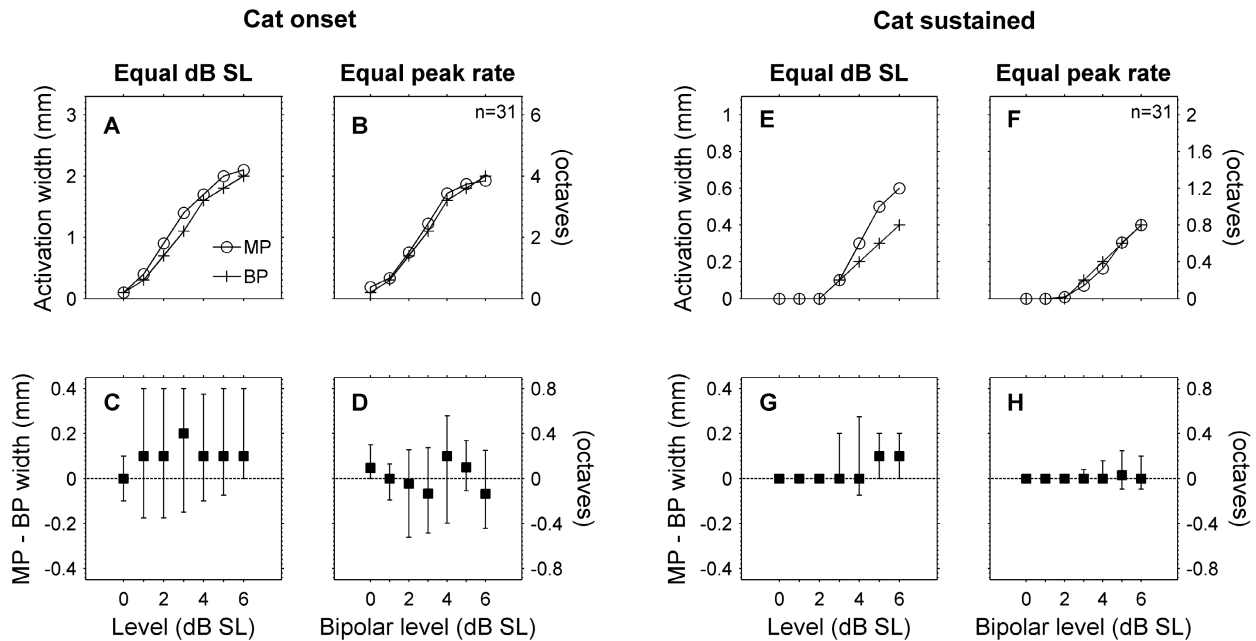
Fig. 14. Monopolar and bipolar activation widths were comparable for equal peak spike rates in cats. **A.** At equal dB SL, monopolar stimuli produced broader onset activation widths than bipolar stimuli (medians shown for 31 total stimulus channels in eight cats). **B.** When compared at equal peak spike rates, monopolar and bipolar stimuli produced nearly equal onset activation widths. **C and D.** Paired differences (medians and interquartile ranges) for the monopolar and bipolar onset activation widths shown in (A) and (B). **E. – F.** Activation widths and paired differences for the sustained time window. When compared at equal dB SL sustained activation widths were slightly broader for monopolar than for bipolar stimulation (E and G). At equal peak spike rates, sustained monopolar and bipolar activation widths were nearly identical (F and H).
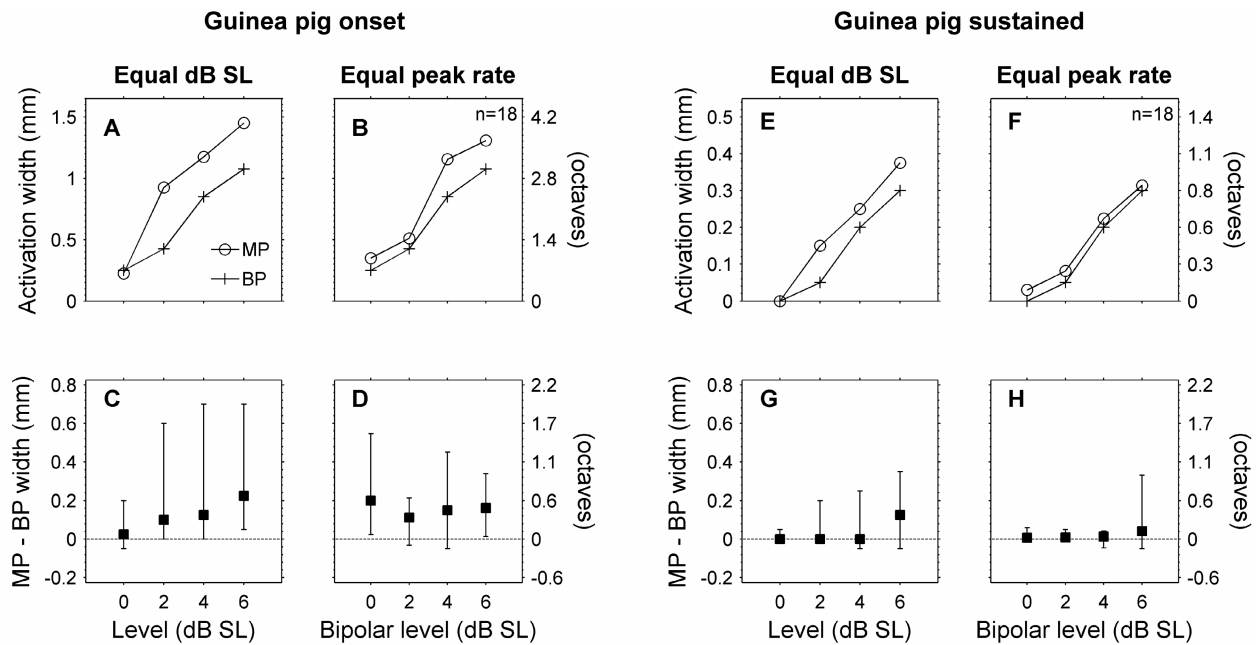
Fig. 15. Monopolar and bipolar activation widths in guinea pigs. (Figure layout as in Fig. 14). **A. – D.** Both at equal dB SL and at equal peak spike rates, onset activation widths were broader for monopolar than for bipolar stimuli. **E. – F.** Sustained activation widths were broader for monopolar stimuli than for bipolar stimuli for equal dB SL (E and G). However, for equal peak spike rates monopolar and bipolar sustained activation widths were nearly identical at levels up to 4 dB SL (F and H). At 6 dB SL, some monopolar channels produced broader sustained activation (large positive interquartile range), but the median difference was near zero.

When peak spike rates were matched to those of 60-dB acoustic tones, both monopolar and bipolar stimuli produced *narrower* sustained activation widths than acoustic stimuli (Fig. 16). In guinea pigs this difference was significant, and both electrical and acoustic stimuli showed relatively small variability in sustained activation widths. Monopolar onset activation, on the other hand, had high variability and median onset widths were broader for monopolar than for acoustic stimuli (difference not significant). Data from one of the two normal cats also showed a trend toward narrower sustained activation for monopolar and bipolar stimulation than for acoustic stimulation.

Similar to our finding for sustained and onset activation *widths*, we found that normalized activation *areas* were significantly smaller for the sustained response than for the onset response to acoustic, monopolar, and bipolar stimuli in guinea pigs and cats (p<0.001, see Fig. 17). The difference between onset and sustained areas generally increased with increasing stimulus level (significant interaction between time window and stimulus level, p<0.001, partial eta squared > 0.5 for a linear interaction contrast). For acoustic tones at 60 dB SL, sustained activation areas were 49% (44–54%) narrower than onset activation areas in guinea pigs and 52% (30–73%) narrower in cats. Sustained activation areas were also narrower than onset activation areas for 6-dB SL pulse trains in monopolar and bipolar configurations (respectively) by 46% (32–60%) and 35% (28–43%) in guinea pigs and 65% (54–75%) and 64% (48–79%) in cats.
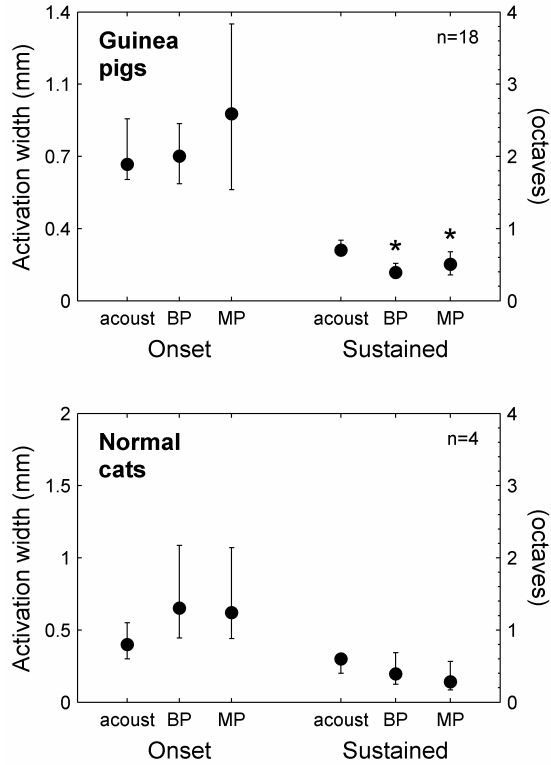
Fig. 16. Sustained activation widths were narrower for electrical than for acoustic stimuli when peak spike rates were matched to 60-dB-SPL acoustic tones. In three guinea pigs, sustained activation widths were significantly narrower for monopolar and bipolar stimuli than for acoustic stimuli (medians and interquartile ranges shown for 18 total electrical stimulus channels and 18 matched acoustic tone frequencies). Bipolar onset activation widths were similar to acoustic. Monopolar onset activation widths, however, had large variability and a trend towards broader activation than acoustic (not significant). For the one normal cat in which acoustic-to-electrical comparisons could be made, trends were similar to those seen in guinea pigs except that bipolar onset activation was more similar to monopolar activation than to acoustic activation. *p<0.05 relative to acoustic tones. (Abbreviations: acoust, acoustic tones.)
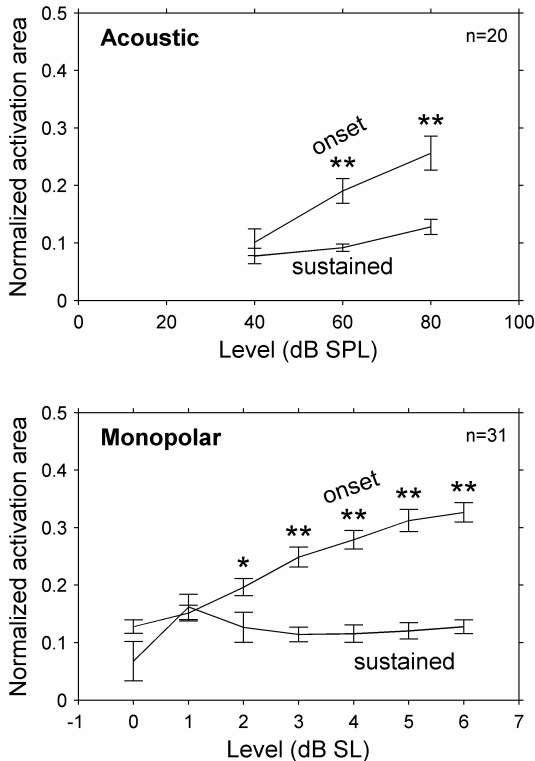
Fig. 17. Normalized activation area was smaller for the sustained time window than for the onset time window in cats. This effect increased with stimulus level, indicating that at higher levels the shape of the sustained response was narrower than that of the onset response (even for normalized peak spike rates). Values are means and error bars are standard errors of the means. Acoustic data are from 20 stimulus frequencies in two cats. Monopolar data are from 31 stimulus channels in eight cats. *p<0.05, **p<0.001 relative to sustained area.

36

DISCUSSION

Our study conducted in both guinea pigs and cats has demonstrated that sustained monopolar intracochlear stimulation can elicit selective activation of the inferior colliculus. Specifically, we found that the extent of inferior colliculus activation produced by 1000-pulse/s monopolar electrical stimuli is narrower for the sustained response than for the onset response. Surprisingly, we also found that for similar peak spike rates, monopolar stimulation produces narrower extents of *sustained* activation than acoustic stimulation. Also somewhat surprisingly, we found that for similar peak spike rates monopolar and bipolar stimulation produce comparable extents of activation.

There are two lines of evidence that support our conclusion that monopolar pulse trains at 1000 pulses/s produce narrower extents of IC activation during the sustained response than during the onset response. First, for monopolar stimuli at 6 dB SL, sustained activation widths were narrower than onset activation widths by 56% in guinea pigs and 74% in cats (Figs. 9 and 10). This same pattern also held true for bipolar and acoustic stimulation and is consistent with previous studies of IC responses to acoustic tones (Aitkin et al., 1994; Harris et al., 1997; Rose et al., 1963; Seshagiri et al., 2007). Interestingly, in the present study onset responses to acoustic and electrical stimuli could be quite broad, extending over several millimeters (or several octaves) of the tonotopic axis of the inferior colliculus at higher levels, whereas sustained responses covered a much narrower extent (for acoustic stimuli at 60 dB SPL the extent was roughly 0.85 octaves—much closer to a neural critical band (Egorova et al., 2008)).

The second line of evidence is that at higher levels normalized activation areas were smaller for the sustained response than for the onset response (Fig. 17). This finding rules out the possibility that onset responses adapted uniformly across IC depths to produce sustained responses that were smaller but the same shape. Instead, it implies that the pattern of sustained activation narrowed relative to onset activation. This narrowing of the sustained response may be due to lateral inhibition, which has been shown to be present at multiple levels of central auditory processing (Ramachandran et al., 1999; Shamma et al., 1993; Young, 2003).

The unexpected finding that for levels that produce similar peak spike rates, monopolar stimulation produces narrower extents of sustained activation than acoustic stimulation is consistent with both guinea pig and cat data. Median sustained activation widths were 30% narrower for monopolar stimulation than for acoustic stimulation in guinea pigs (and 50% narrower in the one cat in which this comparison was possible, Fig. 16). Raw data from eight stimulus channels in one guinea pig qualitatively shows the high degree of similarity between sustained response patterns to monopolar and acoustic stimuli (Fig. 8).

The other somewhat unexpected finding—that for levels that produce similar peak spike rates, monopolar and bipolar stimulation produce similar extents of IC activation—is also supported by data from both cats and guinea pigs. In cats, monopolar and bipolar stimulation produced quite comparable onset activation widths and almost identical sustained activation widths (Fig. 14 B, D, F and H). In guinea pigs, onset activation widths were broader for monopolar stimulation than for bipolar stimulation, but sustained activation widths were similar at levels up to 4 dB SL (Fig. 15 B, D, F and H). One possible reason for the greater similarity between monopolar and bipolar activation widths in cats than in guinea pigs is the difference in stimulating contact spacing for

37

the two species (1 mm in cats versus 0.5 mm in guinea pigs). The closer contact spacing in guinea pigs could have lead to relatively narrower excitation patterns for bipolar stimulation. It is interesting to note that the 1-mm contact spacing used in cats is closer to the contact spacing used in human clinical devices.

The reliability of these findings does not appear to be diminished by the two main methodological limitations of the present study. First, activation widths for equal peak spike rates were not measured directly during experiments, but instead were interpolated from among the electrical stimulus levels tested (Fig. 6). It should be noted, however, that peak spike rates and activation widths increased monotonically with increasing stimulus level (Figs. 5, 9 and 10), suggesting that interpolation between levels was reasonable. This monotonic increase in spike rate with increasing stimulus level contrasts with results from several previous studies that showed non-monotonic rate-level functions in many single-units in the inferior colliculus (Ehret et al., 1988; Nuding et al., 1999; Rose et al., 1963). One possible explanation for this discrepancy is that the present study recorded primarily multi-unit responses. Neurons with monotonic and non-monotonic rate-level functions are frequently adjacent to one another in the inferior colliculus (Seshagiri et al., 2007); therefore recording from multiple neurons simultaneously could yield aggregate rate-level functions that are monotonic.

The second limitation, as mentioned above, was that the multi-site recording probes used recorded primarily multi-unit data and allowed isolation of single neurons on only a few recording sites per animal. Because our goal was to examine the relative selectivity of monopolar, bipolar, and acoustic stimulation in activating a population of auditory neurons distributed across the frequency band laminae of the inferior colliculus, our findings do not rely upon the isolation of single units. However, exemplary data shown in the present study suggest that the tuning of isolatable units to electrical stimuli is similar to the tuning of multi-unit data and, specifically, that this tuning is narrower for the sustained response than for the onset response (Figs. 11-13).

Having argued that our findings are reliable despite methodological limitations, we also offer several explanations for apparent discrepancies between the findings of the present study and previously published studies. First we will consider studies that have compared IC responses to monopolar and acoustic stimulation. Our finding that for similar peak spike rates monopolar stimulation produces narrower extents of sustained activation than acoustic stimulation seems to contradict previous studies that showed much broader IC activation for monopolar stimulation than for acoustic stimulation (Middlebrooks et al., 2007; Snyder et al., 2004). There are at least three possible explanations for this discrepancy. First, in the present study extents of activation for monopolar pulse trains and acoustic tones were decomposed into onset and sustained components before comparing them. In the previous studies, extents of activation were calculated for the response to isolated monopolar pulses (similar to our monopolar onset response) and for the entire acoustic response (a combination of onset and sustained response). Because onset responses are generally much broader than sustained responses for all stimuli, it is not surprising that a comparison between monopolar onset responses and a combination of acoustic onset and sustained responses would indicate that the monopolar response is much broader. A second possible explanation is that the present study compared extents of activation for monopolar and acoustic stimuli that produced similar peak spike rates, whereas the previous studies compared stimuli at a fixed number of decibels above threshold. Because it is not clear

how the loudness of acoustic and electrical stimuli are related on a decibel level scale, it is difficult to choose fixed decibel levels at which to compare these two types of stimuli. Comparing extents of activation at levels that produced similar peak spike rates enabled us to match intensities of monopolar and acoustic responses in a way that was perhaps more appropriate. The third possible explanation for the discrepancy is that the present study used space-filling intracochlear stimulation electrodes, specifically designed for guinea pigs and cats to position stimulating contacts close to the neural targets, whereas the previous studies used conventional, non-space-filling electrodes. It has been shown that non-space-filling electrodes are able to selectively activate the auditory nerve, but not reliably (Liang et al., 1999). The space-filling electrodes used in the present study, on the other hand, have been shown to produce significantly narrower extents of IC activation than non-space-filling banded arrays (Snyder et al., 2008).

Additional interesting discrepancies are seen when we compare the present study to previous studies that characterized IC responses to monopolar and bipolar stimulation. Our finding that monopolar and bipolar stimuli produce similar extents of IC activation when compared at equal peak spike rates contrasts with findings of previous studies that showed monopolar stimulation producing a broader extent of activation across the frequency gradient of the IC than bipolar stimulation at equivalent decibel levels above threshold (Rebscher et al., 2001; Snyder et al., 2004; Snyder et al., 2008). However, as was the case in comparisons between monopolar and acoustic stimuli, it is difficult to choose fixed decibel levels at which to compare monopolar and bipolar stimulus configurations. This is because the thresholds and dynamic ranges vary so widely between monopolar and bipolar stimulation, both among subjects and among different stimulating channels within subjects (Bierer, 2007; Pfingst et al., 2008). Comparing extent of activation for levels that produce similar peak spike rates allowed us to control for the differing growths of monopolar and bipolar response strengths with decibel stimulus level, approximating equivalent effective stimulus intensities for these two stimulus configurations. One previous study compared activation widths for single pulses presented in monopolar and bipolar configurations for stimulus levels that were matched using a d' measure (Middlebrooks et al., 2007). In that study, which used a non-space-filling electrode, monopolar stimulation produced broader activation than bipolar stimulation. It is possible that our use of a space-filling intracochlear electrode explains the much closer match between the selectivity of activation elicited by the monopolar and bipolar configurations in the present study.

Finally, our finding that monopolar and bipolar stimuli produce similar extents of IC activation at suprathreshold levels is in apparent contradiction with the findings of several psychophysical studies that suggest monopolar stimulation produces broader electrical field interactions than bipolar stimulation at near-threshold levels (Bierer, 2007; Boex et al., 2003b; Stickney et al., 2006). A possible explanation for this discrepancy is that near-threshold electrical field interactions may not accurately predict the extent of neuronal activation at suprathreshold levels. Evidence supporting this explanation may be found in the fact that psychophysical studies at suprathreshold levels have shown mixed results for comparisons of monopolar and bipolar stimulation. An early study showed that loudness summation for simultaneous two-channel stimulation was greater for monopolar stimulation in one subject and for bipolar stimulation in another subject (Shannon, 1983a). Psychophysical forward masking using suprathreshold stimuli also shows conflicting results with bipolar stimulation producing narrower masking than monopolar stimulation in some studies (Boex et al., 2003a; Nelson et al., 2008; Shannon, 1983a)

but no difference between the two stimulus configurations in others (Cohen et al., 2001; Kwon et al., 2006). It seems fair to conclude that psychophysical studies at suprathreshold levels have not definitively shown less channel interaction for bipolar stimulation than for monopolar stimulation (Bonham et al., 2008).

Another possible explanation for the disparities between the findings of the present study and those of psychophysical studies is the potential difference in location of stimulating contacts in the cochlea. It has been shown that the placement of intracochlear electrode contacts can account for a significant portion of the performance variability among cochlear implant users; for example, electrodes entering the scala vestibuli are associated with poorer performance (Finley et al., 2008). Although the final location of stimulating electrodes was not verified in our study, three factors reduced the likelihood of our electrodes being placed in the scala vestibuli: they were relatively short, the electrode carriers were specially molded to fit within the first turn of the cochlea, and insertion of the electrodes was through the round window (i.e., precluding direct insertion into the scala vestibuli, as reported in some human subjects (Finley et al., 2008)). As mentioned previously, the space-filling electrode was also designed to place electrode contacts close to spiral ganglion neurons and or peripheral/processes. These factors make it possible that our results could be representative of better-performing cochlear implant users, with stimulating contacts placed in the scala tympani close to neural elements, rather than cochlear implant users as a whole.

Thus, our findings that the extent of IC activation for 1000-pulse/s electrical stimuli is narrower for the sustained response than for the onset response, and that for levels that produce similar peak spike rates, monopolar and bipolar stimulation elicit similar extents of IC activation may help explain the observation that cochlear implant users do not generally perform better with bipolar stimulation than with monopolar stimulation. The unexpected finding that, using a space-filling electrode, monopolar pulse trains produce more selective sustained activation than acoustic tones also suggests that it may indeed be worthwhile to design intracochlear electrodes with higher densities of stimulating contacts that lie close to their target neural elements. With such arrays, it may be possible to provide cochlear implant users with much finer spectral resolution, improving their ability to appreciate music and to understand speech, especially in noisy environments.

Chapter 3: Amplitude Modulation Increases Extent of Activation in the Inferior Colliculus

ABSTRACT

It is well known that in normal hearing listeners, sinusoidally amplitude-modulated (SAM) signals produce psychophysical interactions that can occur across large differences in carrier frequency. Similarly, in cochlear implant users SAM electrical pulse trains can elicit psychophysical interactions across large intracochlear electrode separations. However, the neural correlates of these phenomena are not well understood. This study sought to determine whether SAM stimuli elicit activation across a broader extent of the frequency axis of the inferior colliculus than unmodulated steady-state stimuli, and whether this activation is strongly phase-locked to the SAM stimulus envelope. To address these questions we recorded neuronal activity in the inferior colliculus of guinea pigs, normal cats and chronically deafened cats in response to acoustic stimulation and/or electrical stimulation delivered by a cochlear implant. We found that the extent of inferior colliculus activation was up to 70% broader for SAM stimuli than for unmodulated steady-state stimuli in normal cats and guinea pigs and 160% broader in chronically deafened cats. We also found that this activity was phase-locked to the SAM envelope across a broad extent of the frequency axis of the inferior colliculus. Our results suggest that substantial cross-carrier frequency interactions for SAM stimuli could occur at the level of the inferior colliculus in response to SAM stimuli. They also suggest that responses to amplitude modulation for acoustic stimulation in normal hearing animals and electrical stimulation in chronically deafened animals should be carefully compared to help guide the implementation of new processing strategies for future cochlear implants.

INTRODUCTION

It is well known that when acoustic tones are sinusoidally amplitude-modulated (SAM), they elicit auditory neuronal responses that phase lock to the modulator waveform. Moreover, the same finding has been reported for intracochlear electrical stimulation delivered by a cochlear implant using SAM pulse trains. This phase locking has been implicated in speech processing, sound source localization, and source identification and has been studied extensively at many levels of the auditory system for both acoustic (Creutzfeldt et al., 1980; Frisina et al., 1990; Huffman et al., 1998; Javel, 1980; Moller, 1974; Nelson et al., 1966; Yin et al., 1984) (for reviews see (Frisina, 2001; Joris et al., 2004; Langner, 1992)) and electrical stimuli (Litvak et al., 2003b; Middlebrooks, 2008; Snyder et al., 2000).

Studies employing acoustic stimuli often have characterized neuronal responses using carrier frequencies that fall within a critical band around the neuron's characteristic frequency (CF, the frequency that produces a response at the lowest stimulus intensity; a critical band is roughly 1/3 to 1/2 octave (Zwicker et al., 1957)). However, a number of psychophysical phenomena including modulation detection interference (Grose et al., 2005; Yost et al., 1989) and comodulation masking release (Hall et al., 1984; Verhey et al., 2003) imply that excitatory and/or suppressive effects of SAM tones in the auditory system extend well beyond a critical band. Cross-critical-band phenomena such as modulation detection interference also have been

shown to occur in cochlear implant users (Chatterjee et al., 2004). Despite these interesting and potentially important findings, relatively little is known about how populations of neurons with characteristic frequencies across more than one critical band respond to either acoustic SAM tones or electrical SAM pulse trains.

At the level of the auditory midbrain or inferior colliculus (IC), it has been reported that the transient response to the onset of an unmodulated acoustic tone or electrical pulse train extends farther across the IC tonotopic axis (broader frequency or spectral activation) than the steady-state response, and that this onset response can extend well beyond the width of a critical band (Chapter 2). However, it is not known whether this increase in activation extent also occurs in response to SAM stimuli.

In the present study we recorded in the central nucleus of the inferior colliculus and characterized responses to unmodulated and SAM acoustic tones and electrical pulse trains in guinea pigs, normal cats, and chronically deafened cats. We first asked whether acoustic and electrical SAM stimuli elicit activation across a broader extent of the tonotopic axis of the IC than unmodulated steady-state stimuli. We next examined whether the extent of activation in response to SAM stimuli was different for acoustic tones than for monopolar electrical pulse trains. Finally, for both acoustic and electrical SAM stimuli we explored whether responses phase lock to the modulator waveform across a broad extent of the tonotopic axis of the inferior colliculus.

METHODS

To characterize the spatial extent of SAM activation and to examine phase-locking behavior across the tonotopic axis of the inferior colliculus, we conducted a series of acute neurophysiologic experiments in adult guinea pigs and cats. In these experiments, we recorded neuronal activity in the central nucleus of the inferior colliculus in response to acoustic and intracochlear electrical stimuli. All procedures were approved by the UCSF Institutional Animal Care and Use Committee.

Other than the addition of SAM stimuli in the present study, the anesthesia and surgery, stimulus generation, and multi-unit recording were the same as described in Chapter 2. One normal cat was added to the present study and one chronically deafened cat that was not chronically stimulated (K336, see Appendix) was excluded for reasons that will be described under statistical analyses. Otherwise the animal subjects used in the present study were the same as those in Chapter 2. The specific details of SAM stimulus parameters and data analysis for the present study are described below.

SAM stimulus parameters

The stimuli presented here were identical to the unmodulated acoustic tones and monopolar electrical pulse trains described in Chapter 2, except in the present study we also used signals that were sinusoidally amplitude-modulated (Fig. 1). In order to avoid differences in peak stimulus levels, modulation depth (m in percent) was defined as percentage decrement from each constant, unmodulated stimulus level. That is, for each unmodulated stimulus with constant level A, the corresponding modulated stimulus had a maximum value of A and a minimum value of A

× (100% – *m*). Consequently, each modulated stimulus delivered less total energy than its paired unmodulated stimulus. For both acoustic and monopolar electrical stimulation, the SAM conditions included SAM frequencies of 50-Hz and 125-Hz and a modulation depth of 100%. For monopolar electrical stimuli in a subset of three out of the five chronically deafened cats (K319, K329, K335, see Appendix) a modulation depth of 20% was also examined.

A. Acoustic stimulus (10 kHz, 50-Hz SAM)

B. Responses at depth = 0.75 mm

C. PSTHs at three IC depths

D. Temporal response image
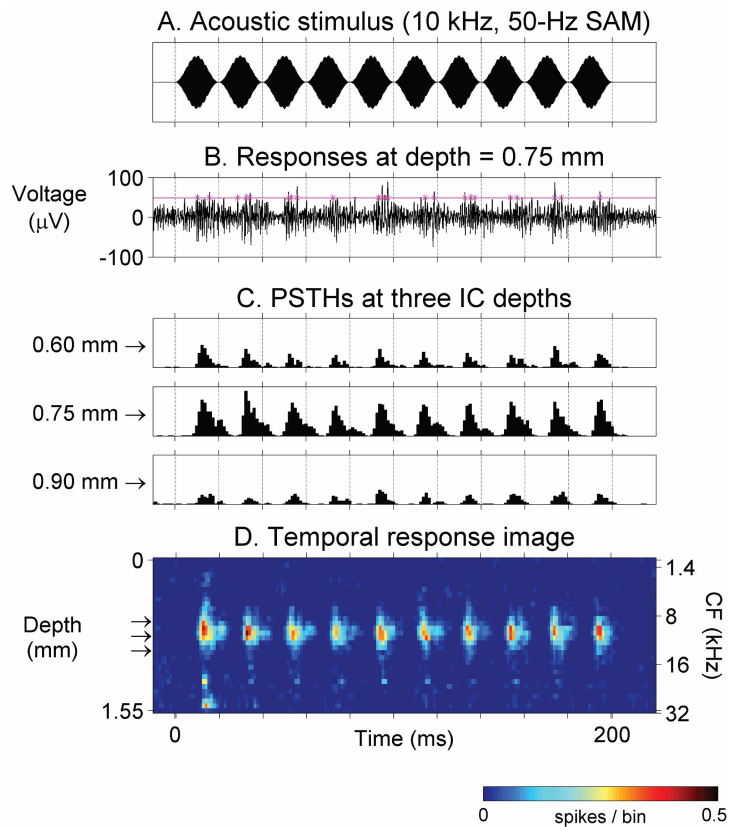
Fig. 1. Example of an inferior colliculus response image for acoustic stimulation in a guinea pig. **A.** Stimulus was a 10-kHz, 60 dB SPL tone with 50-Hz SAM (100% SAM depth). **B.** Multi-unit activity from one of 32 linearly spaced recording sites along the tonotopic (depth) axis of the IC central nucleus. Horizontal line indicates spike detection threshold and asterisks indicate threshold crossings, counted as spikes. **C.** PSTHs were computed from spike times on each recording channel with mean spontaneous activity subtracted. PSTHs at three IC depths are shown here (depths shown to the left of each panel are relative to the most superficial recording site). **D.** The 32 PSTHs are displayed in depth order to form a temporal response image, showing the extent of neuronal activation along the tonotopic axis of the IC and changes in this activity over time. Response strength is indicated by color intensity. Arrows indicate depths of the PSTHs shown in (C) for comparison. Characteristic frequency at a given depth is shown on the right axis indicating the frequency organization of the IC from low frequencies (superficial locations) to high frequencies (deep locations). Note that neuronal activity was phase-locked to the 50-Hz SAM stimulus frequency across a range of IC depths. (Abbreviations: SAM, sinusoidally amplitude-modulated; PSTH, post stimulus time histogram; IC, inferior colliculus; CF, characteristic frequency.)

Data analysis

For each stimulus condition, post stimulus time histograms (PSTHs) with a temporal resolution of 1-ms bins were constructed from data recorded at each recording site (Fig. 1). In addition, temporal response images displaying these PSTHs in IC depth order (Figs. 1 and 2) were constructed to examine patterns of neural activity across all recording sites for each stimulus as described in Chapter 2. An analysis window of 20 – 200 ms after electrical stimulus onset and 23 – 203 ms after acoustic stimulus onset was defined to exclude the response to the stimulus onset. The response to the unmodulated stimulus condition over this analysis window will hereafter be

referred to as the unmodulated steady-state (SS) response. After smoothing the PSTHs using a 2-point moving average filter in the time dimension, period histograms were then constructed for each recording site over this analysis window. Period histogram images (Fig. 3) displayed period histograms for all recording sites in depth order (along the tonotopic axis of the inferior colliculus). A period of 20 ms was used for the 50-Hz SAM and unmodulated steady-state conditions, and a period of 8 ms was used for the 125-Hz SAM condition. The values for a number of metrics were determined from these period histograms including the maximum (max) firing rate at any time bin in the period histogram, the tonic firing rate (the mean number of spikes per time bin), the mean number of spikes per period (n), the vector strength (R) (Goldberg et al., 1969), the p value for significant phase locking (according to the Rayleigh test) (Mardia, 1972), the number of phase-locked spikes per period ($n \times R$), and the SAM time delay (Fig. 4).
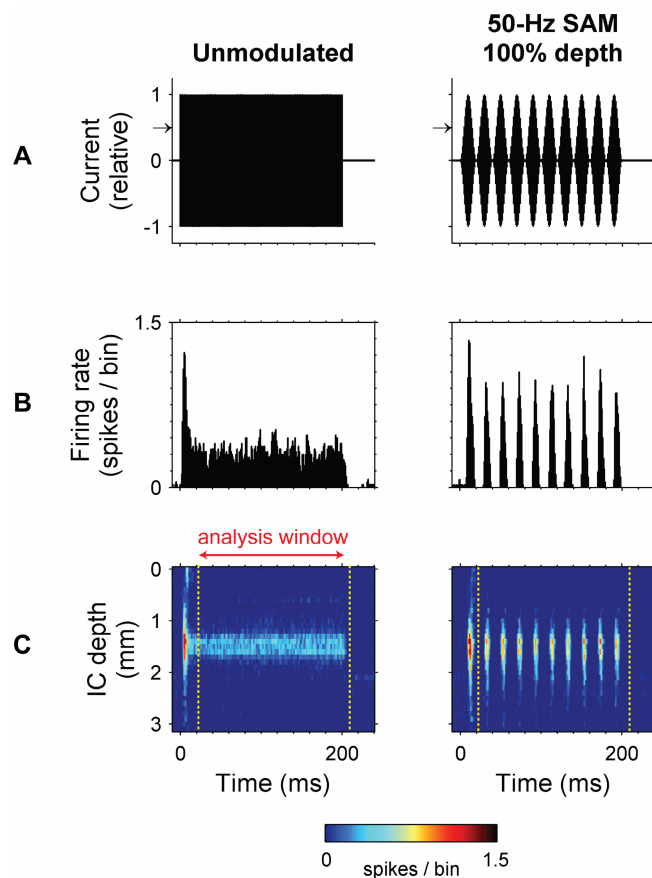
Fig. 2. Post stimulus time histograms and temporal response images for unmodulated and amplitude modulated electrical pulse trains in one chronically deafened cat. **A.** Electrical pulse trains were delivered in the cochlea in monopolar configuration at 1000 pulses/s. Pulses were charge-balanced biphasic with the cathodic phase first (40 μs per phase, and 20-μs interphase gaps). In this example the peak current was 220 μA (6 dB SL) delivered on the third most apical monopole (MP 3). Threshold is indicated by the arrow on the vertical axis. **B.** Post-stimulus time histograms (20 trials, 1-ms time bins) of inferior colliculus responses to the stimuli in (A) are shown for the best recording site (i.e., the site with the highest tonic firing rate). **C.** Temporal response images for the stimuli in (A). Note that for both stimulus conditions the initial onset response was strong and covered a broad extent of the IC tonotopic (depth) axis. An analysis window (20 – 200 ms) was defined to exclude this onset response. Within the analysis window, responses to the SAM stimulus (right panel) were phase locked in time to the SAM period and extended farther across the depth axis than the unmodulated "steady-state" responses (left panel). In other words, the responses to the unmodulated stimulus were more restricted with regard to the IC frequency gradient.

Response-rate profiles and activation widths. To answer the questions related to extent of activation along the tonotopic axis of the IC, two metrics were designed: response-rate profiles and activation widths. Firing rates (maximum or tonic) for each of the 32 recording sites arranged in IC depth order were used to create the response-rate profiles (Fig. 5). To determine activation widths, a rate criterion was first chosen at 0.05 spikes per bin (well above spontaneous activity, but below steady-state firing rates for 60-dB SPL tones). Then, the number of recording

44

sites with maximum firing rates exceeding this criterion was determined and multiplied by the inter-site spacing to give an activation width in units of millimeters. Units of octaves were also estimated by multiplying the activation widths by the number of octaves per millimeter in the IC (as described in Chapter 2). Including the additional normal cat in this study, mean conversion values were 1.8 octaves per millimeter in cats and 2.8 octaves per millimeter in guinea pigs. When calculated using maximum rates, activation widths are termed "max activation widths". When calculated using tonic rates, they are termed "tonic activation widths".
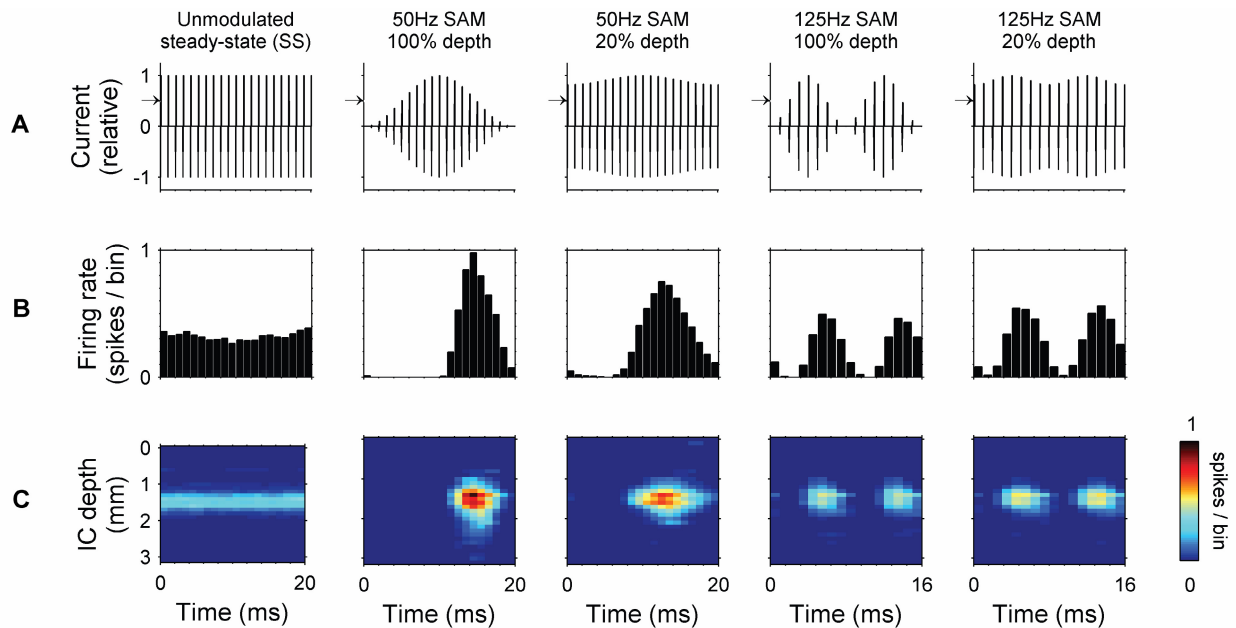
Fig. 3. Construction of period histograms and period histogram images. **A.** One period (50-Hz SAM) or two periods (125-Hz SAM) of monopolar electrical stimuli are illustrated. The arrow on the vertical axis corresponds to threshold for a 6-dB SL stimulus. **B.** Period histograms (1-ms time bins) for responses at the best recording site. The cat, stimulus parameters, and analysis window were the same as in Fig. 2. SAM responses were phase locked to the stimulus and had peak firing rates that exceed the unmodulated steady-state firing rate. Responses to 20% modulation depths were strongly phase locked, even though the positive stimulus pulses shown in (A) were always above threshold. **C.** Period histogram images were formed by displaying the period histograms from the 32 recording sites in depth order, with firing rate indicated by color intensity. Responses to the 50-Hz SAM stimuli (both 100% and 20% modulation depths) extended more broadly across the tonotopic (depth) axis of the IC than unmodulated steady-state responses despite the fact that the unmodulated stimulus delivered greater total energy. The same was true for 125-Hz SAM responses but to a lesser extent.

In addition to activation width comparisons among the unmodulated, 50-Hz SAM, and 125-Hz conditions, max activation widths were also compared between acoustic and monopolar electrical stimuli in the guinea pigs and in one normal cat. Electrical stimulus levels were interpolated to match peak spike rates (Fig. 5) of 60-dB SPL acoustic stimuli as described previously (Chapter 2). Because connecting the electrical current stimulator increased noise levels markedly in two of the three normal cats, direct comparison between acoustic and electrical activation widths was only performed in one normal cat.

Response-rate profiles for pooled data. The response-rate profiles described in Figure 5 were pooled across animals and carrier frequencies or electrical stimulus channels to visualize the median profile for each SAM condition. First, response-rate profiles were plotted for increasing acoustic carrier frequencies or increasingly basal monopolar electrical stimulus channels (Fig. 6). Then, the best recording site was determined for each response-rate profile as the recording site with the highest tonic firing rate. Next, IC depths for each response-rate profile were expressed relative to the best recording site. Finally, firing rates at each depth relative to the best recording site were pooled across all acoustic carrier frequencies (or electrical stimulus channels) and across animals, and the pooled firing rates were summarized with medians and interquartile ranges. The number of stimuli that contributed to the pooled data at each relative depth varied (Fig. 7) because best recording sites were located at different IC depths for different stimuli. Only relative IC depths with at least 4 pooled values were included in order to display meaningful interquartile ranges. In constructing these profiles, a stimulus level of 60 dB SPL was used for acoustic stimuli. For each monopolar electrical stimulus channel in guinea pigs, the stimulus level was chosen to match the stimulus level of an acoustic 60-dB-SPL SAM tone stimulus with a similar best recording site. The electrical level was chosen that elicited peak SAM firing rates closest to those elicited by the 60-dB-SPL SAM tone. In normal and chronically deafened cats a monopolar electrical stimulus level of 4 dB SL was used. Distances along the IC depth axis were expressed in millimeters or in octaves (multiplying the distance in millimeters by the average number of octaves per millimeter). Half-octave and one-octave extents around the best recording site were indicated on the IC depth axis of rate profiles to facilitate comparisons among stimulus conditions.
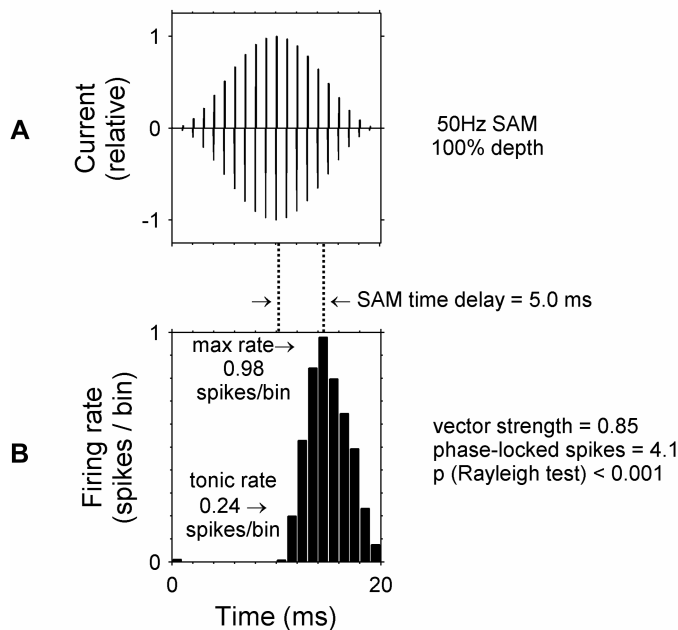
Fig. 4. Firing-rate and phase-locking metrics for period histograms constructed for each recording site. Maximum (max) rate is the firing rate at the time bin with the strongest response whereas tonic rate is the mean firing rate across all time bins. The SAM time delay is the delay from the peak of the SAM stimulus envelope to the peak of the response. The number of phase-locked spikes is the product of the number of spikes per period times the vector strength. The p-value for significant synchrony was determined by the Rayleigh test.
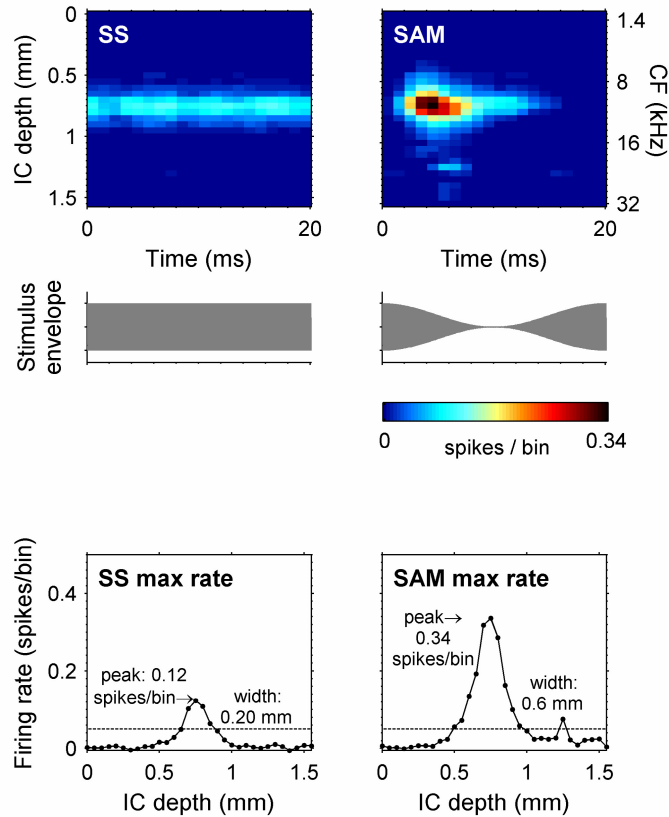
Fig. 5. Construction of response-rate profiles and determination of activation widths. In this example the stimulus was an acoustic tone with a carrier frequency of 10 kHz and intensity of 60 dB SPL, and responses are shown from one guinea pig. The left column shows the unmodulated steady-state (SS) condition and the right column shows the 50-Hz SAM condition (100% modulation depth). A. Period histogram images show that the responses to the acoustic SAM tone (right panel) were strongly phase-locked to the stimulus across a range of depths in the inferior colliculus, and that the extent of responses along the depth axis was substantially broader for the SAM tone than for the unmodulated steady-state tone. B. Response rate profiles were formed by plotting the maximum or tonic firing rate for each period histogram versus IC depth (max rate shown here). Each point along the profile represents the firing rate at one IC recording site. To measure activation width, first a rate criterion was defined as 0.05 spikes per bin. Then, the number of recording sites with firing rates that exceeded this criterion were counted and multiplied by the inter-site spacing for the recording probe (50 μm for guinea pigs and 100 μm for cats). Widths are termed "max activation widths" when calculated using maximum rates and "tonic activation widths" when calculated using tonic rates. Peak firing rate was defined as the highest max firing rate recorded at any of the 32 recording sites.

Phase-locking profiles for pooled data and total vector strength. To determine whether responses phase lock to the modulator waveform across a broad extent of the tonotopic axis of the inferior colliculus, we constructed two additional metrics: phase-locking profiles and total vector strength. Phase-locking profiles were constructed in the same way as the response-rate profiles described above, but using phase-locking measurements (vector strength, phase-locked spike rate, significance of synchrony, SAM time delay, Fig. 4) instead of firing rate. Significance of phase locking was expressed as the proportion of stimuli that produced significant phase locking (p < 0.01) at a given IC depth relative to the best recording site. The SAM time delay values were taken only from period histograms with significant phase locking.

Total vector strength (R_{total}) summarizes the phase locking across recording sites for each stimulus condition. For a given recording site, vector strength (R) can be expressed as the number of phase-locked spikes (PLS) per period divided by the total number of spikes (n) per period: $R = PLS / n$. Analogously, total vector strength is the sum of phase-locked spikes from all 32 sites divided by the sum of the total number of spikes from all 32 sites:

$$R_{total} = \frac{\sum\limits_{i=1}^{32} PLS_i}{\sum\limits_{i=1}^{32} n_i}$$

where i is the recording site number. This metric is a value between zero and one, and represents the average phase locking per spike across all 32 recording sites. Within each animal category (guinea pigs, normal cats, and chronically deafened cats), total vector strength values were pooled across carrier frequencies (for acoustic stimuli) or electrical stimulus channels (for electrical stimuli) and were expressed as a median and interquartile range of the pooled values.
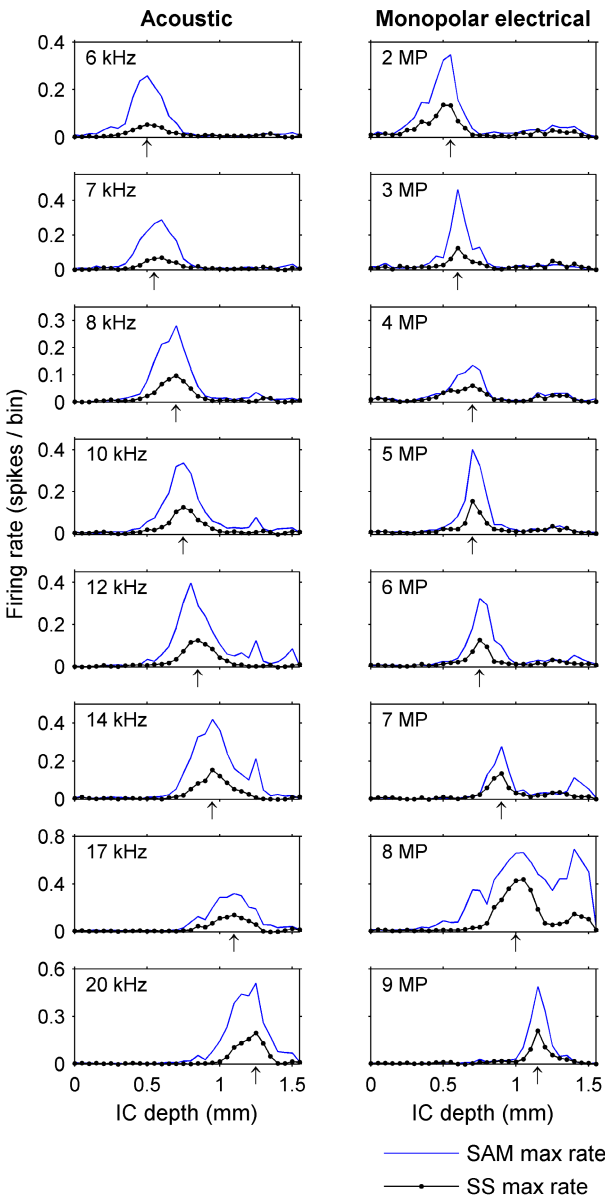
Fig. 6. Maximum response-rate profiles for increasing acoustic carrier frequencies and increasingly basal electrical stimulus channels in one guinea pig. Profiles are shown for unmodulated steady state (SS) stimuli and 50-Hz SAM stimuli (100% modulation depth). Best recording sites for the SS max rate profiles are indicated by vertical arrows on the IC depth axis. Note that SAM max rates exceeded SS max rates across a range of IC depths around the best recording site. For acoustic stimuli, best recording site shifted deeper in the IC with increasing carrier frequency (inset), showing the frequency organization of the inferior colliculus. Analogously, responses to monopolar electrical pulse trains shifted deeper in the inferior colliculus with increasingly basal intracochlear stimulation (channel number inset). For a given electrical stimulus channel, the level was chosen that elicited a peak spike rate closest to that of a 60-dB acoustic tone with similar best recording site. Note that monopolar electrical channel 8 MP had particularly broad tuning. Activation increased strongly with level on this stimulus channel, and it was not possible to match the acoustic peak spike rate very accurately using the 2-dB level steps tested. Otherwise, tuning for monopolar electrical stimuli and acoustic stimuli was similar.

A. Guinea pigs

Acoustic

Stimulus conditions (N)

IC depth relative to best recording site (mm)

Monopolar electrical

IC depth relative to best recording site (mm)

B. Cats, monopolar electrical

Normal cats

Stimulus conditions (N)

IC depth relative to best recording site (mm)

Chronically deafened

IC depth relative to best recording site (mm)
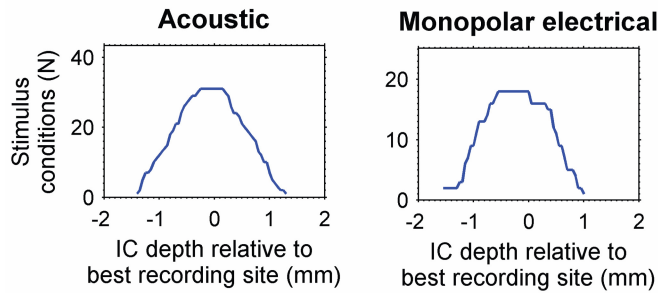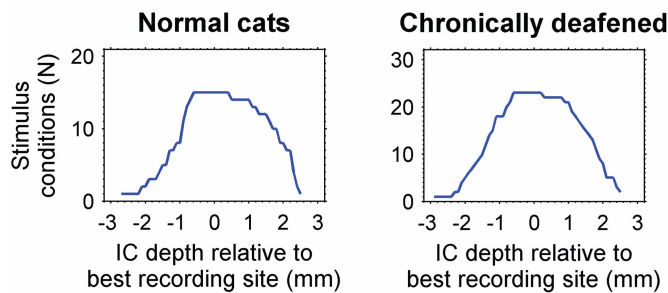
Fig. 7. Number of stimulus conditions contributing to response-rate and phase-locking profiles. The number of stimulus conditions denotes the number of acoustic carrier frequencies or electrical stimulus channels that contributed to pooled data at each depth relative to the best recording site. These numbers are not constant across depths because the best recording site occurred at different IC depths for different stimulus conditions (Fig. 6). The number of stimulus conditions that contributed to pooled data at zero depth (at the best recording site) is equal to the total number of acoustic carrier frequencies or electrical stimulus channels tested in that group (guinea pigs, normal cats, or chronically deafened cats).

Statistical analyses. Data from guinea pigs and cats were analyzed separately. Activation widths were compared using a two-way repeated measures ANOVA with the SPSS software package ("general linear model" command). Each stimulus frequency or electrical stimulus channel in a given animal was considered a subject, and within-subject effects of SAM condition (unmodulated steady-state, 50-Hz SAM, or 125-Hz SAM) and stimulus level (2 dB SL – 6 dB SL) were tested. Activation widths were compared among the three SAM conditions by running two within-subject simple contrast tests.

In cats, the between subjects effect of treatment group (normal or chronically deafened) was also added to the ANOVA test. There was a significant interaction between the effects of SAM condition and treatment group so the normal and chronically deafened cats were analyzed separately. The activation widths of the one chronically deafened cat that was not chronically stimulated (K336, see Appendix) differed significantly from those of the normal cats but did not differ significantly from those of the chronically stimulated cats. However, we chose to exclude this cat to rule out the possibility of differences between normal and chronically deafened cats being caused by a chronic lack of stimulation of the auditory system.

The normality assumption was met for some, but not all, of the cells in the ANOVA tests. However, because non-parametric, two-way repeated measures ANOVA tests are not generally available, displays of median and interquartile ranges for response-rate profiles were constructed to provide a non-parametric confirmation of the ANOVA results.

Activation widths were compared between acoustic and monopolar electrical stimuli using a paired Wilcoxon signed rank test. Separate comparisons were performed for the 50 Hz SAM and

125 Hz SAM conditions. No correction for multiple comparisons was made because neither test resulted in a significant difference (p > 0.05).

RESULTS

In guinea pigs, normal cats and chronically deafened cats, neuronal activation extended more broadly across the tonotopic axis of the inferior colliculus for the 50-Hz SAM condition than for the unmodulated steady state condition. To illustrate these findings, unit responses at one IC location in a chronically deafened cat to unmodulated and 50-Hz SAM intracochlear electrical pulse trains are presented in Figure 8. Unmodulated pulse trains delivered on monopolar stimulus channels 1 MP, 3 MP, and 5 MP elicited transient responses at the stimulus onset. However, only 5 MP, the most basal intracochlear electrode, elicited a sustained (steady-state) response. In contrast, 50-Hz SAM pulse trains (100% modulation depth, modulated downward from the level of the unmodulated stimuli) delivered on 1 MP, 3 MP, and 5 MP all elicited responses throughout the duration of the stimulus. Sustained tuning at this IC depth was, therefore, broader in response to the SAM stimuli than the unmodulated stimuli despite the fact that the unmodulated stimuli delivered more energy. Note that for all three stimulus channels SAM responses were clearly phase locked to the SAM stimulus envelope, and responses to the individual SAM periods looked similar to onset responses.

Effect of SAM on the extent and strength of IC responses

In response to acoustic and monopolar electrical stimulation guinea pigs, maximum response-rate profiles were higher for the 50-Hz SAM condition (SAM max rate) than for the unmodulated steady-state condition (SS max rate) across broad extent of the inferior colliculus (more than 1 octave, Fig. 9A). Maximum response-rate profiles were similar for acoustic and electrical stimuli. However, electrical profiles had more variability, especially as distance from the best recording site increased. For monopolar electrical stimulation in normal cats, SAM max rates were similar to those in guinea pigs. In chronically deafened cats, however, SAM max rates were higher and covered a broader extent of the inferior colliculus than in normal cats or guinea pigs (Fig. 9B).

Consistent with these maximum response-rate profiles, max activation widths were significantly broader for the 50-Hz SAM condition than for unmodulated steady-state condition (Fig. 10). In response to 60 dB SPL acoustic tones, max activation widths were 72% broader for 50-Hz SAM condition (100% modulation depth) than for unmodulated steady state condition in guinea pigs and 47% broader in normal cats. In guinea pigs, max activation widths for 50-Hz SAM tones averaged 450 μm (1¼ octaves) and, in cats, 560 μm (1 octave). In response to 4-dB-SL monopolar electrical pulse trains, max activation widths were broader for the 50-Hz SAM condition (100% modulation depth) than for the unmodulated steady-state condition by 61% in guinea pigs, by 43% in normal cats, and by 160% in chronically deafened cats. This much-larger difference between the 50-Hz SAM and unmodulated steady state conditions in the chronically deafened cats versus the normal cats was highly significant (p<0.001 for interaction between effects of SAM condition and cat treatment group). At 20% modulation depth in chronically deafened cats, the 50-Hz SAM condition elicited activation widths that were 76% broader than activation widths for the unmodulated steady-state condition.
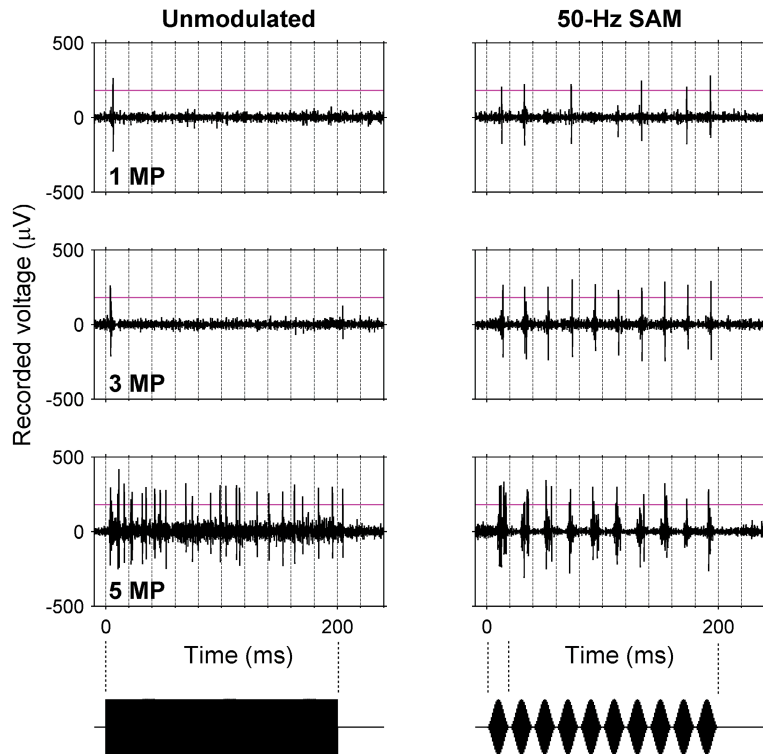
Fig. 8. Unit responses at one inferior colliculus location to unmodulated and 50-Hz SAM electrical pulse trains in a chronically deafened cat. Each row shows responses to a different monopolar stimulus channel (intracochlear stimulation site shifts basally from 1 MP to 5 MP). Stimulus waveforms are shown below each column. Only 5 MP produced sustained responses for unmodulated pulse trains whereas 1MP, 3 MP, and 5 MP all produced sustained responses for 50-Hz SAM pulse trains. Thus, sustained tuning was broader in response to SAM pulse trains even though unmodulated pulse trains delivered more energy. Responses to 50-Hz SAM pulse trains were phase locked to the SAM envelope. Peak current amplitudes were 350 μA, 250 μA, and 450 μA for 1 MP, 3 MP, and 5 MP respectively. (Abbreviations: MP, monopolar.)

Max activation widths for the 125-Hz SAM condition were broader than for the unmodulated steady-state condition in guinea pigs (in response to acoustic and electrical stimulation). In chronically deafened cats, activation widths for the 125-Hz SAM condition were only significantly broader than the unmodulated steady-state condition for 100% modulation depth whereas in normal cats there was no significant difference between the 125-Hz SAM condition and the steady-state unmodulated condition.

Tonic response-rate profiles for pooled data (Fig. 11) show trends that differed from those of the maximum response-rate profiles (Fig. 9). For acoustic stimulation in guinea pigs, tonic rates for the 50-Hz SAM condition (SAM tonic rates) were almost identical to those for the unmodulated steady-state condition (SS tonic rates, Fig. 11A). For monopolar electrical stimulation in guinea pigs and normal cats (Fig. 11A and 11B), SAM tonic rates were actually less than SS tonic rates. In chronically deafened cats, SAM tonic rates were greater than SS tonic rates, but the difference was much less than it was for maximum response-rate profiles. Note that for all of the steady-state unmodulated stimuli, tonic firing rates had relatively narrow tuning (they exceeded the rate criterion across roughly ½ octave centered on the best recording site).

51

A. Guinea pigs

Acoustic

Monopolar electrical

←decreasing CF   increasing CF→

B. Cats, monopolar electrical

Normal cats

Chronically deafened cats
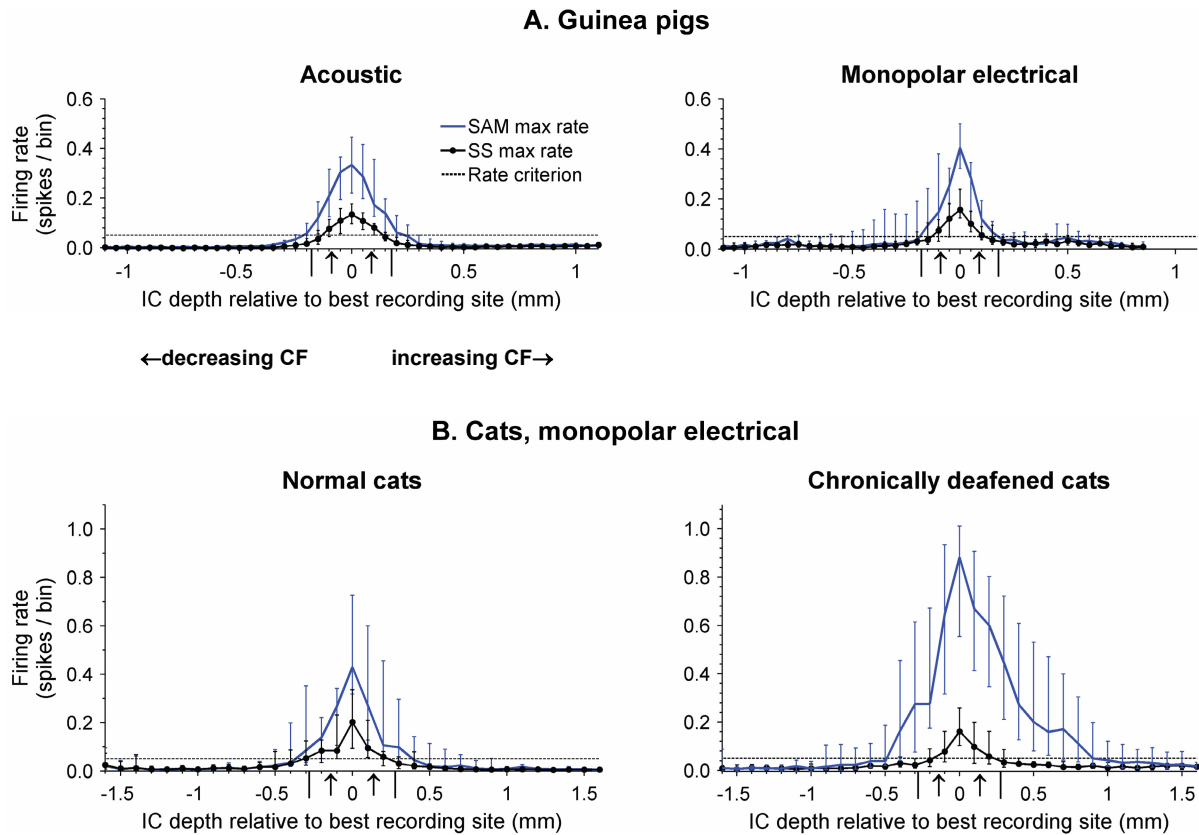
Fig. 9. Maximum response-rate profiles pooled across carrier frequencies or electrical stimulus channels. Lines are medians of the pooled data and error bars are interquartile ranges. Maximum firing rates were greater for the 50-Hz SAM, 100% depth condition (SAM max rate) than for unmodulated steady-state condition (SS max rate) over a broad extent of the depth axis of the inferior colliculus. The distance between the vertical arrows on the IC depth axis is approximately ½ octave along the frequency gradient of the IC, and the distance between the vertical bars is approximately one octave (estimated using the mean number of octaves per IC millimeter in each species). **A.** Median profiles in guinea pigs were similar for acoustic stimuli (60 dB SPL) and monopolar electrical stimuli (at levels producing comparable SAM max rates). However, variability was higher for the electrical stimuli. For both, SAM max rate profiles exceeded the rate criterion over a span of roughly one octave. **B.** Maximum firing rates are shown for monopolar electrical stimulation (4 dB SL) in normal and chronically deafened cats. SAM max rates in normal cats were similar to those in guinea pigs. In chronically deafened cats they were higher and covered a larger extent of the frequency gradient of the inferior colliculus. See Figure 7 for sample sizes at each relative IC depth.
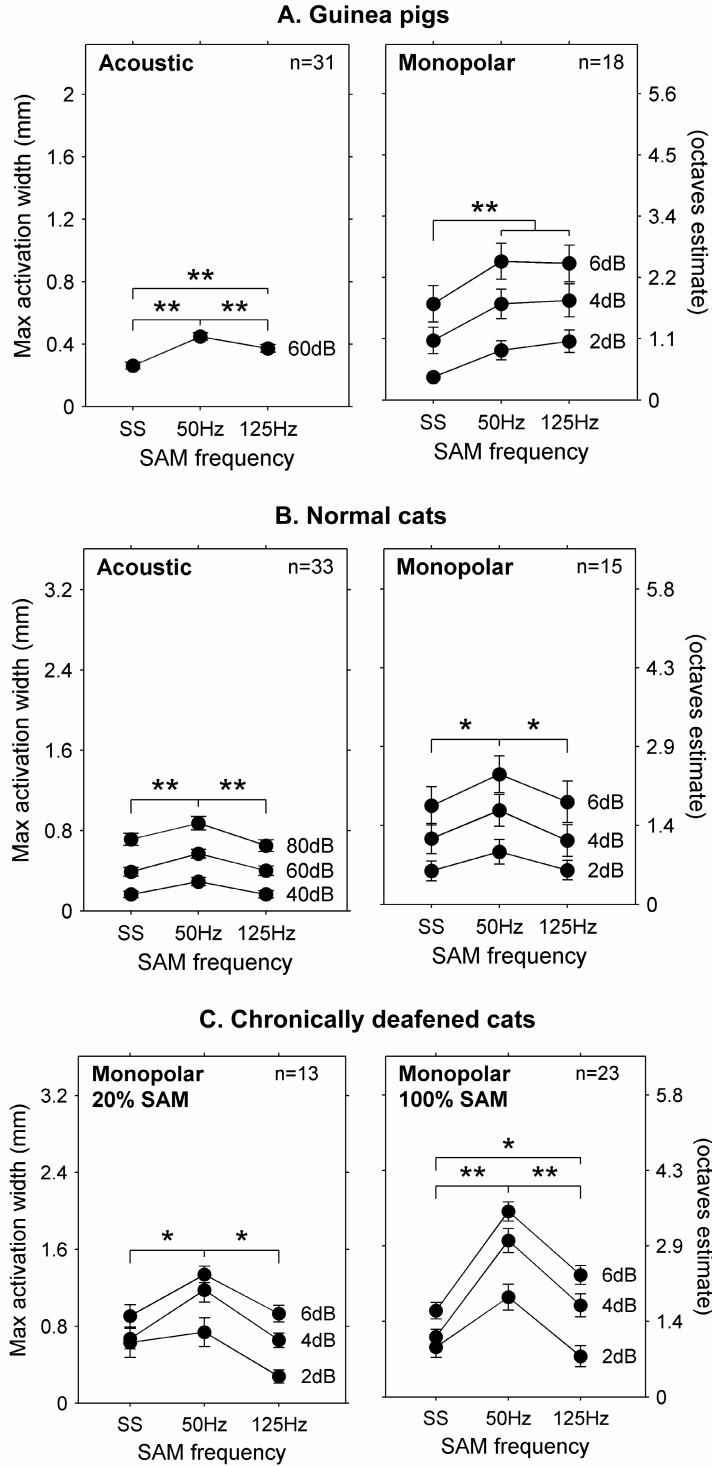
Fig. 10. Max activation widths were broader for the 50-Hz SAM condition than for the unmodulated steady-state condition in guinea pigs, normal cats, and chronically deafened cats. Acoustic and/or monopolar electrical activation widths are shown for maximum (max) responses to unmodulated steady-state (SS), 50-Hz SAM, and 125-Hz SAM conditions. SAM depth was 100% (in a subset of three chronically deafened cats a SAM depth of 20% was also tested). Despite the fact that SAM stimuli delivered less energy than SS stimuli, max activation widths were significantly broader for 50-Hz SAM stimuli than for SS stimuli. Activation widths for 125-Hz SAM stimuli were broader than for SS stimuli in guinea pigs and for the 100% SAM depth condition in chronically deafened cats. Values shown are means and standard errors of the mean. Sample size (n) is the number of acoustic carrier frequencies or electrical stimulus channels tested in the three guinea pigs, three normal cats, or five chronically deafened cats. Values in octaves were estimated by multiplying activation widths by the mean number of octaves per IC millimeter in each species. Although odd dB SL levels were also tested in cats, only even levels are shown for clarity. *p≤0.05, **p≤0.001.

A. Guinea pigs

(Acoustic panel, left)

←decreasing CF   increasing CF→

B. Cats, monopolar electrical
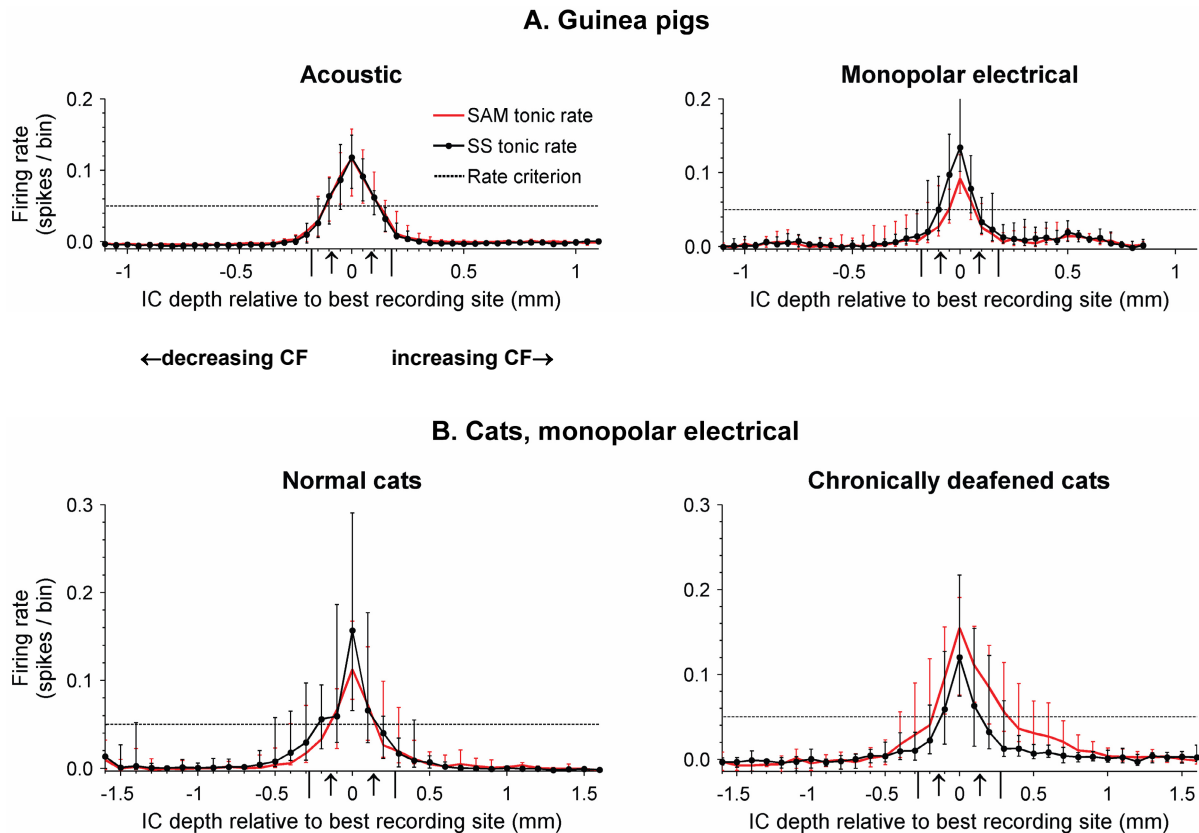
Fig. 11. Tonic response-rate profiles for pooled data in guinea pigs (A) and cats (B). In contrast to the patterns for max rates (Fig. 9), SAM tonic rates were very similar to SS tonic rates (the two were nearly identical for acoustic stimulation in guinea pigs). Median profiles of SS tonic rates were all narrowly tuned, exceeding the rate criterion over an extent of roughly ½ octave. Other figure details as in Figure 9.

Consistent with these tonic response-rate profiles, tonic activation widths for unmodulated steady-state and SAM conditions were relatively similar (Fig. 12). Widths were significantly broader for the SAM condition than for the unmodulated steady-state condition for 125-Hz SAM condition in guinea pigs and the 50-Hz SAM condition in chronically deafened cats (both monopolar electrical stimulation at 100% SAM depth). For acoustic stimulation in normal cats, tonic activation widths were only slightly broader for the 50-Hz SAM condition than for the unmodulated steady-state condition.

When peak firing rates for monopolar electrical stimuli and 60 dB SPL acoustic stimuli were matched, electrical and acoustic SAM stimuli produced similar max activation widths (Fig. 13). In guinea pigs, median activation widths were narrower for monopolar electrical stimuli than for acoustic stimuli by 8.9% and 19% for 50-Hz SAM and 125-Hz SAM respectively, but the differences were not statistically significant. For the one cat where this comparison could be made, monopolar electrical stimulation produced 5% broader activation than acoustic stimulation for 50-Hz SAM and 25% narrower activation for 125-Hz SAM (not significant).
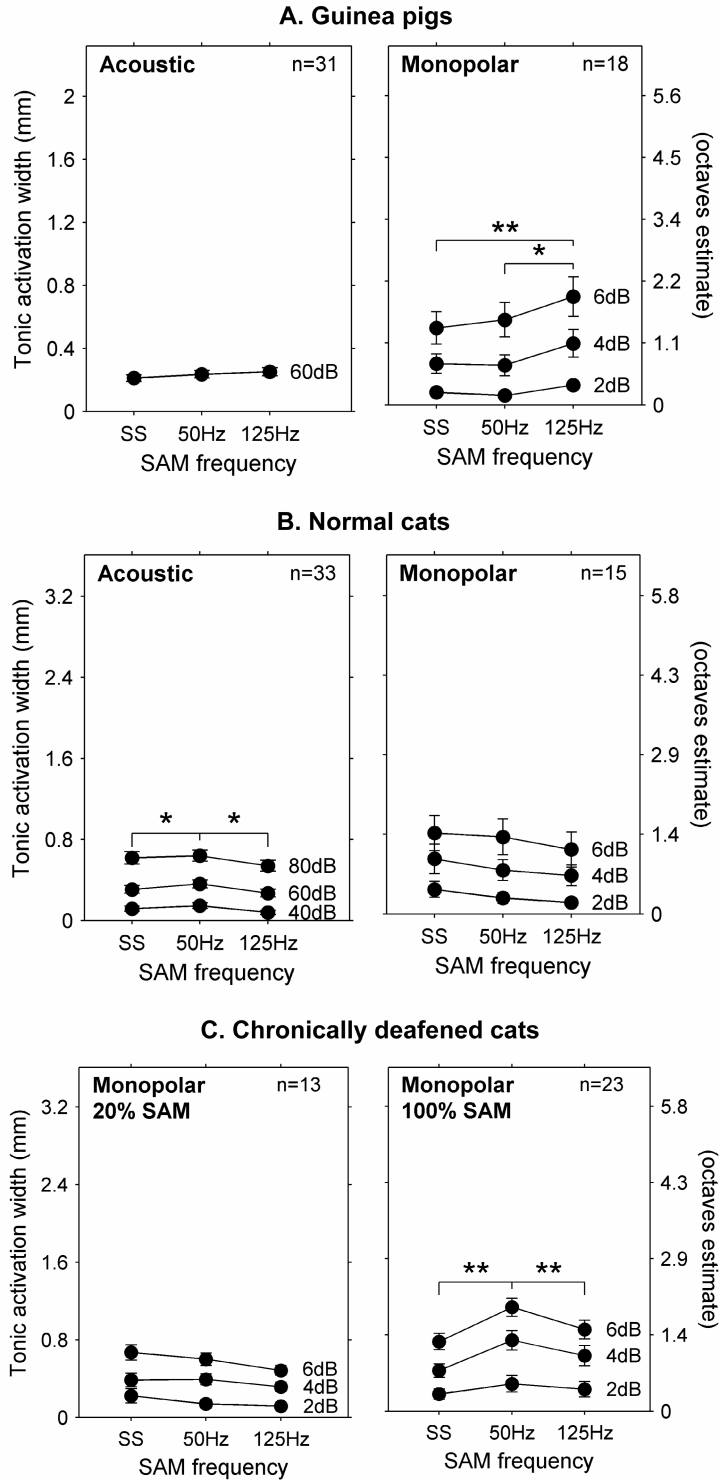
Fig. 12. Effect of amplitude modulation condition on tonic activation widths. With a few exceptions, tonic activation widths were similar for the SS, 50-Hz SAM, and 125-Hz SAM conditions. Figure details as in Fig. 10.
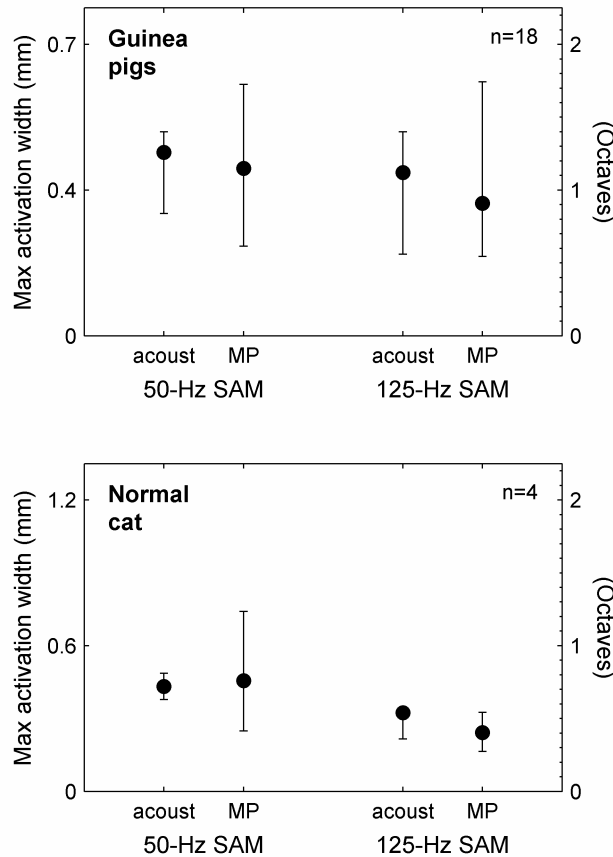
Fig. 13. Max activation widths were comparable for acoustic and monopolar electrical stimuli matched for equal peak spike rates. Acoustic SAM activation widths were not significantly different from electrical SAM activation widths in the three guinea pigs studied and in the one cat where this comparison could be made (p>0.05). Modulation depth was 100%. Values shown are medians and interquartile ranges. The number of acoustic tone frequencies and electrical stimulus channels compared were 18 and 4 for the three guinea pigs and one cat, respectively. (Abbreviations: acoust, acoustic; MP, monopolar electrical.)

Phase locking across the tonotopic axis of the IC

For acoustic and monopolar electrical stimulation in guinea pigs, normal cats, and chronically deafened cats, responses to 50-Hz SAM stimuli with a 100% modulation depth had vector strengths that exceeded that of the modulator waveform, were significantly phase locked, and had constant SAM time delays across a broad extent of the depth axis in the inferior colliculus. In guinea pigs, 60 dB SPL acoustic stimuli elicited responses with median vector strengths that exceeded the vector strength of the modulator waveform (0.5) over an extent of more than 360 μm, or roughly one octave, centered around the best recording site (Fig. 14). The median vector-strength profile was relatively flat across this one-octave span (ranging between 0.54 and 0.63). This relatively high, flat vector strength resulted in the profile of phase-locked spike rate resembling that of the SAM max rate (the phase-locked spike rate is equal to the product of the vector strength and the response rate). Phase locking was significant for 90% or more of the pooled values throughout the one octave span around the best recording site, and it continued to be significant for more than 50% the pooled values across a span of 800 μm (roughly 2.3 octaves). Median SAM time delays were constant (and equal to the delay at the best recording site) across more than one octave around the best recording site.

Phase-locking metrics for monopolar electrical stimuli (at intensities such that peak spike rates were similar to those of 60-dB SPL acoustic stimuli) in guinea pigs were similar to those of acoustic stimuli, but with higher vector strengths near the best recording site. Median vector strength profiles ranged between 0.54 and 0.76 within the one octave span around the best

56

recording site. Outside this range, they exhibited somewhat more variability than the vector strengths for acoustic stimulation. Similar to that for acoustic stimulation, the profile of phase-locked spikes resembled that of the SAM max rate. Phase locking was significant for 80% or more of the pooled values across the one octave span around the best recording site, and at least 50% of pooled values had significant phase locking over an extent of 510 μm (about 1.5 octaves). Median SAM time delays were within 1 millisecond of the delay at the best recording site across more than a one-octave span.

Profiles of phase-locking metrics for monopolar stimulation in normal cats (50-Hz SAM, 100% depth) were similar to those in guinea pigs (Fig. 15). However, in chronically deafened cats phase locking was stronger than in normal cats or guinea pigs. Median vector strengths in the chronically deafened cats ranged from 0.89 to 0.91 in the one octave span around the best recording site, and they exceeded the vector strength of the modulator waveform (0.5) over a span of 1800 μm (about 3.2 octaves). The peak value for the median profile of phase-locked spikes was 3.1 spikes per period (compared to 1.8 spikes per period in normal cats). At least 50% of the pooled values had significant phase locking over a span of 2100 μm (about 3.8 octaves). As in guinea pigs, median SAM time delay for both normal and chronically deafened cats was within 1 millisecond of the time delay at the best recording site over a span of more than one octave.

As a metric of average phase locking across IC depths, total vector strength was generally higher for the 50-Hz SAM condition than for the 125-Hz SAM condition (Table 1). For the 50-Hz SAM condition (100% SAM depth, vector strength of the modulator waveform = 0.5) in both guinea pigs and normal cats, median values of total vector strength for responses to $40 - 80$ dB SPL acoustic stimuli ranged from 0.46 to 0.57. In these same animals, median total vector strengths for responses elicited by $2 - 6$ dB SL monopolar electrical stimulation had a somewhat larger range (0.40 to 0.66) but still were not far from the 0.5 vector strength of the modulator waveform. Total vector strength for acoustic stimulation in normal cats (where multiple stimulus levels were tested) did not increase monotonically with stimulus level. In contrast, for monopolar electrical stimulation vector strength increased monotonically with stimulus level in almost all cases.

In chronically deafened cats, total vector strength for responses to monopolar electrical stimulation exhibited a stronger level dependence. For 50-Hz SAM at 100% modulation depth, a level of 2 dB SL elicited responses with a median total vector strength of 0.37 (lower than those in normal cats and guinea pigs) whereas levels of $4 - 6$ DB SL produced responses with total vector strengths of $0.74 - 0.86$ (considerably higher than in normal cats and guinea pigs). At a modulation depth of 20%, $2 - 6$ dB SL stimuli produced median total vector strengths from 0.24 to 0.70, greatly exceeding the 0.05 vector strength of the modulator waveform.
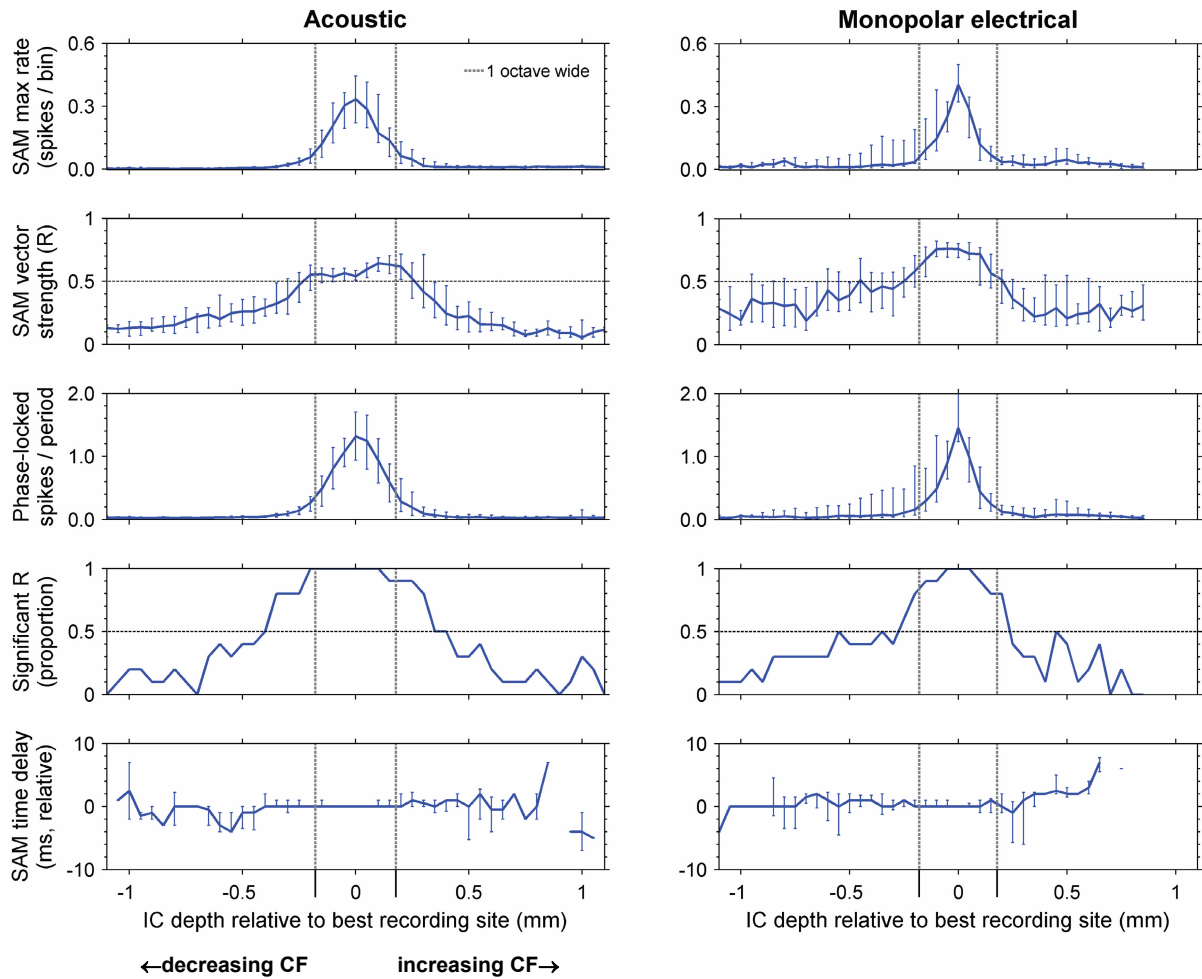
Fig. 14. Phase-locking profiles summarizing pooled data for IC responses in guinea pigs. Responses were to acoustic and monopolar electrical stimulation with 50-Hz SAM (100% SAM depth). SAM max rates are reproduced from Figure 9 for comparison with phase-locking profiles. For both acoustic and electrical stimulation, median SAM vector strength (R) exceeded the vector strength of the modulator waveform (0.5, indicated by the horizontal line) across a span of more than one octave. Profiles of phase-locked spikes resembled the profile of SAM max rates. Stimuli produced significant phase locking (significant R, p<0.01) across a broad extent of the IC (even where SAM max rates were close to zero); the horizontal line at 0.5 shows the boundary where the proportion of stimuli producing significant phase locking was 50%. SAM time delay was constant (equal to the delay at the best recording site) over a span of more than one octave. Values shown are medians and interquartile ranges. The distance between the vertical lines represents approximately one octave.
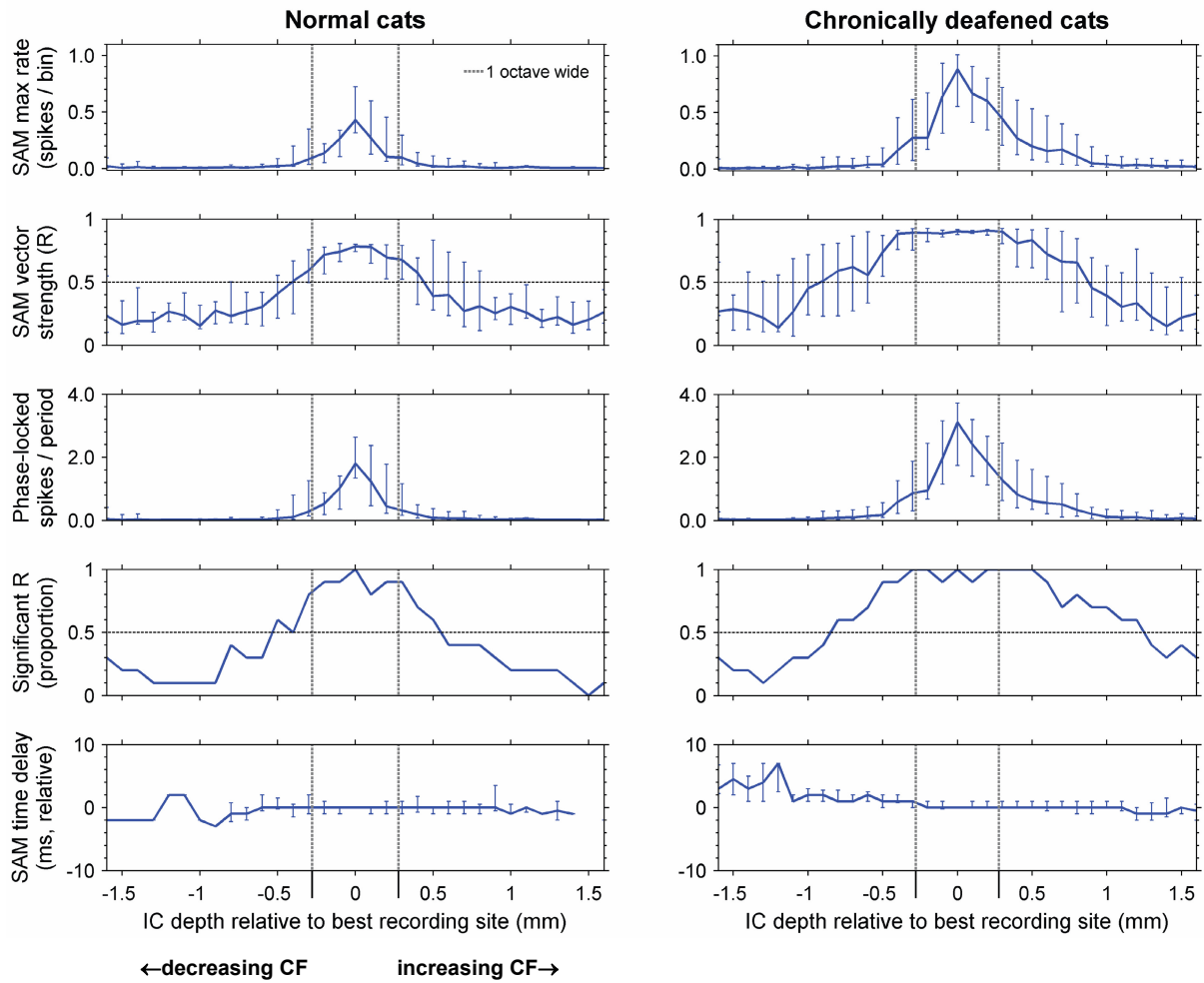
Fig. 15. Phase-locking profiles summarizing pooled data for responses recorded in normal and chronically deafened cats. Phase-locking profiles in normal cats were similar to those in guinea pigs (Fig. 14). In chronically deafened cats, however, vector strengths were higher (they were near 0.9 over a one-octave span around the best recording site), phase locked spikes were higher, and vector strengths were significant over a broader extent of the IC than in normal cats or guinea pigs. Other figure details as in Figure 14.

59

Table I. Effect of modulation frequency and stimulus level on total vector strength

	Acoustic stimulus level (dB SPL)	Electrical stimulus level (dB SL)	Total vector strength[1]		Sample size[2]
			50-Hz SAM	125-Hz SAM	
Guinea pigs 100% SAM depth	60		0.48 (0.42 - 0.51)	0.40 (0.35 - 0.49)	31
		2	0.40 (0.31 - 0.52)	0.42 (0.32 - 0.53)	18
		4	0.56 (0.50 - 0.62)	0.49 (0.36 - 0.56)	18
		6	0.60 (0.54 - 0.68)	0.42 (0.32 - 0.60)	18
Normal cats 100% SAM depth	40		0.51 (0.34 - 0.60)	0.29 (0.23 - 0.39)	29
	60		0.57 (0.52 - 0.58)	0.34 (0.30 - 0.43)	29
	80		0.46 (0.41 - 0.50)	0.30 (0.22 - 0.34)	29
		2	0.45 (0.36 - 0.59)	0.27 (0.24 - 0.39)	15
		4	0.62 (0.47 - 0.71)	0.38 (0.29 - 0.53)	15
		6	0.66 (0.54 - 0.73)	0.44 (0.27 - 0.59)	15
Chronically deafened cats					
100% SAM depth		2	0.37 (0.25 - 0.68)	0.20 (0.16 - 0.40)	23
		4	0.74 (0.54 - 0.89)	0.50 (0.33 - 0.70)	23
		6	0.86 (0.81 - 0.90)	0.67 (0.61 - 0.71)	23
20% SAM depth		2	0.24 (0.16 - 0.39)	0.18 (0.13 - 0.25)	13
		4	0.51 (0.40 - 0.68)	0.35 (0.23 - 0.54)	13
		6	0.70 (0.61 - 0.74)	0.58 (0.54 - 0.63)	13

[1]Values shown are medians (interquartile ranges. For comparison, the vector strength of the modulator waveform is 0.50 for 100% SAM depth and 0.050 for 20% SAM depth.

[2]Number of acoustic carrier frequencies or electrical stimulus channels tested across animal subjects.

DISCUSSION

These studies have demonstrated several fundamental features of the representation of SAM stimuli in the auditory midbrain of guinea pigs, normal cats, and chronically deafened cats. First, both acoustic and electrical 50-Hz SAM stimuli elicit activation across a broader extent of the tonotopic axis of the inferior colliculus than unmodulated steady-state stimuli, even when the SAM stimuli have only half the average intensity of the unmodulated stimuli. In addition, data indicate that the extents of activation in response to SAM stimuli are not different for acoustic tones and monopolar electrical pulse trains when intensities of the two types of stimulation are matched by peak spike-rates. Further, both acoustic and electrical SAM stimuli elicit responses that phase-lock to the modulator waveform across a broad extent of the tonotopic axis of the inferior colliculus.

These findings are supported by several lines of evidence. Specifically, at least three results indicate that activation extends more broadly across the tonotopic axis of the IC for 50-Hz SAM stimuli than for unmodulated steady-state stimuli. First, maximum activation widths were broader for 50-Hz SAM stimuli than for unmodulated steady-state stimuli (Fig. 10). In normal cats and guinea pigs, mean differences for 100% SAM depths versus unmodulated stimuli were about 50% - 70% for acoustic stimulation at 60 dB SPL, and roughly 45 – 60% for monopolar electrical stimulation at 4 dB SL. In chronically deafened cats the mean difference for monopolar electrical stimulation at 4 dB SL was even greater at 160%. Next, 50-Hz SAM max rate profiles exceeded SS max rate profiles across an extent of more than one octave (Figs. 6 and 9). Finally, an example of unit responses showed considerably broader sustained tuning to 50-Hz SAM pulse trains than to unmodulated pulse trains. These findings are particularly compelling because the SAM intensities were modulated downward from the unmodulated intensities and thus delivered substantially less energy.

The finding that the extents of activation in response to SAM stimuli are not different for acoustic tones as compared to monopolar electrical pulse trains is supported by results in guinea pigs and data from one normal cat. For equal peak spike rates, maximum activation widths for acoustic and monopolar electrical stimulation had similar medians (Fig. 13). Maximum and tonic SAM response rate profiles for equal peak spike rates also showed similar tuning for acoustic and monopolar electrical stimuli in guinea pigs (Fig. 9A, Fig. 11A).

For both acoustic and electrical SAM stimuli, the finding that responses phase-lock to the modulator waveform across a broad extent of the tonotopic axis of the inferior colliculus is supported by profiles of phase-locking metrics and by total vector strength measurements in guinea pigs and cats. Median vector strengths exceeded the 0.5 vector strength of the 100% SAM depth modulator waveform over an extent of about one octave centered around the best recording site for acoustic and electrical stimulation (Figs. 14 and 15). Furthermore, phase locking was significant for at least 50% of SAM stimuli across an extent of more than 2 octaves for acoustic stimuli in guinea pigs, more than 1.5 octaves for monopolar electrical stimuli in guinea pigs and normal cats, and greater than 3 octaves for monopolar electrical stimuli in chronically-deafened cats. The SAM time delay was nearly constant across an extent of more than one octave for both acoustic and electrical stimuli. Also, total vector strength measurements showed values that were close to or that exceeded the vector strength of the modulator waveform for 50-Hz SAM acoustic and electrical stimuli in guinea pigs and cats (Table I).

In considering this evidence, some possible explanations and comparisons with previous studies can be made. Tuning seems to be similarly narrow for 50-Hz SAM and unmodulated steady-state conditions when examining the tonic rate (Figs. 11, 12), but 50-Hz SAM activation becomes more intense and broadens at a specific time during its period, phase locked to the modulator envelope and constant in phase across the responding portion of the inferior colliculus. This heightening and broadening of SAM activation could underlie the ability of listeners to detect and discriminate the SAM envelope (Churcher et al., 1934; Kay, 1982; Shannon, 1992), while narrow tonic tuning could help preserve their the ability to discriminate the carrier (Small, 1955). The observation that this broadening of activation occurs even for low electrical modulation depths (Fig. 10, 20% modulation below the peak intensity, equivalent to 11% modulation above and below a reference level) could help account for the ability of many cochlear implant users to detect amplitude modulation at very low modulation depths (Fu, 2002). Furthermore, the higher

and broader maximum SAM activation could also be associated with the increase in loudness reported for some acoustic and electrical SAM stimuli relative to unmodulated stimuli (McKay et al., 2010; Zhang et al., 1997).

The finding that 50-Hz SAM stimuli elicit activation across a broader extent of the tonotopic axis of the IC than unmodulated steady-state stimuli is also related to the finding reported in Chapter 2 that activation in response to the onset of an unmodulated stimulus extends more broadly than sustained activation. In both cases, activation in response to a dynamic stimulus produces a broader representation across the frequency gradient of the IC than activation in response to a constant stimulus. For acoustic tones at 60 dB SL, mean onset activation for unmodulated tones extended across a range of $2 - 3$ octaves (Chapter 2). Acoustic tones at 60 dB in the present study produced activation widths of $1 - 1.25$ octaves for the 50-Hz SAM condition and $0.7 - 0.73$ octaves for the unmodulated steady-state condition. The broad onset activation for unmodulated tones followed by narrower steady-state activation may represent wideband activation followed by a wideband suppression of some kind (perhaps refractoriness, adaptation, or inhibition) around the relatively narrow region of sustained activation. This pattern of excitation and suppression seems to alternate for a SAM stimulus, producing a maximum activation that is broad and a minimum activation that can even disappear at some times during the SAM period (Fig. 3). Furthermore, significant synchrony to the SAM envelope extends even more broadly across the IC than maximum SAM response rates would suggest (Figs. 14 and 15).

This possible combination of wideband excitation and suppression is consistent with a number of psychophysical observations. One simple observation is that for acoustic pure tones, durations of less than $10 - 20$ ms sound like clicks, whereas longer durations take on a tonal quality (Gabor, 1947). This could be related to the broad response across the tonotopic axis of the IC at the tone onset followed by the narrower steady state response. Another phenomenon is overshoot, in which a probe tone can be masked by a preceding tone, distant in frequency, provided that the two tones have onsets that are close in time to one another. In this case it is possible that the broad onset response to the masker tone suppresses the response to the distant probe tone. In the realm of SAM stimuli a number of psychophysical phenomena show interactions for carrier-frequency differences that exceed a critical band such as comodulation masking release and modulation detection interference (Grose et al., 2005; Verhey et al., 2003). In some cases these interactions can occur for carrier-frequency differences of up to 3-octaves. These interactions also often occur for binaural stimuli, and wideband inhibition has been proposed as one possible mechanism. Previous results have shown binaural interactions (Fitzpatrick et al., 2009) and wideband inhibition (Li et al., 2006) for IC responses to SAM tones, suggesting that the IC may be an interesting place to investigate correlates of these cross-critical-band phenomena.

With regard to speech reception, it seems likely that detection of onset of utterances, differentiation of phonemes and speaker localization, which are all related to sound onset (Ter-Mikaelian et al., 2007), might benefit from a broader representation of the onset response in the IC (Chapter 2). In contrast, precise spectral information contained in vowels (Xu et al., 2008) may be better represented by the narrower steady-state response. Broader responses to amplitude-modulations in speech might aid in speaker localization and auditory grouping, which are phenomena that depend on processing envelope information (Joris et al., 2004).

The finding that the extents of activation in response to SAM stimuli are not different for acoustic tones versus monopolar electrical pulse trains is also related to the findings for unmodulated stimuli presented in Chapter 2. In that chapter, it was shown that onset responses tended to be broader for monopolar electrical stimulation than for acoustic stimulation, but that sustained responses were similar or narrower for monopolar electrical stimulation. It appears that activation widths in response to SAM stimuli lie somewhere between those of onset and sustained responses and that there is no consistent difference between monopolar and acoustic SAM activation widths, at least for the 50-Hz and 125-Hz envelopes investigated. For both onset responses (Chapter 2) and SAM maximum responses (this Chapter), monopolar electrical stimulation elicited more variable activation than acoustic stimulation, indicating that in a minority of cases the extent of monopolar activation in response to dynamic stimuli could be quite broad (Fig 9A).

Phase-locking results for acoustic SAM tones results reported in the present study are consistent with those from previous studies, but the present observations extend these results to include neurons with characteristic frequencies far from the SAM carrier frequency. The high vector strengths observed in the present study were comparable to values reported for SAM tones in the auditory nerve (Joris et al., 1992) and inferior colliculus (Nelson et al., 2007); but in the present study these high vector strengths were also observed for neurons with characteristic frequencies across a span of about one octave centered at the best recording site (Fig. 14). The relatively constant SAM delays across neurons with different characteristic frequencies seen in the present study are also consistent to results seen in the auditory nerve (Joris, 1996). However, in that study phase was only measured for characteristic frequencies up to 0.2 octaves distant from the carrier frequency, whereas in the present study constant delays were for characteristic frequencies more than 1 octave away from the acoustic carrier frequency (Fig. 14). This broad, constant SAM time delay could be particularly useful for a cross-critical-band coincidence detector at a higher processing center.

Our finding that total vector strengths (Table 1) were higher for the 50-Hz SAM condition than for the 125-Hz SAM condition is consistent with previous neurophysiologic and psychophysical findings. For acoustic SAM tones with best frequency carriers, it has been reported that single IC neurons tend to have best modulation frequencies ranging from 10 – 100 Hz (Nelson et al., 2007). Similarly, a study of IC responses to SAM electrical pulse trains reported that maximum modulation following frequencies had mean values of 34 Hz and 42 Hz for band-pass and low-pass neurons, respectively (Snyder et al., 2000). The results of the present study are also consistent with psychophysical evidence in humans, which show acoustic modulation transfer functions having a low pass cutoff of roughly 50 Hz (Viemeister, 1979) and similar characteristics for electrical modulation transfer functions (Busby et al., 1993). It may be that the period of the 50-Hz SAM condition (20 ms) allows the neurons to recover from refractory effects, inhibition, or adaptation after each period whereas the shorter period of the 125-Hz SAM condition (8 ms) allows less recovery.

With regard to level effects, the non-monotonic functions of total vector strength versus acoustic level in our study are consistent with non-monotonic vector strength versus level functions observed in the auditory nerve and cochlear nucleus (Joris et al., 1992; Moller, 1974). The contrasting monotonic increases of total vector strength with electrical stimulus level are consistent with cochlear implant psychophysics (Shannon, 1992).

Having argued that the findings of the present study are consistent with findings of previous neurophysiologic and psychoacoustic studies, we now comment on some alternative explanations of our results. We suggested that the broader extents of onset and SAM maximum activation compared to steady-state activation could be due to a combination of wideband excitation and suppression in the IC. It might be proposed instead that the broad extent of responses to tone onsets and SAM tones are caused by the broad spectral bandwidth of these signals relative to an unmodulated tone of long duration (Kay, 1974). This broad spectral bandwidth would tend to excite a larger portion of the basilar membrane and produce a broader extent of neuronal responses at the tone onset and for SAM tones. While these spectral bandwidth differences do exist, it seems unlikely that they are the only or even the primary cause of the large differences we observed in the extent of neuronal activation. For one reason, the tone onset was not a step function, but had had a cosine on-ramp of 2-3 milliseconds to prevent a sudden transition (reducing the spectral bandwidth of the tone onset). Also, the 50-Hz SAM tones, which effectively had an on-ramp of 5 milliseconds, also showed a broader response for the stimulus onset than for later periods (Fig. 1). However, the most convincing evidence against this possibility is that the responses to electrical stimulation also showed a large difference between the extent of onset or SAM activation and unmodulated steady-state activation, and electrical stimulation in a deafened animal completely bypasses basilar membrane mechanics.

It could also be argued that the broad phase locking and constant SAM time delays for electrical stimulation are due to stimulus artifacts. We believe this is highly unlikely for two reasons. First, SAM time delays were constant relative to the delay at the best recording site, and for electrical stimulation the SAM time delay at the best recording site was on the order of 5 ms (Figs. 3 and 4). We would expect SAM time delays for electrical artifacts to have essentially zero time delay because of their near instantaneous transmission from stimulating to recording electrode. Second, phase locking and constant SAM time delays were also broad for responses to acoustic SAM tones, for which there are no electrical stimulus artifacts.

It is also worthwhile to discuss some limitations of the present study. One potentially important limitation was that our study was carried out in anesthetized animals (a mixture of ketamine and xylazine was used in guinea pigs and sodium pentobarbital was used in cats). One study reported that sodium pentobarbital increases inhibitory effects in the IC, altering response latencies and firing patterns in some IC neurons (Kuwada et al., 1989). Another study, however, has shown that although a mixture of ketamine and sodium pentobarbital has a profound effect on the temporal response properties of neurons in the auditory cortex, it has only a mild effect in the IC (Ter-Mikaelian et al., 2007). While this second study reported only small effects of anesthesia on the IC phase-locking metrics reported in the present study, it would be interesting to repeat the experiments described here in an unanesthetized preparation to investigate further the possible effects of anesthesia.

Another potential limitation was that our study focused largely on multi-unit data rather than single-unit data. The multi-site recording probes we used had relatively large recording site areas that did not always allow isolation of single units, but did allow recording of multi-unit responses on almost every recording site. Because our aim was not to characterize the responses of single units, but to characterize the population response of neurons across the tonotopic axis of the inferior colliculus, it was advantageous for us to use these multi-site probes. Furthermore, a

previous study has shown that for single and multi-unit responses in the IC temporal response properties correspond closely (Langner et al., 1988).

A third potential limitation was that data collection was limited to a single IC penetration in each animal, and we specifically selected a penetration that had robust sustained responses. Some of the other penetrations in the IC tended to show primarily onset responses with weak or absent sustained responses. It is not clear whether the processing of SAM stimuli would have been different in these other penetrations. However, because previous studies found that most IC neurons that do not respond to amplitude modulation are "onset only" neurons (Condon et al., 1996; Shaddock Palombi et al., 2001), it seems likely that neurons along penetrations with robust sustained responses would respond better to SAM stimuli than neurons along penetrations with primarily onset responses.

After having addressed the limitations of the present study, we now discuss the somewhat surprising finding that chronically deafened cats exhibited broader extents of 50-Hz SAM activation and stronger phase locking in response to monopolar electrical stimulation than did normal (acutely deafened) cats. It does not seem that the difference between normal and chronically different cats was simply due to a level difference because their unmodulated steady-state responses at 4 dB SL were similar (Figs. 9B and 11B). It is possible that this difference is related to the observation that the auditory nerve shows stronger phase locking for electrical stimulation in acutely deafened cats than for acoustic stimulation in normal hearing cats (Litvak et al., 2001; Litvak et al., 2003a). This difference has been attributed to the lack of spontaneous activity in the auditory nerve of acutely deafened cats causing neurons to loose their stochastic firing properties and entrain to the stimulus period. It could be that a similar effect caused the difference between chronically deafened and acutely deafened cats, and that spontaneous activity throughout the auditory system decreased over time in the chronically deafened cats.

It is also possible that chronic stimulation played a role in causing difference between normal and chronically deafened / stimulated cats. Chronic electrical stimulation has been reported in previous studies to produce several long term changes in responses of IC neurons including increased temporal resolution for higher stimulation rates (Vollmer et al., 1999) and broader IC tuning for chronic stimulation on a single bipolar channel (Leake et al., 2000; Moore et al., 2002). However, chronic deafness itself may have also played a role. This is suggested by the observation that activation width patterns for the one chronically deafened, *non*-stimulated cat were significantly different from the normal cats, but not significantly different from the chronically deafened, stimulated cats (see Methods: statistical analyses). Because only one non-stimulated, chronically deafened cat was studied, more experiments will need to be performed to determine the contributions of chronic stimulation and chronic deafening to the differences seen relative to acutely deafened cats.

In summary, we found that SAM stimuli can elicit activation across a broad extent of the tonotopic axis of the inferior colliculus, that this activation is strongly phase locked to the SAM stimulus, and that activation patterns do not differ markedly for acoustic and electrical stimulation in normal / acutely deafened animals. Coupled with the broad extents of activation observed for onset responses in Chapter 2, our results suggest that a number of cross-critical-band interactions could take place at the level of the inferior colliculus. Furthermore, our results suggest that the spatial extent and temporal properties of IC activation for a wide range of stimuli

including speech should be compared for acoustic stimulation in normal animals and electrical stimulation in chronically deafened animals with a view towards implementing speech processing strategies that replicate normal acoustic patterns with electrical stimulation in cochlear implant users.

Conclusion

A 32-channel recording system with fast-recovery from electrical stimulus artifacts was designed, implemented, and applied *in vivo* to study neuronal responses to cochlear implant stimulation in animal models. The system was shown to accurately and efficiently record neuronal responses to intracochlear electrical stimulation at clinically relevant rates of up to 2000 pulses per second, making it a valuable tool for the study of central auditory responses to complex multichannel stimulation delivered by contemporary cochlear implants. In addition to being well-suited to the study of channel interactions in cochlear implants, the system could also prove useful in the analysis of responses to multichannel stimulation delivered by other neural prostheses.

This recording system was applied *in vivo* in guinea pigs and cats to characterize responses in the auditory midbrain (inferior colliculus) to acoustic and electrical intracochlear stimulation. Results indicated that the extent of activation of the inferior-colliculus (i.e. the inferred spectral tuning) for 1000-pulse/s electrical stimuli is broad for the initial onset phase of the response and substantially narrower for the subsequent sustained response. In addition, analysis of data comparing monopolar and bipolar modes of stimulation revealed that when stimulation levels are matched to produce similar peak spike rates, monopolar and bipolar stimulation elicit similar extents of activation in the inferior colliculus. Together, these two findings may help explain the observation that despite some indications of narrower tuning for bipolar stimulation using single pulses in animal studies, human cochlear implant users do not generally perform better with bipolar stimulation than with monopolar stimulation using high-rate pulse trains modulated by speech signals. The unexpected finding that, using a space-filling cochlear-implant electrode, monopolar pulse trains produce more selective sustained activation than acoustic tones also suggests that it may indeed be worthwhile to design intracochlear electrodes with higher densities of stimulating contacts that lie close to their target neural elements. With such arrays, it may be possible to provide cochlear implant users with much finer spectral resolution than current systems allow.

The study of inferior-colliculus responses to acoustic and electrical sinusoidally amplitude-modulated stimuli demonstrated that 50-Hz SAM stimuli generally elicit activation across a broad extent of the tonotopic axis of the inferior colliculus and that this activation is strongly phase locked to the SAM envelope. Data also revealed that SAM activation patterns do not differ markedly for acoustic and electrical stimulation in normal (acutely deafened) control animals, when signals are matched appropriately for intensity. Coupled with the broad extents of activation observed for onset responses, these results suggest that a number of cross-critical-band interactions may commonly occur at the level of the inferior colliculus for both acoustic and cochlear-implant stimulation.

Together, these results suggest that it would be extremely interesting and valuable to study the spatial extent and temporal properties of IC activation for a wide range of stimuli including speech and to directly compare responses elicited by acoustic stimulation and electrical stimulation. These comparisons could reveal the relative similarities and differences in neuronal processing for acoustic and electrical speech sounds such as onsets of phonemes, sustained vowels, and speech tokens from multiple talkers. A good starting point for these investigations of

multiple sound sources might be to use simpler stimuli such as SAM acoustic tones and electrical pulse trains delivered on multiple carrier frequencies or stimulus channels. These studies would be likely to yield insights into the current limitations experienced by cochlear implant users, as well as suggest new cochlear-implant processing strategies that could elicit response patterns more closely approximating normal acoustic responses. Ultimately, such research should help cochlear-implant users realize the benefits of more normal auditory perception in challenging conditions such as listening to music or tonal languages, and speech understanding with multiple talkers in noisy environments.

References

Aitkin, L., Tran, L., Syka, J. 1994. The responses of neurons in subdivisions of the inferior colliculus of cats to tonal, noise and vocal stimuli. Exp Brain Res 98, 53-64.

Azin, M., Chiel, H.J., Mohseni, P. 2007. Comparisons of FIR and IIR implementations of a subtraction-based stimulus artifact rejection algorithm, Proceedings of the 29th Annual International Conference of the IEEE EMBS. pp. 1437-40.

Bierer, J.A. 2007. Threshold and channel interaction in cochlear implant users: evaluation of the tripolar electrode configuration. J Acoust Soc Am 121, 1642-53.

Bierer, J.A., Middlebrooks, J.C. 2004. Cortical responses to cochlear implant stimulation: channel interactions. J Assoc Res Otolaryngol 5, 32-48.

Bilger, R.C., Black, F.O. 1977a. Auditory prostheses in perspective. Ann Otol Rhinol Laryngol Suppl 86, 3-10.

Bilger, R.C., Hopkinson, N.T. 1977b. Hearing performance with the auditory prosthesis. Ann Otol Rhinol Laryngol Suppl 86, 76-91.

Boex, C., Kos, M.I., Pelizzone, M. 2003a. Forward masking in different cochlear implant systems. J Acoust Soc Am 114, 2058-65.

Boex, C., de Balthasar, C., Kos, M.I., Pelizzone, M. 2003b. Electrical field interactions in different cochlear implant systems. J Acoust Soc Am 114, 2049-57.

Boex, C., Baud, L., Cosendai, G., Sigrist, A., Kos, M.I., Pelizzone, M. 2006. Acoustic to electric pitch comparisons in cochlear implant subjects with residual hearing. J Assoc Res Otolaryngol 7, 110-24.

Bonham, B.H., Litvak, L.M. 2008. Current focusing and steering: modeling, physiology, and psychophysics. Hear Res 242, 141-53.

Brown, E.A., Ross, J.D., Blum, R.A., Yoonkey, N., Wheeler, B.C., DeWeerth, S.P. 2008. Stimulus-artifact elimination in a multi-electrode system. IEEE Transactions on Biomedical Circuits and Systems 2, 10-21.

Busby, P.A., Tong, Y.C., Clark, G.M. 1993. The perception of temporal modulations by cochlear implant patients. J Acoust Soc Am 94, 124-31.

Cai, S., Ma, W.L., Young, E.D. 2009. Encoding intensity in ventral cochlear nucleus following acoustic trauma: implications for loudness recruitment. J Assoc Res Otolaryngol 10, 5-22.

Chatterjee, M. 1999. Effects of stimulation mode on threshold and loudness growth in multielectrode cochlear implants. J Acoust Soc Am 105, 850-60.

Chatterjee, M., Oba, S.I. 2004. Across- and within-channel envelope interactions in cochlear implant listeners. J Assoc Res Otolaryngol 5, 360-75.

Churcher, B.G., King, A.J., Davies, H. 1934. The minimum perceptible change of intensity of a pure tone. Philos. Mag. 18, 927-939.

Cohen, L.T., Saunders, E., Clark, G.M. 2001. Psychophysics of a prototype peri-modiolar cochlear implant electrode array. Hear Res 155, 63-81.

Condon, C.J., White, K.R., Feng, A.S. 1996. Neurons with different temporal firing patterns in the inferior colliculus of the little brown bat differentially process sinusoidal amplitude-modulated signals. J Comp Physiol A 178, 147-57.

Creutzfeldt, O., Hellweg, F.C., Schreiner, C. 1980. Thalamocortical transformation of responses to complex auditory stimuli. Exp Brain Res 39, 87-104.

DeMichele, G.A., Troyk, P.R. 2003. Stimulus-resistant neural recording amplifier, Proceedings of the 25th Annual International Conference of the IEEE Engineering in Medicine and Biology Society, Vol. 4. pp. 3329-32.

Egorova, M., Ehret, G. 2008. Tonotopy and inhibition in the midbrain inferior colliculus shape spectral resolution of sounds in neural critical bands. Eur J Neurosci 28, 675-92.

Ehret, G., Merzenich, M.M. 1988. Neuronal discharge rate is unsuitable for encoding sound intensity at the inferior-colliculus level. Hear Res 35, 1-7.

Finley, C.C., Holden, T.A., Holden, L.K., Whiting, B.R., Chole, R.A., Neely, G.J., Hullar, T.E., Skinner, M.W. 2008. Role of electrode placement as a contributor to variability in cochlear implant outcomes. Otol Neurotol 29, 920-8.

Fitzpatrick, D.C., Roberts, J.M., Kuwada, S., Kim, D.O., Filipovic, B. 2009. Processing temporal modulations in binaural and monaural auditory stimuli by neurons in the inferior colliculus and auditory cortex. J Assoc Res Otolaryngol 10, 579-93.

Freeman, J.A. 1971. An electronic stimulus artifact suppressor. Electroencephalography and Clinical Neurophysiology 31, 170-2.

Friesen, L.M., Shannon, R.V., Cruz, R.J. 2005. Effects of stimulation rate on speech recognition with cochlear implants. Audiol Neurootol 10, 169-84.

Frisina, R.D. 2001. Subcortical neural coding mechanisms for auditory temporal processing. Hear Res 158, 1-27.

Frisina, R.D., Smith, R.L., Chamberlain, S.C. 1990. Encoding of amplitude modulation in the gerbil cochlear nucleus: I. A hierarchy of enhancement. Hear Res 44, 99-122.

Fu, Q.J. 2002. Temporal processing and speech recognition in cochlear implant users Neuroreport 13, 1635-9.

Gabor, D. 1947. Acoustical quanta and the theory of hearing. Nature 159, 591-4.

Gnadt, J.W., Echols, S.D., Yildirim, A., Honglei, Z., Paul, K. 2003. Spectral cancellation of microstimulation artifact for simultaneous neural recording in situ. IEEE Transactions on Biomedical Engineering 50, 1129-35.

Goldberg, J.M., Brown, P.B. 1969. Response of binaural neurons of dog superior olivary complex to dichotic tonal stimuli: some physiological mechanisms of sound localization. J Neurophysiol 32, 613-36.

Grose, J.H., Hall, J.W., 3rd, Buss, E. 2005. Across-channel spectral processing. Int Rev Neurobiol 70, 87-119.

Hall, J.W., Haggard, M.P., Fernandes, M.A. 1984. Detection in noise by spectro-temporal pattern analysis. J Acoust Soc Am 76, 50-6.

Harris, D.M., Shannon, R.V., Snyder, R., Carney, E. 1997. Multi-unit mapping of acoustic stimuli in gerbil inferior colliculus. Hear Res 108, 145-56.

Hashimoto, T., Elder, C.M., Vitek, J.L. 2002. A template subtraction method for stimulus artifact removal in high-frequency deep brain stimulation. J Neurosci Methods 113, 181-6.

Heffer, L.F., Fallon, J.B. 2008. A novel stimulus artifact removal technique for high-rate electrical stimulation. Journal of Neuroscience Methods 170, 277-84.

Huffman, R.F., Argeles, P.C., Covey, E. 1998. Processing of sinusoidally amplitude modulated signals in the nuclei of the lateral lemniscus of the big brown bat, Eptesicus fuscus. Hear Res 126, 181-200.

Javel, E. 1980. Coding of AM tones in the chinchilla auditory nerve: implications for the pitch of complex tones. J Acoust Soc Am 68, 133-46.

Joris, P.X. 1996. Envelope coding in the lateral superior olive. II. Characteristic delays and comparison with responses in the medial superior olive. J Neurophysiol 76, 2137-56.

Joris, P.X. 2009. Recruitment of neurons and loudness. Commentary on "Encoding intensity in ventral cochlear nucleus following acoustic trauma: implications for loudness recruitment" by Cai et al. J. Assoc. Res. Otolaryngol. DOI: 10.1007/s10162-008-0142-y. J Assoc Res Otolaryngol 10, 1-4.

Joris, P.X., Yin, T.C. 1992. Responses to amplitude-modulated tones in the auditory nerve of the cat. J Acoust Soc Am 91, 215-32.

Joris, P.X., Schreiner, C.E., Rees, A. 2004. Neural processing of amplitude-modulated sounds. Physiol Rev 84, 541-77.

Kay, R.H. 1974. The physiology of auditory frequency analysis. Prog Biophys Mol Biol 28, 109-88.

Kay, R.H. 1982. Hearing of modulation in sounds. Physiol Rev 62, 894-975.

Kileny, P.R., Zwolan, T.A., Telian, S.A., Boerst, A. 1998. Performance with the 20 + 2L lateral wall cochlear implant. Am J Otol 19, 313-9.

Kral, A., Hartmann, R., Mortazavi, D., Klinke, R. 1998. Spatial resolution of cochlear implants: the electrical field and excitation of auditory afferents. Hear Res 121, 11-28.

Kuwada, S., Batra, R., Stanford, T.R. 1989. Monaural and binaural response properties of neurons in the inferior colliculus of the rabbit: effects of sodium pentobarbital. J Neurophysiol 61, 269-82.

Kwon, B.J., van den Honert, C. 2006. Effect of electrode configuration on psychophysical forward masking in cochlear implant listeners. J Acoust Soc Am 119, 2994-3002.

Langner, G. 1992. Periodicity coding in the auditory system. Hear Res 60, 115-42.

Langner, G., Schreiner, C.E. 1988. Periodicity coding in the inferior colliculus of the cat. I. Neuronal mechanisms. J Neurophysiol 60, 1799-822.

Leake, P.A., Hradek, G.T., Snyder, R.L. 1999. Chronic electrical stimulation by a cochlear implant promotes survival of spiral ganglion neurons after neonatal deafness. J Comp Neurol 412, 543-62.

Leake, P.A., Snyder, R.L., Rebscher, S.J., Moore, C.M., Vollmer, M. 2000. Plasticity in central representations in the inferior colliculus induced by chronic single- vs. two-channel electrical stimulation by a cochlear implant after neonatal deafness. Hear Res 147, 221-41.

Li, H., Sabes, J.H., Sinex, D.G. 2006. Responses of inferior colliculus neurons to SAM tones located in inhibitory response areas. Hear Res 220, 116-25.

Liang, D.H., Lusted, H.S., White, R.L. 1999. The nerve-electrode interface of the cochlear implant: current spread. IEEE Trans Biomed Eng 46, 35-43.

Litvak, L., Delgutte, B., Eddington, D. 2001. Auditory nerve fiber responses to electric stimulation: modulated and unmodulated pulse trains. J Acoust Soc Am 110, 368-79.

Litvak, L.M., Delgutte, B., Eddington, D.K. 2003a. Improved temporal coding of sinusoids in electric stimulation of the auditory nerve using desynchronizing pulse trains. J Acoust Soc Am 114, 2079-98.

Litvak, L.M., Smith, Z.M., Delgutte, B., Eddington, D.K. 2003b. Desynchronization of electrically evoked auditory-nerve activity by high-frequency pulse trains of long duration. J Acoust Soc Am 114, 2066-78.

Mardia, K.V. 1972. Statistics of directional data. London: Academic.

McGill, K.C., Cummins, K.L., Dorfman, L.J., Berlizot, B.B., Luetkemeyer, K., Nishmura, D.G., Widrow, B. 1982. On the nature and elimination of stimulus artifact in nerve signals evoked and recorded using surface electrodes. IEEE Transactions on Biomedical Engineering BME-29, 129-37.

McKay, C.M., Henshall, K.R. 2010. Amplitude modulation and loudness in cochlear implantees. J Assoc Res Otolaryngol 11, 101-11.

Merzenich, M.M., White, M.W. 1977. Cochlear implant: the interface problem. In: Hambrecht, F.T., and Reswich, J.B., (Ed.), Functional Electrical Stimulation: Applications in Neural Prosthesis. Dekker, New York. pp. 321-340.

Middlebrooks, J.C. 2004. Effects of cochlear-implant pulse rate and inter-channel timing on channel interactions and thresholds. Journal of the Acoustical Society of America 116, 452-68.

Middlebrooks, J.C. 2008. Auditory cortex phase locking to amplitude-modulated cochlear implant pulse trains. J Neurophysiol 100, 76-91.

Middlebrooks, J.C., Snyder, R.L. 2007. Auditory prosthesis with a penetrating nerve array. J Assoc Res Otolaryngol.

Moller, A.R. 1974. Responses of units in the cochlear nucleus to sinusoidally amplitude-modulated tones. Exp Neurol 45, 105-17.

Moore, C.M., Vollmer, M., Leake, P.A., Snyder, R.L., Rebscher, S.J. 2002. The effects of chronic intracochlear electrical stimulation on inferior colliculus spatial representation in adult deafened cats. Hear Res 164, 82-96.

Morris, D.J., Pfingst, B.E. 2000. Effects of electrode configuration and stimulus level on rate and level discrimination with cochlear implants. J Assoc Res Otolaryngol 1, 211-23.

Nelson, D.A., Donaldson, G.S., Kreft, H. 2008. Forward-masked spatial tuning curves in cochlear implant users. J Acoust Soc Am 123, 1522-43.

Nelson, P.C., Carney, L.H. 2007. Neural rate and timing cues for detection and discrimination of amplitude-modulated tones in the awake rabbit inferior colliculus. J Neurophysiol 97, 522-39.

Nelson, P.G., Erulkar, S.D., Bryan, J.S. 1966. Responses of units of the inferior colliculus to time-varying acoustic stimuli. J Neurophysiol 29, 834-60.

Nuding, S.C., Chen, G.D., Sinex, D.G. 1999. Monaural response properties of single neurons in the chinchilla inferior colliculus. Hear Res 131, 89-106.

Pfingst, B.E., Burkholder-Juhasz, R.A., Zwolan, T.A., Xu, L. 2008. Psychophysical assessment of stimulation sites in auditory prosthesis electrode arrays. Hear Res 242, 172-83.

Pfingst, B.E., Franck, K.H., Xu, L., Bauer, E.M., Zwolan, T.A. 2001. Effects of electrode configuration and place of stimulation on speech perception with cochlear prostheses. J Assoc Res Otolaryngol 2, 87-103.

Ramachandran, R., Davis, K.A., May, B.J. 1999. Single-unit responses in the inferior colliculus of decerebrate cats. I. Classification based on frequency response maps. J Neurophysiol 82, 152-63.

Rebscher, S.J., Snyder, R.L., Leake, P.A. 2001. The effect of electrode configuration and duration of deafness on threshold and selectivity of responses to intracochlear electrical stimulation. J Acoust Soc Am 109, 2035-48.

Rebscher, S.J., Hetherington, A.M., Snyder, R.L., Leake, P.A., Bonham, B.H. 2007. Design and fabrication of multichannel cochlear implants for animal research. J Neurosci Methods 166, 1-12.

Rose, J.E., Greenwood, D.D., Goldberg, J.M., Hind, J.E. 1963. Some discharge characteristics of single neurons in the inferior colliculus of the cat. I. Tonotopical organization, relation of spike counts to tone intensity and firing patterns of single elements. J Neurophysiol 26, 294-320.

Ryan, A.F., Miller, J.M., Wang, Z.X., Woolf, N.K. 1990. Spatial distribution of neural activity evoked by electrical stimulation of the cochlea. Hear Res 50, 57-70.

Schreiner, C.E., Langner, G. 1997. Laminar fine structure of frequency organization in auditory midbrain. Nature 388, 383-6.

Seshagiri, C.V., Delgutte, B. 2007. Response properties of neighboring neurons in the auditory midbrain for pure-tone stimulation: a tetrode study. J Neurophysiol 98, 2058-73.

Shaddock Palombi, P., Backoff, P.M., Caspary, D.M. 2001. Responses of young and aged rat inferior colliculus neurons to sinusoidally amplitude modulated stimuli. Hear Res 153, 174-80.

Shamma, S.A., Fleshman, J.W., Wiser, P.R., Versnel, H. 1993. Organization of response areas in ferret primary auditory cortex. J Neurophysiol 69, 367-83.

Shannon, R.V. 1983a. Multichannel electrical stimulation of the auditory nerve in man. II. Channel interaction. Hear Res 12, 1-16.

Shannon, R.V. 1983b. Multichannel electrical stimulation of the auditory nerve in man. I. Basic psychophysics. Hear Res 11, 157-89.

Shannon, R.V. 1992. Temporal modulation transfer functions in patients with cochlear implants. J Acoust Soc Am 91, 2156-64.

Sher, A., Chichilnisky, E.J., Dabrowski, W., Grillo, A.A., Grivich, M., Gunning, D., Hottowy, P., Kachiguine, S., Litke, A.M., Mathieson, K., Petrusca, D. 2007. Large-scale multielectrode recording and stimulation of neural activity. Nuclear Inst. and Methods in Physics Research, A 579, 895-900.

Small, A.M. 1955. Some parameters influencing the pitch of amplitude modulated signals. J Acoust Soc Am 27, 751-760.

Snyder, R.L., Bierer, J.A., Middlebrooks, J.C. 2004. Topographic spread of inferior colliculus activation in response to acoustic and intracochlear electric stimulation. J Assoc Res Otolaryngol 5, 305-22.

Snyder, R.L., Middlebrooks, J.C., Bonham, B.H. 2008. Cochlear implant electrode configuration effects on activation threshold and tonotopic selectivity. Hear Res 235, 23-38.

Snyder, R.L., Vollmer, M., Moore, C.M., Rebscher, S.J., Leake, P.A., Beitel, R.E. 2000. Responses of inferior colliculus neurons to amplitude-modulated intracochlear electrical pulses in deaf cats. J Neurophysiol 84, 166-83.

Stickney, G.S., Loizou, P.C., Mishra, L.N., Assmann, P.F., Shannon, R.V., Opie, J.M. 2006. Effects of electrode design and configuration on channel interactions. Hear Res 211, 33-45.

Ter-Mikaelian, M., Sanes, D.H., Semple, M.N. 2007. Transformation of temporal properties between auditory midbrain and cortex in the awake Mongolian gerbil. J Neurosci 27, 6091-102.

Tong, Y.C., Millar, J.B., Clark, G.M., Martin, L.F., Busby, P.A., Patrick, J.F. 1980. Psychophysical and speech perception studies on two multiple channel cochlear implant patients. J Laryngol Otol 94, 1241-56.

Venkatraman, S., Elkabany, K., Long, J.D., Yimin, Y., Carmena, J.M. 2009. A system for neural recording and closed-loop intracortical microstimulation in awake rodents. IEEE Transactions on Biomedical Engineering 56, 15-22.

Verhey, J.L., Pressnitzer, D., Winter, I.M. 2003. The psychophysics and physiology of comodulation masking release. Exp Brain Res 153, 405-17.

Viemeister, N.F. 1979. Temporal modulation transfer functions based upon modulation thresholds. J Acoust Soc Am 66, 1364-80.

Vollmer, M., Snyder, R.L., Leake, P.A., Beitel, R.E., Moore, C.M., Rebscher, S.J. 1999. Temporal properties of chronic cochlear electrical stimulation determine temporal resolution of neurons in cat inferior colliculus. J Neurophysiol 82, 2883-902.

Wagenaar, D.A., Potter, S.M. 2002. Real-time multi-channel stimulus artifact suppression by local curve fitting. Journal of Neuroscience Methods 120, 113-20.

Wichmann, T. 2000. A digital averaging method for removal of stimulus artifacts in neurophysiologic experiments. J Neurosci Methods 98, 57-62.

Wilson, B.S., Finley, C.C., Lawson, D.T., Wolford, R.D., Eddington, D.K., Rabinowitz, W.M. 1991. Better speech recognition with cochlear implants. Nature 352, 236-8.

Xu, L., Pfingst, B.E. 2008. Spectral and temporal cues for speech recognition: implications for auditory prostheses. Hear Res 242, 132-40.

Yin, T.C., Kuwada, S., Sujaku, Y. 1984. Interaural time sensitivity of high-frequency neurons in the inferior colliculus. J Acoust Soc Am 76, 1401-10.

Yost, W.A., Sheft, S., Opie, J. 1989. Modulation interference in detection and discrimination of amplitude modulation. J Acoust Soc Am 86, 2138-47.

Young, E.D. 2003. Cochlear Nucleus. In: Shepherd, G.M., (Ed.), The Synaptic Organization of the Brain, 5th ed. Oxford University Press, New York.

Zeng, F.G., Rebscher, S., Harrison, W.V., Sun, X., Feng, H. 2008. Cochlear Implants:System Design, Integration and Evaluation. IEEE Rev Biomed Eng 1, 115-142.

Zhang, C., Zeng, F.G. 1997. Loudness of dynamic stimuli in acoustic and electric hearing. J Acoust Soc Am 102, 2925-34.

Zhang, F., Miller, C.A., Robinson, B.K., Abbas, P.J., Hu, N. 2007. Changes across time in spike rate and spike amplitude of auditory nerve fibers stimulated by electric pulse trains. J Assoc Res Otolaryngol 8, 356-72.

Zwicker, E., Flottorp, G., Stevens, S.S. 1957. Critical Band Width in Loudness Summation. J Acoust Soc Am 29, 548-557.

Zwolan, T.A., Kileny, P.R., Ashbaugh, C., Telian, S.A. 1996. Patient performance with the Cochlear Corporation "20 + 2" implant: bipolar versus monopolar activation. Am J Otol 17, 717-23.

Appendix I: Circuit Schematics
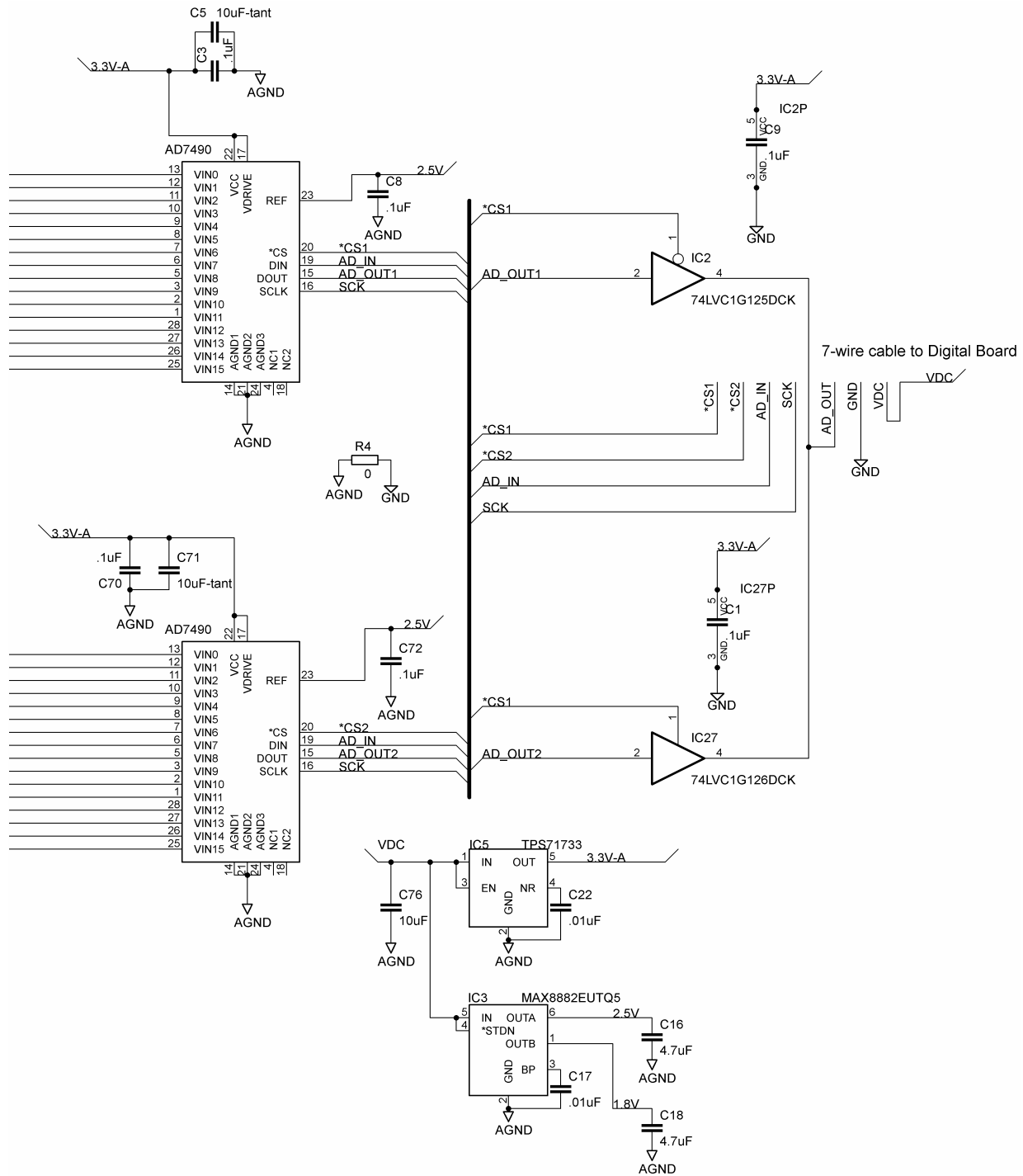
Fig. 1. Circuit schematic for the headstage. Horizontal wires extending to the left edge of the figure are the 32 total inputs to the two AD7490 A-D converters. Each A-D converter input connects to the output of one amplifier (amplifier schematic shown in Chapter 1). The outputs of the A-D converters are multiplexed onto the AD_OUT line and passed to the digital board.
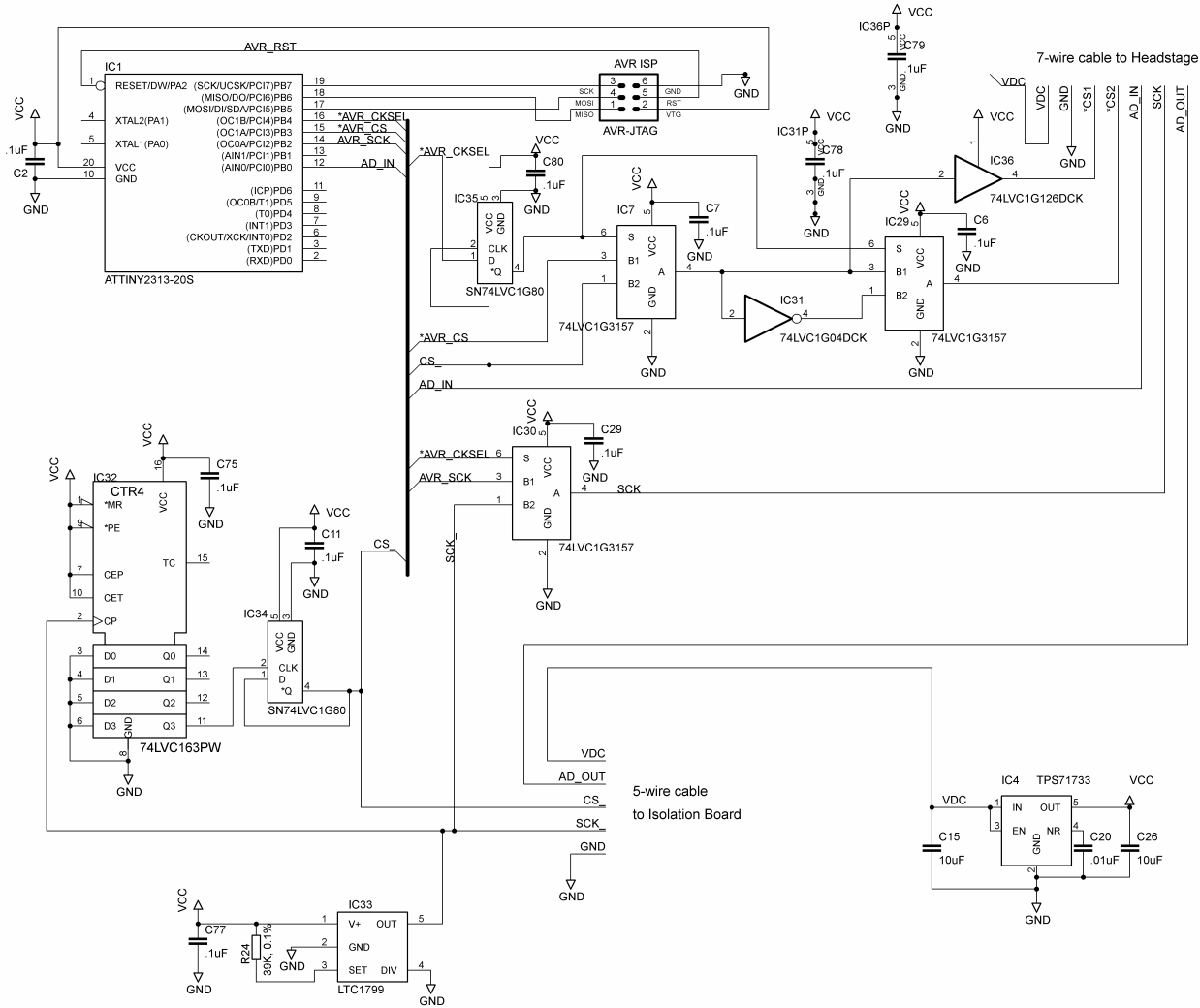
Fig. 2. Circuit schematic for the digital board. This board generates serial clock (SCK), chip select (CS), and input (AD_IN) signals for the A-D converters. It receives the A-D outputs multiplexed on the AD_OUT line from the headstage and passes this signal (along with SCK and CS) to the isolation board (Fig. 3).
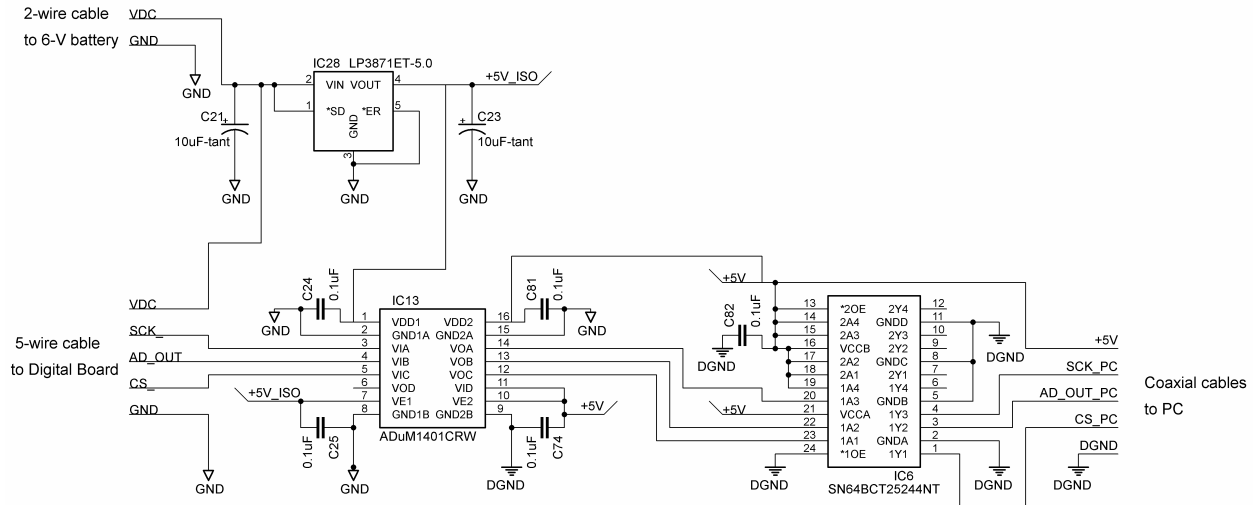
Fig. 3. Circuit schematic for the isolation board. This board passes the three digital output signals (CS, SCK, and AD_OUT) through an inductive digital isolator (Analog Devices ADuM1401) and a digital line driver (Texas Instruments 64BCT25244), then relays them to the PC over 50-Ω-terminated coaxial cables. The isolation board receives 5-V power and ground on the non-isolated side from the PC and 6-V power and ground on the isolated side from four "D" cell batteries connected in series.
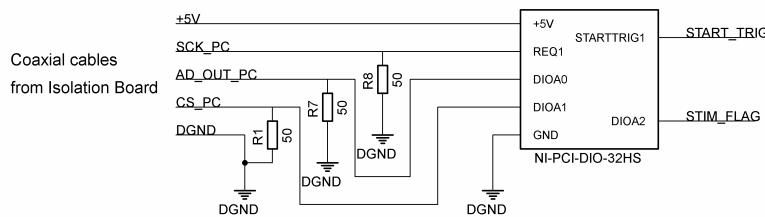
Fig. 4. Connection diagram for the PC digital I/O card. The NI-PCI-DIO-32HS digital I/O card operates in buffered pattern I/O mode. A pulse on the START_TRIG line triggers the beginning of an acquisition, and the SCK signal provides the data transfer clock (on falling edges). Data words from the two A-D converters are multiplexed on the AD_OUT line. Output words are 16-bits long and are framed by transitions in the CS line. The STIM_FLAG line is high while there is an electrical stimulus current being delivered on an intracochlear electrode and low otherwise. This provides information about stimulus times and durations for artifact blanking. Note that additional 32-channel recording systems could be connected simultaneously to the NI-PCI-DIO-32HS using one additional digital line per 32-channel system (another AD_OUT line). The other lines could be shared among the recording systems. Given the ability of the NI-PCI-DIO-32HS to acquire 32-bit words and the fact that only two bits are being used by signals other than AD_OUT (i.e. CS and STIM_FLAG), 30 recording systems could be connected simultaneously to the NI-PCI-DIO-32HS for a total channel count of 960 recording channels. The cost beyond the initial 32 channels would be about $300 per additional 32-channel system (see Chapter 1 for cost breakdown). However, it is likely that at higher channel counts the ability of the PC to acquire and store data fast enough would become an issue. National Instruments does offer newer digital I/O card models, which could be useful in this regard.

Appendix II: AVR Microcontroller C Code

PROGRAM CODE

```
/* spi-adc-v1.c

This program configures an ADC (AD7490) to convert on a specified sequence
of channels. It is currently written for an ATtiny2313 mcu (Atmel, 8-bit AVR).

*/

#include "pins.h"
#include <inttypes.h>
#include <avr/io.h>
#include <avr/interrupt.h>
#include <avr/sleep.h>


//Pin toggle commands
#define SCK_HIGH            sbi(PORTB, PIN_SCK)
#define MOSI_HIGH           sbi(PORTB, PIN_MOSI)
#define MOSI_LOW            cbi(PORTB, PIN_MOSI)
#define CS_HIGH                 sbi(PORTB, PIN_CS)
#define CS_LOW              cbi(PORTB, PIN_CS)
#define SCK_LOW             cbi(PORTB, PIN_SCK)
#define SCK_HIGH            sbi(PORTB, PIN_SCK)


// ADC control register bit numbers for AD7490.
//Lower Byte
#define CODING  4           // 0-3 are always zeros
#define RANGE       5
#define WK_TRI  6
#define SHADOW  7
//Upper Byte
#define PM0         0
#define PM1     1
#define ADD0    2
#define ADD1    3
#define ADD2    4
#define ADD3    5
#define SEQ     6
#define WRITE   7


/* Create ADC control bytes. Sets up for continuous conversion
on a sequence of channels (i.e., SEQ=0, SHADOW=1). The first channel is
channel zero (ADD3:0 = 0000). Normal power mode (PM1=PM0=1).
Weak pullups on ADC output are disabled (WK_TRI=0). The ADC input
range is set from 0->Vref (RANGE=1). The coding is straight binary
(CODING=1) */

//Upper Byte
#define ADC_CR_UP  (1<<WRITE) | (0<<SEQ) | (0<<ADD3) | (0<<ADD2) | \
                   (0<<ADD1) |  (0<<ADD0) |(1<<PM1)  | (1<<PM0)

//Lower Byte (the four LSBs are always zeros)
#define ADC_CR_LO  (1<<SHADOW)| (1<<WK_TRI)| (1<<RANGE) | (1<<CODING)


//Create shadow register bytes. Tells ADC which channels to convert
#define SHADOW_UP  0xFF
#define SHADOW_LO  0xFF

static uint8_t SPI_out_up = 0xFF;    //temporary variable for SPI output
static uint8_t SPI_out_lo = 0xFF;    //temporary variable for SPI output
static uint8_t SPI_out = 0xFF;       //temporary variable for SPI output
static uint8_t TIM0_count;           //counts number of Timer0 interrupts
```

```
static uint8_t TIM1_count;               //counts number of Timer1 interrupts


/*ISR (INT1_vect)
{
        sbi(PORTB, PIN_SCK_SEL);         //select external sck
        cbi(PORTB, PIN_SCK_SEL);
        GIMSK = (0<<INT1);
        sbi(PORTB, PIN_SCK_SEL);
        cbi(PORTB, PIN_SCK_SEL);

        sleep_cpu();                     //put cpu into idle mode to save power
}
*/


ISR (TIMER1_COMPA_vect)
{
        /* This interrupt routine is called when the counter of TIMER1 reaches the
        value stored in OCR1A. TIMER1 is then reset and begins counting again.
        TIMER1 is used to toggle CS for the ADC.

        The first time this interrupt is called, there has just been a falling
        edge of CS. The next time will be a rising edge. It keeps alternating like
        this. The purpose of this routine is to load the output words for the ADC
        on rising edges of CS and start SCLK (TIMER0) for a data transfer on falling
        edges. The first data word has already been initialized before this
        routine is called the first time. After the control words have been loaded
        into the ADC, this routine starts running SCLK and CS signals continuously
        at higher speeds. The ADC will continuously convert using the most recent
        control information. */

        TIM1_count++;  //keeps track of whether CS just rose or fell


        /* If positive edge of CS (TIM1_count even) load the output bytes for ADC,
        stop and reset Timer0, and return. */
        if (!(TIM1_count & 1))
        {
                //Already set up to output 0xFFFF for 2nd falling edge of CS (do nothing)
                if (TIM1_count==2)
                {
                }

                //Load ADC control registers for 3rd falling edge of CS
                if (TIM1_count==4)
                {
                        SPI_out_up = ADC_CR_UP;
                        SPI_out_lo = ADC_CR_LO;
                }

                //Load ADC shadow registers for 4th falling edge of CS
                if (TIM1_count==6)
                {
                        SPI_out_up = SHADOW_UP;
                        SPI_out_lo = SHADOW_LO;
                }

                //Load continuous conversion control word for ADC (WRITE=0)
                if (TIM1_count==8)
                {
                        SPI_out_up = 0x00;
                        SPI_out_lo = 0x00;
                }


                if (TIM1_count>8)
                //Setup the timers to run continuously at higher speeds
                {
                        OCR0A = 0;
                        TIMSK &=  ~(1<<OCIE0A);                 //disable TIMER0 interrupt
                        TIMSK &=  ~(1<<OCIE1A);                 //Disable TIMER1 interrupt
```

```
                    cbi(PORTB, PIN_SCK_SEL);                //select external sck

            }

            return;
        }

        /* This section of code only runs after a falling edge of CS. It loads the
        output word msb into the data output to the ADC (MOSI). It then starts
        Timer0 (SCLK) */

        SPI_out = SPI_out_up<<1; //load output word msb into carry flag of SREG


        if (SREG & 1)
            {
                    MOSI_HIGH;      //if msb=1, set MOSI high
            }
        else
            {
                    MOSI_LOW;       //if msb=0, clear MOSI
            }



        //Start TIMER0 (SCLK)
        TCCR0B = (0<<FOC0A) | (0<<FOC0A) | (1<<WGM02) | (0<<CS02) |
                    (0<<CS01) | (1<<CS00);
        return;
}



ISR (TIMER0_COMPA_vect)
{
        /* This interrupt routine is called when the counter of TIMER0 reaches the
        value stored in OCR0A. TIMER0 is then reset and begins counting again.
        TIMER0 is used to toggle SCLK for the ADC.

        Before this routine is called, spi_out has already been loaded with the
        upper byte to send to the ADC. spi_out_lo has the bottom byte loaded.

        The first time this interrupt is called, there has just been a falling
        edge of SCLK. The next time will be a rising edge. It keeps alternating like
        this. The purpose of this routine is to output the next bit onto MOSI before
        the next falling edge of SCLK. The first bit has already been initialized
        before this routine is called so it is output on the first falling edge
        of SCLK. After 16 bits have been clocked out, this routine turns off TIMER0
        and resets it for the next output word.*/

        TIM0_count++;  //keeps track of whether SCLK just rose or fell


        if (TIM0_count==32) //after 16 bits clocked out, stop/reset TIMER0. Return.
            {
            //Stop TIMER0
            TCCR0B = (0<<FOC0A) | (0<<FOC0A) | (1<<WGM02) | (0<<CS02) |
                        (0<<CS01) | (0<<CS00);

            //Reset TIMER0
            TCNT0=0x00;
            TIM0_count=0;
            return;
        }

        /*If falling edge of SCLK (TIM0_count odd), check to see if need to load
        bottom byte of SPI output (i.e. already clocked out 8 bits). Return. */
        if (TIM0_count & 1)
        {
                if(TIM0_count==15)
                {
```

```c
                       SPI_out=SPI_out_lo;
            }
    return;
    }


    //If rising edge of SCLK, load the next bit of the current output byte.
    SPI_out = SPI_out<<1; //load output bit into msb into carry flag of SREG

    if (SREG & 1)
    {
            MOSI_HIGH;              //if bit=1, set MOSI high
    }
    else
    {
            MOSI_LOW;               //if bit=0, clear MOSI
    }

    /* Now MOSI has the next bit for the ADC. Next time there is a falling edge
    of SCLK this bit will be captured by the ADC */
    return;
}


int main (void) {

//set brown out fuses

    SREG |= (1<<7);                 //global interrupt enable

    //enable idle mode and set INT1 mode to rising edge
    MCUCR |= (0<<SM1) | (1<<SE) | (0<<SM0);


    ACSR |= (1<<ACD);                       //turns off analog comparator to save power


    //setup uC for ADC interface
    PORTA = 0xFF;                   // enable pullups
    PORTB = 0xFF;
    PORTD = 0xFF;


    //Setup TIMER0

    TIMSK |=  (1<<OCIE0A); //enable TIMER0 output compare match interrupt

    //OCR0A is the TIMER0 output compare register. Needs to be large enough so
    //that there is time to do everything in TIMER0 interrupt routine before
    //next TIMER0 compare match
    OCR0A = 100;    //this value could probably be made smaller, if needed

    //Initialize TIMER0 output pin (OC0A) to 1 by writing a 1 to 1<<FOC0A. Can't
    //be in Fast PWM Mode to do this.
    TCCR0A = (0<<COM0A1) | (1<<COM0A0) | (0<<COM0B1) | (0<<COM0B0) |
                    (1<<WGM01)  | (0<<WGM00);

    TCCR0B = (1<<FOC0A) | (0<<FOC0B) | (0<<WGM02) | (0<<CS02) |
                    (0<<CS01)   | (0<<CS00);

    //Setup TIMER0 for Fast PWM Mode
    TCCR0A = (0<<COM0A1) | (1<<COM0A0) | (0<<COM0B1) | (0<<COM0B0) |
                    (1<<WGM01)  | (1<<WGM00);


    //Setup & start TIMER1

    //OCR1A is the TIMER1 output compare register. Needs to be large enough so
    //that there is time to go through 16 falling edges of SCLK (TIMER0)
    OCR1A = 80;

    TIMSK |=  (1<<OCIE1A); //enable TIMER1 output compare match interrupt
```

```
        //Initialize TIMER1 output pin (OC1A) to 1 by writing a 1 to 1<<FOC1A. Can't
        //be in Fast PWM Mode to do this.
        TCCR1A = (0<<COM1A1) | (1<<COM1A0) | (0<<COM1B1) | (0<<COM1B0) |
                        (0<<WGM11)  | (0<<WGM10);

        TCCR1B = (0<<WGM13) | (1<<WGM12) | (0<<CS02) |
                        (0<<CS01)  | (0<<CS00);

        TCCR1C = (1<<FOC1A) | (0<<FOC1B);

        sbi(DDRB, PIN_MOSI);            //set MOSI as output
        sbi(DDRB, PIN_CS);              //set CS as output
        sbi(DDRB, PIN_SCK);             //set SCK as output
        sbi(DDRB, PIN_SCK_SEL);         //set SCK_SEL as output
        sbi(PORTB, PIN_SCK_SEL);        //initialize clock select to one
        cbi(DDRB, PIN_MISO);            //set MISO as input

        cbi(DDRD, PIN_INT1);            //set INT1 pin as an input

        //Setup TIMER1 for Fast PWM Mode
        TCCR1A = (0<<COM1A1) | (1<<COM1A0) | (0<<COM1B1) | (0<<COM1B0) |
                        (1<<WGM11)  | (1<<WGM10);

        //Use a prescaler of 64 on the io clk to make sure TIMER1 is slow enough
        TCCR1B = (1<<WGM13) | (1<<WGM12) | (0<<CS02) |
                        (1<<CS01)  | (1<<CS00);


        volatile int i=1;

        while(i)
                //Go to sleep and wait for next interrupt. TIMER0 (SCLK) will only start
                //after a falling edge of CS (TIMER1). There will be 16 falling edges of
                //SCLK. Then SCLK will stop and there will be a rising edge of CS. The
                //TIMER1 interrupt will then prepare for the next falling edge of CS.
                {
                //EIFR = (0<<INTF1);
                sleep_cpu();
                }


        return 0;
}
```

HEADER FILE

```
//pins.h

#ifndef pin_h           //port pins for ATtiny2313

#define PIN_INT1 3

#define PIN_CS 3
#define PIN_SCK 2
#define PIN_MOSI 0
#define PIN_MISO 1
#define PIN_SCK_SEL 4
#define sbi(port,pin)  port |= _BV(pin)
#define cbi(port,pin)  port &= ~_BV(pin)
#define high(pin) sbi(PORTB, pin)
#define low(pin) cbi(PORTB, pin)

#endif
```

Appendix III: Chronically Deafened Cats

Six of the eight cats in this study were deafened as neonates by daily subcutaneous injections of neomycin sulfate (60 mg/kg) (Leake et al., 1999) and received varying electrical stimulation regimes and drug treatments (Table I). For all six animals, neomycin injections were started at day 1 after birth; click-evoked auditory brainstem responses were used to monitor hearing loss beginning after 16 days of treatment, at 2-3 days intervals. Neomycin treatment was discontinued after 16-21 injections when absence of responses to clicks at 90 dB SPL indicated a profound hearing loss. All six cats were implanted unilaterally at 4-7 weeks of age with an intracochlear electrode having six to eight stimulating contacts. Four cats also received a subcutaneous mini osmotic pump (Rebscher et al., 2007) for direct infusion of brain-derived neurotrophic factor (BDNF, 94 µg/ml, 3 animals) or artificial perilymph (1 animal) into the inner ear. One animal received systemic treatment with rasagiline (1 mg/kg daily). Five cats also received chronic electrical stimulation for 4 hours per day, 5 days a week, for a period of 13 to 23 weeks. Four of these five animals received electrical stimulation with biphasic pulse trains (90 µs/phase) delivered by Clarion™ CII speech processor. Levels of stimulation were controlled by the loudness of environmental sounds with maximum stimulation levels set at 6 dB above electrically evoked ABR thresholds, but no more than 500 µA. The remaining animal was stimulated with continuous trains of charge-balanced biphasic pulses (200 µsec/phase) delivered at 300 pulses/s with 30-Hz sinusoidal amplitude modulation (100% modulation depth). In this animal stimulation levels were set at 2 dB above electrically evoked ABR thresholds. Chronically deafened cats were studied in acute physiological experiments immediately following completion of the electrical stimulation and drug treatment protocols.

Table 1. Electrical stimulation and drug treatment histories for eight cats.

Cat No.	Age at implantation, weeks	Age at stimulation, weeks	Stimulation period, weeks	Stimulus	Drug treatment	Age at study, weeks
K335	7.5	9	17	BP 1,2 & 5,6 – Speech processor, 1100 pps	none	26
K327*	6	7	23	BP 1,3** & 5,6 – Speech processor, 1100 pps	Rasagiline, systemic, 10 weeks	30
K336*	5.5	Not stimulated	-	-	Artificial perilymph, infusion pump, 10 weeks	16
K313	5	10	13	BP 1,2 & 5,6 – Speech processor, 1100 pps	BDNF, infusion pump, 11 weeks	23
K319	5	8	20	BP 1,2 & 5,6 – Speech processor, 1100 pps	BDNF, infusion pump, 11 weeks	28
K329	4	7	22	BP 1,2 & 5,6: 300pps/30Hz;	BDNF, infusion pump, 10 weeks	29
K328	Normal hearing cat	-	-	-	-	26
K338	Normal hearing cat	-	-	-	-	31

*Cats that received dexamethasone through the osmotic pump during the first several days after cochlear implantation.

**K327 had 1,3 bipolar pair stimulated for most of the stimulation period due to the failure of wire # 2.

Abbreviations: BP, bipolar; pps, pulses per second.

Leake, P.A., Hradek, G.T., Snyder, R.L. 1999. Chronic electrical stimulation by a cochlear implant promotes survival of spiral ganglion neurons after neonatal deafness. J Comp Neurol 412, 543-62.

Rebscher, S.J., Hetherington, A.M., Snyder, R.L., Leake, P.A., Bonham, B.H. 2007. Design and fabrication of multichannel cochlear implants for animal research. J Neurosci Methods 166, 1-12.